Tu-Pos279

BINDING SITE STUDIES OF PROTEIN SYNTHESIS INITIATION FACTORS EIF-4F AND EIF-(ISO)4F USING A PHOTOAFFINITY ANALOG. ((D.E Friedland[a], M.T. Shoemaker*, and D.J. Goss[a])) [a]Chem. Dept., Hunter College of CUNY, NY, NY 10021; *Division of Medicinal Chemistry, University of Kentucky, Lexington KY 40536.

Understanding the molecular basis for recognition of the 5′ terminal cap of eucaryotic cellular mRNA by protein synthesis initiation factors (eIF's) requires determination of the amino acids involved in the binding of the m^7GpppG cap structure to eIF's. In order to investigate this, photoaffinity labeling with a cap analog, (α-^{32}P)8N_3GTP was used in binding site studies with two wheat germ eIF's known to bind at or near the m^7G cap; eIF-4F and eIF-(iso)4F. Competitive inhibition of this analog by m^7GTP indicated probe specificity for interaction at the binding site of both proteins. The binding site in both cases was located on the small subunit, (26kDa for eIF-4F and 28kDa for eIF-(iso)4F). Aluminum(III)-chelate chromatography and reverse phase HPLC were used to isolate the binding site peptide resulting from trypsin or chymotrypsin digestion of photolabeled protein. Grant Support: NSF MCB9303661, AHA-NYC.

Tu-Pos280

CONTRIBUTION OF AMINO ACIDS 317-328 AT THE C-TERMINAL REGION TO LACTOSE REPRESSOR STRUCTURE AND FUNCTION. ((Likun Li and Kathleen S. Matthews)) Department of Biochemistry & Cell Biology, Rice University, Houston, Texas 77251

Leucine heptad repeats at the C-terminal region of the *lac* repressor protein are required for tetramer assembly (Chakerian *et al.* (1991) *J. Biol. Chem.* **266**, 1371; Alberti *et al.* (1991) *New Biol.* **3**, 57). Deletion of up to 32 amino acids from the C-terminus yielded dimeric protein with normal inducer binding activity and ~150-fold diminished operator binding; deletion of 43 or 64 amino acids yielded lower levels or no protein in the cell extracts (Chen & Matthews (1992) *J. Biol. Chem.* **267**, 13843; Betz (1986) *Gene* **42**, 283). To further investigate the region between -32 and -43 amino acids, three deletion mutants eliminating the C-terminal 34, 36 and 39 amino acids were constructed using site-specific mutagenesis. All three proteins were present in cells based on reaction with monoclonal antibody to the repressor protein; however, cell extracts containing the -36 or -39 mutant protein did not bind to IPTG, indicating that the structures of the polypeptide chains in these mutants were altered significantly from wild-type. Although the -34 amino acid repressor protein was found to be a dimer by gel filtration, in contrast to other dimeric repressors examined, this mutant had 6.5-fold lower inducer binding activity than wild-type protein. Furthermore, no cooperativity for inducer binding was found at pH 9.2 for the -34 amino acid mutant. Apparent operator binding affinity for the -34 amino acid repressor was ~300-fold lower than wild-type. These results suggest that Arg326 and/or Lys325, present in the -32 amino acid repressor, contribute to forming the proper tertiary and perhaps also quaternary structure necessary for inducer and operator affinity. Further investigation of the contributions of these amino acids to repressor structure and function is in progress. (Supported by NIH grant GM22441 and Welch Grant C-576).

STRIATED MUSCLE PHYSIOLOGY AND ULTRASTRUCTURE I

Tu-Pos281

INCREASE IN FORCE PER CROSS-BRIDGE BY EMD 57033, A CALCIUM-SENSITIZING AGENT. (T. Kraft[#], I. Lues*, B. Brenner[#])) [#]Medical School, Hannover, FRG; *Pha. Res. Div., E. Merck, Darmstadt, FRG.

EMD 57033 (E. Merck, Darmstadt, Germany) was found to increase the isometric force of cardiac muscle fibers without an equivalent increase in fiber ATPase (Leijendekker,W. & Herzig, J., Pflug.Arch. 421, 1992). Since isometric force can be modulated by cross-bridge turnover kinetics and other factors such as force per cross-bridge, we studied the effects of EMD 57033 on cross-bridge turnover kinetics (f_{app}, g_{app}), on fiber stiffness, and on the shape of plots of force vs. length change during ramp-shaped stretches and releases (T-plots) of fully activated skinned single fibers of rabbit psoas muscle.
With 50μM EMD 57033, isometric force increased by more than 50% and ATPase/force decreased by about 30% while k_{redev} and fiber stiffness remained unchanged. Thus, the large increase in force cannot be explained by a decrease in g_{app} alone nor by a simultaneous change in g_{app} and f_{app}. Comparing the shape of T-plots recorded with and without EMD 57033 revealed an increase in force generated by a cross-bridge. However, it was not by redistribution among the force generating states, favoring those of higher force contribution (c.f. Brenner, PNAS 88, 1991). Instead, in each of the force generating states the force generated by a cross-bridge appears to be increased by EMD 57033.

Tu-Pos282

TRIMETHYLAMINE N-OXIDE (TMAO) DOES NOT SIMPLY REVERSE THE EFFECTS OF HIGH IONIC STRENGTH ON CONTRACTION OF SKINNED RABBIT PSOAS MUSCLE FIBERS. ((S.V. Zhelamsky, R.T.H. Fogaça and R.E. Godt)) Dept. of Physiology. & Endo., Medical College of GA, Augusta GA 30912.

In skinned psoas fibers, elevation of ionic strength (Γ/2) from 165 to 315 mM decreases maximal force (Fmax) and stiffness (Smax) at pCa 4, and Ca^{2+} sensitivity (Ca_{50}), while the ratio of maximal ATPase/force (tension-cost) increases ≈ 30%. The rate constant of force redevelopment (pCa 4) after release & restretch (k_{tr}) was slightly increased (≈ 14 %). In a two-state cross-bridge model (e.g., Brenner, *P.N.A.S. 85*:3265, 1988), higher tension-cost suggests that increased Γ/2 accelerates the apparent detachment rate of cross-bridges. The effect of Γ/2 on Fmax, Smax, and Ca_{50} is consistent with fewer strongly-attached bridges available to switch on the thin filament. The protein stabilizer TMAO (0.3M) reverses the effect of high Γ/2 on Fmax and Smax (Andrews et al., *Biophys. J. 59*:456a, 1991), presumably by increasing the number of strong bridges. However, TMAO decreases Ca_{50}, which is apparently inconsistent with an increase in strong bridges. At both high and low Γ/2, TMAO decreases tension-cost slightly (≈ 10%), and substantially slows k_{tr} (≈ 50%), i.e., TMAO decreases the apparent rates of attachment and detachment. (0.3M sucrose does not affect k_{tr} or Ca_{50}.) The effects on k_{tr} and Ca_{50} suggest that TMAO may also stabilize the switched off state of the thin filament. (Support: NIH AR 31636 & HL 36059, and the Office of Naval Research).

Tu-Pos283

EFFECT OF CALPONIN ON SKINNED RABBIT PSOAS MUSCLE. ((S. Heizmann*, F.W.M. Lu[#], J.M. Chalovich[#] & B. Brenner*)) Medical School of Hannover*, FRG and East Carolina Univ. Med. School[#], USA

In searching for inhibitors of cross-bridge binding to actin we studied the effects of calponin on stiffness of skinned skeletal muscle fibers. **Solution studies** show that calponin (1) weakens the binding of S-1-AMP-PNP to actin (2) inhibits actin-activated ATPase activity even in the presence of tropomyosin-troponin and (3) binds tightly to actin-tropomyosin-troponin in the presence and absence of Ca^{++}. **In Fibers** in relaxing conditions (μ=50 mM), calponin inhibits stiffness by <20% while the active force decreases by >85% at both 50 mM and 170 mM ionic strength. To see if the decrease in active force results from slowing the transition into the force generating state (kinetic effect) the rate constant of force redevelopment after a period of lightly loaded shortening (k_{redev}) was studied. Calponin has no effect on k_{redev} that can account for the observed inhibition of active force. Calponin, however, reduces fiber stiffness, in both rigor and in the presence of 4 mM MgPPi, to 33-50% of the initial values. All effects of calponin are 80-90% reversed after 30 min in relaxing solution at μ=170 mM. Our data suggest that inhibition of strong cross-bridge binding to actin contributes to the reduction of active force by calponin. However, it is possible, that part of the inhibitory effect is due to interference of calponin with the Ca^{++}-activation mechanism of the skeletal muscle system. (Supported by DFG 849/1-4, NATO 900257, and NIH AR40540).

Tu-Pos284

DYNAMICS AND ORIENTATION OF SPIN-LABELED TROPOMYOSIN RECONSTITUTED IN RABBIT PSOAS MUSCLE FIBERS ((Danuta Szczesna and Piotr G. Fajer)) Inst. Molec. Biophysics, Florida State Univ., Tallahassee, FL 32306. (Spon. by Z. Grabarek)

We have used EPR spectroscopy to study the rotational motions and orientation of a maleimide-labeled rabbit tropomyosin (MSL-Tm) reconstituted in ghost muscle fibers. Fibers were depleted of intrinsic myosin, troponin and tropomyosin (85±5%) with Hasselbach-Schneider solution and MSL-Tm was added back to 95±5% of the initial level as quantified by SDS electrophoresis.
EPR of myofibrils and oriented fibers showed that:
(*i*) the mobility of labeled domains of tropomyosin was decreased by 1.4 times on the binding of MSL-Tm to actin in myofibrils. The rotational correlation time, τ_r = 5.7 ns for free MSL-Tm in solution, and 7.7 ns for tropomyosin reconstituted in myofibrils;
(*ii*) dynamics of reconstituted tropomyosin were not affected by the further reconstitution of troponin in the presence or absence of Ca^{2+};
(*iii*) myosin-S1 infused into the reconstituted fibers increased the motion of MSL-Tm to τ_r = 6.1 ns;
(*iv*) the orientation of reconstituted tropomyosin was not changed by either troponin in the presence of Ca^{2+} or myosin-S1.

Tu-Pos285

FLUORESCENCE POLARIZATION OF ACETAMIDOTETRAMETHYLRHODAMINE (ATR) COVALENTLY BOUND TO SH-1 IN RABBIT *PSOAS* MUSCLE FIBERS FOLLOWING RAPID LENGTH CHANGES. ((C.L. Berger, S. Karki and Y.E. Goldman)) Univ. of Penn., Phila. PA 19104.

In order to relate structural changes of myosin with force production, we studied the motions of skeletal muscle cross-bridges during force transients elicited by rapid length changes (2-8 nm/h.s. in ~150 μs) of fibers in active and rigor contractions. Orientation of the cross-bridges was monitored by fluorescence polarization of single fibers labeled at SH-1 (Cys-707 of the myosin heavy chain) using iodo-ATR (Molecular Probes, Inc. lot 9A). The polarization ratios $Q_\parallel = (I_\parallel - I_\perp)/(I_\parallel + I_\perp)$ and $Q_\perp = (I_\perp - I_\parallel)/(I_\perp + I_\parallel)$ were obtained at 500 μs instrumental rise-time (10-90%) using 84 kHz modulation of the exciting light polarization (Tanner et al., *J. Mol. Biol.* 223:185-203, 1992) and a Wollaston prism to resolve the ∥ and ⊥ fluorescence. In rigor $Q_\parallel = 0.395 \pm 0.002$ and $Q_\perp = 0.624 \pm 0.004$ (mean ± s.e.m., n = 8). As shown in the Fig. for $\Delta l \cong 2$ nm/h.s., repeated cycles of stretches and releases caused virtually no change in polarization ratio signals ($\Delta Q_\parallel = 0.002 \pm 0.001$ and $\Delta Q_\perp = -0.002 \pm 0.001$, n = 8). This result was independent of the amplitude of the applied step up to ~8 nm/h.s. tested. Similar results were obtained following quick releases in fibers actively contracting at 5 mM MgATP and ~30 μM free Ca^{2+}, 200 mM ionic strength, 20°C. The changes in $Q_\parallel$ and $Q_\perp$ were <0.006, even for the largest length steps that reduced force transiently to <37% of isometric force. Although the fluorescence polarization ratios sense probe angle rather than protein orientation, if the region of myosin near Cys-707 tilted in these length step experiments, the ATR probes would be expected to follow. Thus, possible concerted angle changes, associated with rigor cross-bridge compliance or with active force production, appear to occur away from this region of the molecule. Supported by the MDA & NIH.

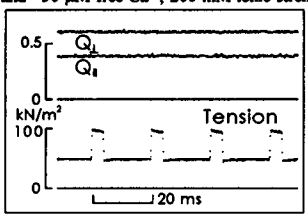

Tu-Pos286

EPR STUDIES OF ORIENTATION AND DYNAMICS OF MSL-TROPONIN C RECONSTITUTED IN RABBIT SKELETAL MUSCLE ((H.C. Li and P.G. Fajer)) Dept. of Biol. Sci. Florida State University, Tallahassee, FL 32306 *(Spon. by D. Easton)*

Rabbit skeletal Troponin C (TnC) was labeled with maleimide spin label (MSL) at its single cysteine residue (Cys-98) and reconstituted into an oriented skinned fiber system, to investigate its calcium dependent dynamics and orientation. Reconstitution was achieved by incubating TnC-depleted fiber with MSL-TnC. Fibers depleted of 70% of endogeneous TnC showed 60-100% loss of active tension, and reconstitution of 95% of original protein concentration restored 80% of the original tension.

EPR spectra indicate that the mobility of MSL-TnC in the reconstituted fiber system (correlation time 50ns) is only 0.1 that in solution. No further changes in mobility of reconstituted TnC were observed on the addition of Ca^{2+} or MgATP. The EPR spectra of oriented fiber bundles show broad orientational distribution of the labeled TnC domain. The distribution becomes significantly narrower when Ca^{2+} is removed, and is accompanied by the reorientation of the label's principal axis towards the long axis of the filaments. This orientational change is more pronounced when the myosin heads are detached during fiber relaxation.

Tu-Pos287

CHANGES IN CROSSBRIDGE ORIENTATION AND MOBILITY DUE TO LATTICE COMPRESSION. ((B.B. Adhikari and P. G. Fajer)) Inst. of Mol. Biophysics, Florida State Univ., Tallahassee, FL 32306. *(Spon. L. Makowski)*

Tension generation in muscle fibers is dependent on the filament lattice spacing. Decreasing the lattice spacing of skinned rabbit psoas muscle fibers by osmotic compression using dextran T-500, initially increases the tension, which reaches a maximum when the lattice is compressed by about 10% [1]. With further compression the tension gradually decreases [2], reaching zero at a lattice compression of 60%. Using conventional and saturation transfer EPR spectroscopy, we have studied the crossbridge orientation and mobility in MSL labeled rabbit psoas fibers at various levels of compression. In the compression range studied (from 0% to 60%), we noted distinct spectral changes. Specifically we found that:
(i) in rigor, the orientation and mobility of myosin heads did not change at any level of applied compression;
(ii) no spectral changes were seen in contracting fibers during the initial phase of compression (<10%), above this level however the inhibition of active tension was paralleled by the ordering of the myosin heads and inhibition of their mobility;
(iii) in relaxed fibers, increasing compression caused a proportional increase in crossbridge ordering and a corresponding decrease in their mobility.
We therefore conclude that it is necessary for the myosin heads to retain their broad orientational distribution and microsecond mobility to enter the force producing state(s).

[1] Gulati, J., and Babu, A. 1985. Biophys. J. 48:781.
[2] Kawai, M. et al. 1993. Biophys. J. 64:187.

Tu-Pos288

THE ROTATIONAL DYNAMICS OF GIZZARD REGULATORY LIGHT CHAINS FUNCTIONALLY INCORPORATED INTO SCALLOP MYOFIBRILS. ((Sampath Ramachandran, Osha Roopnarine and David D. Thomas)) U. of Minnesota, Minneapolis, MN 55455. (Spon. by David Levitt).

We have used **time-resolved phosphorescence anisotropy (TPA)** to probe the rotational dynamics of chicken gizzard myosin regulatory light chain (GRLC) incorporated into scallop (*Placopecten magellanicus*) myofibrils. GRLC was specifically labeled at Cys 108 with eosin-5-maleimide (EoM) and introduced into RLC-depleted (calcium-insensitive) scallop myofibrils. The calcium-dependent ATPase activity was restored, showing that the labeled GRLC was functionally incorporated. TPA was performed at 4°C. In rigor, a rapid initial decay (1-3 μs) was followed by no change in anisotropy up to 1 millisecond. In relaxation (rigor + 5 mM MgATP), the amplitude of the initial decay was much greater than in rigor, and was followed by a slower decay (5-10 μs). In contraction, the decay had a slightly smaller amplitude than in relaxation. These results are consistent with light chains undergoing **rapid microsecond motions even in rigor**, the amplitude of which is increased upon addition of ATP. We thank Dr. Andrew G. Szent-Györgyi for helpful discussions.

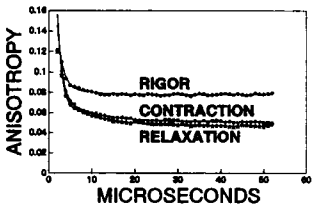

Tu-Pos289

THE LIGHT CHAIN BINDING REGION OF THE MYOSIN HEADS IN MUSCLE FIBERS IS MORE DYNAMICALLY DISORDERED THAN THE SH1 REGION ON THE HEAVY CHAIN.
((Osha Roopnarine, Andrew. G. Szent-Györgyi*, and David D. Thomas)). University of Minnesota Medical School, Minneapolis, MN 55455, *Brandeis University, Waltham, MA 02254.

We have covalently attached an indane-dione **spin label**, InVSL, to the sulfhydryls of rabbit skeletal regulatory light chains (RLC) and to Cys 55 in *Mercenaria* RLC. The spin-labeled RLC were exchanged into RLC-depleted rabbit or scallop (*Placopecten magellanicus*) muscle fiber bundles. The conventional EPR spectrum of the fiber bundles indicated that all the spin labels in all preparations were immobile on the nanosecond time scale but **orientationally disordered** in rigor, relaxation, and contraction. **Saturation-transfer EPR (ST-EPR)** shows that this disorder is **not static, but is dynamic on the microsecond time scale.** In contrast, previous results with InVSL and other spin labels attached to Cys 707 **(SH1)** on the heavy chain show rigid and uniform orientation in rigor, with dynamic (microsecond) disorder only in relaxation and contraction. In fact, more rotational disorder and motion is observed for light chain labels in rigor than for SH1 labels in relaxation. These results support the proposal that **the light chain binding region ("neck") of the myosin head is more flexible and dynamic than is the portion of the head closer to actin.** This flexibility within the myosin head may play a crucial role in the mechanism of force generation.

Tu-Pos290

MICROSECOND ROTATIONAL DYNAMICS OF MUSCLE CROSS-BRIDGES DETECTED AT TWO DISTINCT SITES. ((David W. Hayden, Sampath Ramachandran and David D. Thomas)) Dept. of Biochemistry, University of Minnesota Medical School, Minneapolis, MN 55455. (Sponsored by Richard Linck)

Most spectroscopic measurements of crossbridge motion have focussed on SH1 (Cys 707). However, recent models suggest independent movement of domains within the myosin head, so a complete description of the molecular dynamics requires probes at several distinct sites. Therefore, we have studied the microsecond rotational motions of a phosphorescent probe, eosin maleimide (EoM), **attached specifically to two distant sites on the myosin head** in rabbit psoas myofibrils. Motions of the light-chain-binding region were detected with EoM bound to Cys108 of chicken gizzard regulatory light chains (RLC), which were incorporated into RLC-depleted rabbit psoas myofibrils. Alternatively, EoM was attached directly to SH1 in intact myofibrils, providing a probe of the ATP-binding region. **Time-resolved phosphorescence anisotropy** (TPA) was performed under physiological ionic conditions at 4 °C. In rigor, neither site showed rotational motion on the 1 to 800 μsec time scale. **At each site, the addition of ATP induced large-amplitude microsecond rotational motion both in the presence and absence of calcium.**

Tu-Pos291

THE ROTATIONAL DYNAMICS OF GIZZARD REGULATORY LIGHT CHAINS FUNCTIONALLY INCORPORATED INTO SCALLOP MYOFIBRILS. ((Sampath Ramachandran, Osha Roopnarine and David D. Thomas)) U. of Minnesota, Minneapolis, MN 55455. (Spon. by David Levitt).

We have used **time-resolved phosphorescence anisotropy (TPA)** to probe the rotational dynamics of chicken gizzard myosin regulatory light chain (GRLC) incorporated into scallop (*Placopecten magellanicus*) myofibrils. GRLC was specifically labeled at Cys 108 with eosin-5-maleimide (EoM) and introduced into RLC-depleted (calcium-insensitive) scallop myofibrils. The calcium-dependent ATPase activity was restored, showing that the labeled GRLC was functionally incorporated. TPA was performed at 4°C. In rigor, a rapid initial decay (1-3 μs) was followed by no change in anisotropy up to 1 millisecond. In relaxation (rigor + 5 mM MgATP), the amplitude of the initial decay was much greater than in rigor, and was followed by a slower decay (5-10 μs). In contraction, the decay had a slightly smaller amplitude than in relaxation. These results are consistent with light chains undergoing **rapid microsecond motions even in rigor**, the amplitude of which is increased upon addition of ATP. We thank Dr. Andrew G. Szent-Györgyi for helpful discussions.

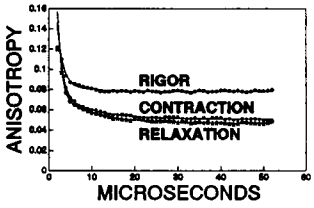

Tu-Pos292

DIFFRACTION INTENSITY PROFILES FROM MULTI-STRAND HELICES WITH DISORDER WITH APPLICATION TO MYOSIN. G.F. Elliott, Open University Oxford Research Unit, Oxford OX1 5HR UK; C.R. Worthington, Carnegie Mellon University, Pittsburgh, PA.

In order to take account of disorder within helices we have directly computed the autocorrelation function (a.c.f.) for the disordered helix [Acta Cryst. A45: 645(1989)]. The Fourier transform of the a.c.f. gives the diffraction intensity profiles. This theory has been extended to multi-strand helices. The following disorders have been treated: stagger between individual strands [Biophys. J. 59: 165a (1991)] , a rotational offset of individual strands and a variation in the locations of the subunits within the individual strands. We have used this theory to examine various disorder models of myosin. The myosin helix has three strands and shows a series of extra meridional refections that are forbiddden if it had a strict 3-fold symmetry as often assumed . The introduction of stagger within the individual strands gives rise to extra reflections but the intensities are weak compared to the observed diffraction recorded in X-ray experiments using synchrotron radiation in Japan [1991] and the UK [1993]. The Yagi et. al. [Biophys. J. 33:121(1981)] model is one of the first models proposed and is thought to explain the observed diffraction. In this model the subunit separations are systematically changed but without stagger between strands. The layer-line intensity profiles have been calculated and , in particular, the meridional intensities give a poor match with the observed even with the use of a large temperature factor. A variation of the Yagi-type model which has limited substitution disorder along the strands but again without any stagger gives a much better match especially with the 2nd meridional order although the model is not ideal as the 5th meridional order persists. Other disorder models for myosin are under study and will be described.

Tu-Pos293

INTEGRATED INTENSITIES OF MYOSIN LAYER LINES ARE NOT AFFECTED BY WEAK ATTACHMENT OF CROSS-BRIDGES TO ACTIN AT 20°C. ((S.Xu^{+}, S.Malinchik^{+}, D.Gilroy^{+}, B.Brenner*, L.Yu^{+})) $^{+}$NIH; *Hannover Medical School, Germany.

In skinned rabbit psoas muscle at low temperature cross-bridges can attach to actin in large fractions under relaxing conditions. Nonetheless, 2D X-ray diffraction patterns showed that myosin layer lines (M-LL) were present (Podolsky & Matsuda, PNAS, 1984; Yu et al. BJ, 1993), suggesting that the structure of weakly attached cross-bridges differs from that of rigor cross-bridges. However, at low temperature, M-LL are weak and diffuse, making quantitative analysis difficult. Presently, we recorded diffraction patterns at 20°C with the ionic strength (μ) varying between 170 mM and 50 mM. Force level was continuously monitored to be always <1-2% of isometric force, and optical diffraction patterns were stable. Under these conditions, the equatorial I_{11}/I_{10} changes from 0.30 to 0.55. M-LL are strong, showing features typical of helical arrangements of cross-bridges. From fiber stiffness and biochemistry, it is estimated that at 20°C the fraction of cross-bridges weakly attached to actin ranges between 8-10% (μ=170mM) and ≥50% (μ=50mM) (Kraft & Brenner, unpublished results). In spite of significant changes in the fraction of weakly bound cross-bridges, radially integrated intensities (between 0.002 and 0.006Å^{-1}) do not change significantly for the first five M-LL, while at μ=50 mM the sixth layer line is stronger. The results support the idea that weak attachment does not disrupt the thick filament based arrangement of cross-bridges in relaxed muscle. (NATO 930448).

Tu-Pos294

STUDIES OF THE CONFIGURATIONS OF WEAKLY ATTACHED AND FORCE GENERATING CROSSBRIDGES. MODELLING OF EQUATORIAL X-RAY DIFFRACTION PATTERNS. ((S.Malinchik and L.Yu)) NIH

Recent equatorial X-ray diffraction results provided direct evidence of a structural difference between weakly attached and force generating crossbridges (B.Brenner and L.Yu, PNAS, 1993). To determine the nature of the structural changes, model calculations are being carried out to find the best fit for the experimental data. The shape of S-1 (Rayment et al., Science., 1993) is simulated by spheres of appropriate radii. Configuration, position, and attachment of the head are described by spatial angles and radial distance from the center of thick filament. R-factor (<4%) and averaged standard deviation of calculated intensities (<18%) are used as criteria for acceptable parameters. To simulate weakly attached cross-bridges, we assume the attachment is non-stereo specific, keeping the shape of S-1 constant but varying spatial angles and radial position. For contracting muscle, in contrast, the light chain (LC) binding part of S-1 is allowed to bend. We found that for weakly bound crossbridges a wide distribution of attachment angles is acceptable. For contracting state, this distribution has to be narrower, while the LC binding part of S-1 can assume a wide range of axial angles. In addition, another required change from weakly attached to force generating configurations is that the crossbridges need to move radially by 5-10Å closer to actin. The results are consistent with the idea that force generation involves a transition from a non-stereo specific attachment to a stereo-specific attachment, with an increased interaction surface between S-1 and actin.

Tu-Pos295

CHANGES IN THICK FILAMENT STRUCTURE AT VARIOUS LATTICE SPACINGS IN RELAXED AND CONTRACTING SKELETAL MUSCLE. ((Quanning Li, Barry Millman and Tom Irving)) Biophysics Group, Department of Physics, University of Guelph, Guelph, Ontario, N1G 2W1, Canada and MacCHESS, Department of Biochemistry, Cornell University, Ithaca, NY, 14853, USA.

The filament lattice structure of intact frog sartorius muscle was studied by X-ray diffraction over a range of lattice spacings induced by changes in osmolarity. Detailed two-dimensional diffraction patterns were obtained from relaxed and contracting muscle in less than half a second using the synchrotron source at Cornell (CHESS). In relaxed muscle, when the lattice shrinks by 20%, the relative intensities of the (2nd, 4th and 5th) meridional reflections decrease by 30 - 50%. As well, the second sampling peak on the third myosin layer-line becomes weaker when the lattice shrinks, as do the inner peaks on the first layer-line. On the other hand, outer reflections on the first layer-line become stronger at smaller lattice spacings. Analysis of equatorial patterns at smaller spacings show that upon activation, the total amount of mass transferred to the thin filament in contracting muscle is insensitive to changes in lattice spacing. Though some myosin head mass is shifted away from the equatorial 1,0 planes, there is little shift of mass along the 1,1 lattice planes. A model for the distribution of myosin heads in different states is proposed to account for changes observed.

Tu-Pos296

THE A-BEE-Z PROBLEM OF ACTIN FILAMENT ROTATION IN INSECT FLIGHT MUSCLE.
((R.J. Edwards, C. Lucaveche, M.K. Reedy)) Duke University, Durham, NC 27710.

There is ample evidence that the actin filaments in the overlap zone of both bee and waterbug flight muscle present a helical array of target zones around each thick filament. However, Squire (J. Mus. Res. **13**, 183-89) has pointed out that Cheng and Detherage's 3D reconstruction of the bee Z-band (J. Cell Biol. **108**, 1761-74), when extrapolated into the A-band, implies rings of target zones rather than helices. This discrepancy might be resolved if there are three-fold screw axes at the lattice and trigonal positions of the insect Z-band instead of three-fold rotation axes; thus making the insect Z-band $P3_221$, instead of P312 as assumed by C&D. We have examined bee Z-bands using EM and filtered images. Thin longitudinal sections show that the diagonal lattice planes arising from the helical target zones continue into the Z-band, suggesting that the azimuthal orientation of the actin filaments, as revealed by local decoration of the thin filaments, follows the same helical pattern in the A and Z bands. Transverse sections of the Z-band show diffraction spots out to 6 nm resolution, and filtered images from 50-90 nm sections clearly show a connecting density (dubbed C-4 by C&D) at the trigonal position, which appears three-fold in projection. We are currently pursuing 10-30 nm oblique sections as a means of detecting the three-fold screw axes which would be present if the insect Z-band is $P3_221$ as we suspect. (Supported by NIH AR14317 and NSF Predoctoral Fellowship.)

Tu-Pos297

X-RAY DIFFRACTION STUDIES OF SKINNED FIBERS OF THE RABBIT PSOAS MUSCLE DURING HIGH-SPEED SHORTENING. ((R. Stehle*, T. Kraft*, J. Harries*, B. Brenner*)) *Medical School Hannover, FRG; *Daresbury Laboratory, UK.

We previously proposed that during rapid shortening <5% of cross-bridge occupy the strong-binding states observed under isometric conditions. Equatorial X-ray patterns recorded during rapid shortening under our conditions, however, are about half-way between isometric and relaxed patterns or patterns recorded in the presence of ATPγS. To account for this discrepancy we tested for (i) incomplete substrate saturation in the activated fiber, (ii) effects of filament sliding on weak interactions, and (iii) a possible slow time course for developing a fully relaxed-type pattern. Neither changes in [MgATP] from 0.25-5mM nor filament sliding per se sufficiently affected the equatorial intensities. We also found no relevant effect when employing a multiple-release protocol so as to allow for longer time to establish a relaxed type pattern. This suggests that during rapid shortening either the fully relaxed arrangement of cross-bridges in weak-binding states is disrupted, e.g. by the few strong interactions, or cross-bridges occupy states that only kinetically correspond with the weak-binding states but have different structural properties. (Supported by DFG, Br 849/1-4 and EC Large Facilities Programme.)

Tu-Pos298

CHARACTERIZATION OF CROSS-BRIDGE STATES DURING HIGH-SPEED SHORTENING. EFFECT OF INORGANIC PHOSPHATE (P_i) AND TEMPERATURE (T). ((R. Stehle, and B. Brenner)) Medical School Hannover, FRG.

We previously demonstrated evidence suggesting that during rapid shortening only a very small fraction of cross-bridges occupies the strong-binding states observed in isometric contraction (Stehle & Brenner, Biophys. J., 1993, Brenner, ibid). Instead, >95% of cross-bridges appear to occupy states similar to those found in the presence of ATPγS at high Ca^{++}, i.e. weak-binding states such as those found in relaxed muscle fibers but with slower attachment/detachment kinetics. To test this concept, we increased $[P_i]$ or decreased T to reduce occupancy of the strong-binding states. If stiffness during high-speed shortening has almost no contribution from strongly bound cross-bridges, P_i and T should only affect isometric stiffness. Isotonic stiffness should essentially be unaffected.

Addition of 7.5mM P_i or decrease in T from 5 to 1°C decreased isometric stiffness by some 30-40%, independent of the speed of stretch or release. Apparently both interventions reduced occupancy of strong-binding states under isometric conditions. Yet, during rapid shortening fiber stiffness was essentially unaffected by both interventions, consistent with only very few cross-bridges occupying strong-binding states under this condition. (Supported by DFG Br849/1-4.)

Tu-Pos299

DIRECT RECORDING OF TIME-RESOLVED X-RAY DIFFRACTION DURING TETANUS RISE OF SINGLE MUSCLE FIBERS USING A CCD AREA DETECTOR.
((Eric F. Eikenberry[1], Fredrik Osterberg[2], T.C. Irving[3], G. Cecchi[4], M.A. Bagni[4], C.C. Ashley[5] and P.J. Griffiths[5])) [1]Department of Pathology, Robert Wood Johnson Medical School, Piscataway; [2]Department of Physics, Princeton University, Princeton; [3]MacCHESS, Department of Biochemistry, Cornell University, Ithaca; [4]Dipartimento di Scienze Fisiologiche, Universita degli Studi di Firenze, Florence; and [5]University Laboratory of Physiology, Oxford.

Cecchi, *et al.* (*Biophys. J. 59* (1991), 1273-1283) have reported time resolved x-ray diffraction studies of single muscle fibers during the rise of tetanic tension. Those studies used a one-dimensional wire counter with a sampling time of 10 ms to record equatorial x-ray intensity during tetanus rise, while simultaneously monitoring sarcomere length and tension.

Using a similar protocol we have produced time-resolved two-dimensional x-ray diffraction patterns using synchrotron undulator radiation at 7.6 keV (0.19 nm; CHESS A2 station). The time-resolved patterns were recorded with a quantum-limited large format (1k x 1k) CCD detector operated as a streak camera in which one dimension of the detector recorded time with a sampling interval of 1 ms, while the other dimension recorded distance along the equator in the conventional manner. When displayed as an image, this gives a direct visualization of the evolution with time of the equatorial x-ray pattern.

The equatorial (10) and (11) reflections from single fibers of *Rana temporaria* tibialis anterior muscle were recorded. During fixed-end tetanus rise, the previously reported transient increase in equatorial spacing was clearly defined. In addition, a marked transient increase in disorder of the second kind was seen, which gives information on the cooperative movement of groups of fibril components. This detector will potentially be of utility in investigating the dynamic structure of muscle at the very high flux beam lines that are becoming available.

The same detector has also been used to record crystallographic data with exceptionally high precision (R_{sym} = 2%). Only a software selection is required to switch between streak camera and conventional modes of operation.

Tu-Pos300

BIREFRINGENCE OF MUSCLE: CROSS-BRIDGE ORIENTATION IN THE ACTIVE STATE OF MUSCLE.
((P.S. Blank, X. Wu, and F.D. Carlson)) NICHD, NHLBI, NIH, Bethesda, MD 20892 and Johns Hopkins Univ., Baltimore, MD 21218

Birefringence, was measured at 15 °C during the relaxed, rigor, and active states of single, skinned, rabbit psoas muscle fibers. The sarcomere length was 2.36 μm. The transitions from the relaxed to rigor and active states were accompanied by significant decreases in birefringence: 1.90 +/- 0.01 (relaxed), 1.75 +/- 0.01 (rigor), 1.65 +/- 0.01 (active) (mean +/- sem x 10^{-3}, n = 8, p < 0.0005). If the intrinsic birefringence of the activated state was comparable to that measured in the relaxed or rigor states then the average cross-bridge angle in the activated state was between 70 - 90 degrees from the fiber axis with the largest isotropic distribution ranging from 50 - 90 degrees. These values are consistent with a minimum cross-bridge rotation of 20 degrees towards the fiber axis during the transition between the active and rigor state. However, equal cross-bridge orientations in the active and rigor states are possible, if the intrinsic birefringence of the activated state is significantly less than that of the rigor state. A structural change in the cross-bridge during the active state, which results in a 10% decrease in the intrinsic birefringence would be consistent with the absence of cross-bridge rotation during the transition between the active and rigor states. Supported in part by USPHS 12803 to F.D.C.

Tu-Pos301

X-RAY DIFFRACTION MEASUREMENTS OF THE EXTENSIBILITY OF THE ACTIN AND MYOSIN FILAMENTS IN MUSCLE. ((Hugh Huxley, Alex Stewart & Hernando Sosa)) Rosenstiel Center, Brandeis University, Waltham, MA 02254, ((Tom Irving)), MacCHESS, Dept. of Biochemistry, Cornell University, Ithaca, New York 14853.

Using a small angle scattering system that we have assembled on the high flux multipole wiggler beam line at CHESS (Cornell) we have been able to make very accurate spacing measurements of certain wide angle meridional reflections from contracting muscles. In particular we have studied the behavior of the first actin meridional reflection (at a spacing of approximately 27.3Å), the second order of this reflection (13.65Å) and the 15th order myosin meridional reflection at approximately 28.6Å. Interestingly, all these reflections show large increases in intensity (up to a factor of 2) during isometric contraction. They also undergo significant changes in spacing which can be measured with great accuracy in an arrangement which allows patterns at different levels of tension during a single experimental series to be compared side-by-side on the same imaging plate. During isometric contraction the actin 27.3Å reflection increases in spacing by between 0.3 and 0.35%, and other actin reflections, including the 59Å and 51Å off-meridional reflections show corresponding changes in spacing. When tension is augmented or diminished by applying moderate speed length changes to a contracting muscle, changes in spacing can again be seen. These correspond to changes in the range of 0.2 to 0.25% when scaled to full isometric tension, suggesting non-linearity at low tension levels, where somewhat larger changes can be seen. Myosin filaments also show changes of axial period of about 0.2%, in addition to the well-known larger change associated with activation. An actin spacing change of 0.25% - 0.3% can be measured during a 2 millisecond time frame immediately following a quick release, showing that the elastic behavior is rapid. These observations of filament extensibility may necessitate some revision of the interpretation of a number of mechanical experiments in muscle, on which it has usually been assumed that virtually all of the elasticity resides in the crossbridges. Supported by NIH ARE38899, by a grant from the Lucille P. Markey Charitable Trust (H.E.H.), and by NIH RR01646-09 (MacCHESS).

Tu-Pos302

THE EFFECT OF 2,3 BUTANEDIONE MONOXIME (BDM) ON THE CROSSBRIDGE TRANSITION FROM WEAKLY TO STRONGLY BOUND STATES IN SKINNED RABBIT SKELETAL MUSCLE FIBERS. ((M. Regnier, C. Morris, and E. Homsher)) Physiol. Dept., Medical School, UCLA, Los Angeles, Ca. 90024.

BDM suppresses force production and stiffness in contracting muscle. Force suppression is >90% at 20 to 30 mM BDM and is completely reversible. Biochemical studies have shown that while steady state myosin ATPase is reduced in BDM, the equilibrium constant for ATP cleavage and the Pi burst rate are increased. Herrmann et al (Biochem. 31:12227, 1992)) suggest that the inhibition of force is produced by an inhibition of Pi release from the AM.ADP.Pi crossbridge state. This interpretation implies that the BDM inhibits the formation of strongly bound crossbridges and/or inhibits force generation by the crossbridges once they do bind. To test this hypothesis we examined the effects of BDM on the rate of tension decline (k_{Pi}) produced when [Pi] is suddenly increased by the photolysis of caged-Pi in an isometrically contracting muscle fiber. k_{Pi} is thought to reflect the rate of a force-generating isomerization and the subsequent release of inorganic phosphate. Further the effect of BDM on the rate of tension redevelopment (k_{tr}) after a sudden release and restretch of fibers was measured. k_{tr} is thought to indicate the rate of transition from the weakly bound to force generating state and thus includes the rates for strong crossbridge attachment and force generation. In BDM, the k_{Pi} declines in parallel with the decline in isometric force; e.g., at 3 mM BDM, force is reduced to 60 % of control and k_{Pi} is reduced to 65% . Similarly k_{tr} is reduced by 45% in 3 mM BDM. These effects are in striking contrast to the effects of calcium concentration on kPi, force, and k_{tr}; i.e., a rise in pCa reduces k_{tr} and force dramatically, but has little or no effect on k_{Pi}. The effect of 3 mM BDM can largely be explained by a reduction in the rate of the force generating isomerization. (Supported by NIH Grant AR 30988).

Tu-Pos303

EFFECTS OF 2,3-BUTANEDIONE-MONOXIME (BDM) ON CROSS-BRIDGE FUNCTION IN MUSCLE. ((Liang Zhao and Roger Cooke)) Dept. of Biochemistry & Biophysics and Cardiovascular Research Institute, University of California, San Francisco, CA 94143.

The effects of BDM on fiber mechanics and on cross-bridge orientation have been investigated. Cross-bridge orientation was measured via electron paramagnetic resonance (EPR) spectroscopy of maleimide spin probes rigidly attached to cys-709 (SH1) on the myosin head. Previous work by a number of investigators has shown that BDM is an uncompetitive inhibitor that reversibly binds to and stabilizes the intermediate states, actin•myosin•ADP•P_i and myosin•ADP•P_i, of the actomyosin cycle. Increasing BDM concentrations caused a decrease in both active tension and stiffness, but to different amounts. At a low level of BDM (5 mM), fiber tension and stiffness were 50% and 70% of control values (in the absence of BDM), respectively. At 20mM BDM, tension was almost abolished, only 5-10% of control, but stiffness remained high, about 40% of control. These results show that at high levels of BDM, cross-bridges attach to actin but do not generate force. The EPR spectrum of active control fibers consisted of two components, a disordered component and an ordered component (18% of total spins). Increasing BDM was found to decrease the ordered component. At 5 mM BDM, the ordered fraction of probes was decreased to about 50% of control. When the BDM level was increased to 20 mM, the probes were almost totally disordered. These results show that in the presence of BDM myosin heads are attached to actin in states that are disordered as measured by probes attached to cys-709. Supported by AR30868.

Tu-Pos304

HIGH LEVELS OF PHOSPHATE AND LOW pH DECREASE MUSCLE TENSION AND STIFFNESS, BUT DO NOT DISORDER PROBES ATTACHED TO CYS-709 ON MYOSIN. ((Liang Zhao and Roger Cooke)) Dept. of Biochemistry & Biophysics and Cardiovascular Research Institute, University of California, San Francisco, CA 94143. (Spon. by J. Finer-Moore)

We have studied the effects of high levels of phosphate (P_i) and low pH on the isometric tension and on the orientation of myosin heads in glycerinated rabbit psoas muscle fibers. A comparison of the fiber's response under two different conditions was made. The first was in the absence of P_i at pH 7.0, the second at 60 mM P_i and pH 6.2. ([MgATP] = 5 mM, μ = 230 mM, 25°C for both conditions). Mechanical measurements showed that the simultaneous increase of P_i to 60 mM and decrease of pH to 6.2 caused a 70% decrease in tension and 40% decrease in stiffness, measured by step changes in length. However, electron paramagnetic resonance spectroscopy of probes attached to cys-709 showed that the ordered fraction seen was almost identical for both control and high P_i, low pH fibers. These results suggest that there is a weak-binding, actin•myosin•ADP•P_i state, in which the orientation of at least a large portion of the catalytic domain of the myosin head is similar to that seen at the end of the powerstroke in rigor. This EPR result is opposite to that found in the presence of BDM, a molecule which has similar effects on fiber mechanics, but stabilizes an actin•myosin•ADP•P_i state that is disordered. (See abstract by L. Zhao this meeting). Together these two results suggest that there are multiple forms of this state some of which have ordered probes while others do not. Supported by AR30868.

Tu-Pos305

MYOSIN LIGHT CHAIN 3 MODULATES SHORTENING VELOCITY IN CHICKEN FAST MUSCLE FIBERS. ((Peter J. Reiser)) Oral Biology, The Ohio State University, Columbus, OH 43210. (Sponsored by A. C. Kirby)

Results from several laboratories have demonstrated a correlation between shortening velocities and alkali light chain (LC1, LC3) ratios in single fibers from mammalian fast muscles. Lowey, Waller and Trybus recently reported (Nature 365:454-456, 1993) that the sliding velocity of actin filaments on coverslips bound with myosin isolated from chicken pectoralis (fast) muscle was dependent on the light chain complement of the reconstituted myosin. The previous results obtained from mammalian muscle and the recent results of Lowey and co-workers consistently demonstrate greater velocities associated with myosin LC3. The objective of the present study was to determine whether a similar association exists in single muscle fibers of chicken pectoralis muscle. The maximal shortening velocity of seven randomly-chosen skinned fibers from adult pectoralis ranged from 3.14 to 5.87 fiber lengths/sec. The LC3/(LC1 + LC3) ratio in the same fibers, determined from densitometric scans of silver-stained SDS gels, ranged from 0.22 to 0.41. Variations in the LC ratio and shortening velocity were associated in a very linear manner. The slope of this relationship in fibers of the pectoralis muscle, where there is almost exclusively one isoform of myosin heavy chain expressed at the adult stage, is about twice as steep as that in mammalian fast muscle (Greaser, Moss & Reiser, J. Physiol., 406:85-98, 1988), where multiple isoforms of MHC are expressed. Thus, it is concluded that LC3 modulates shortening velocity in avian and mammalian fast muscle fibers but there appears to be a greater influence of LC3 on velocity in avian muscle. Supported by NIH grant AR39652.

Tu-Pos306

THE EFFECT OF ALTERED Ca^{2+} BINDING TO MYOSIN REGULATORY LIGHT CHAIN ON TENSION GENERATION IN SKINNED SKELETAL MUSCLE FIBERS ((GM Diffee, ML Greaser, F Reinach*, and RL Moss, Dept of Physiol. and Muscle Biology Lab, Univ of Wisconsin, Madison, WI, 53706, and *Inst. of Chemistry., Univ. of Sao Paulo, Brazil))

To examine the role of Ca^{2+} binding to the regulatory light chain (RLC) of myosin in the generation of tension by skeletal muscle fibers, we exchanged a mutant RLC (D12A) having reduced affinity for Ca^{2+} (Reinach et al, Nature 322:80-83, 1986) for endogenous RLC in skinned rabbit psoas fibers. Up to 90% of the endogenous RLC was replaced by D12A RLC by incubating the fibers in 25mM KCl/10mM EDTA/10mM Imidazole/2mM DTT, and 2 mg/ml of D12A RLC, for 30 min. at 37 °C. Following exchange, maximum tension (at pCa 4.5) decreased to an average 39.4% of pre-exchange tension (n = 22), and the amount of decrease was directly related to the extent of D12A exchange. Fiber stiffness changed in proportion to tension, suggesting that reduced tension was due to a decrease in the number of bound cross-bridges. Decreases in both tension and stiffness were partially reversed following re-exchange of native RLC for D12A. To test that these effects were specifically due to the mutation, RLC exchange was performed using a wild-type RLC. Although a small tension decline was observed (mean = 80.8% of control, n = 14), the decrease was not proportional to the extent of exchange and was not reversed by re-exchange of the native RLC. The results indicate that Ca^{2+} binding to myosin RLC plays a role in tension generation in skeletal muscle fibers, possibly by stabilizing the tension generating intermediate. **Supported by NIH AR08226 and HL25861.**

Tu-Pos307

NATURE OF SYNCHRONOUS LENGTH OSCILLATIONS DURING LOADED SHORTENING OF FROG MUSCLE FIBRES ((K.A.P. Edman and N.A. Curtin*)) Dept. of Pharmacology, University of Lund, S-223 62 Lund, Sweden and *Dept. of Physiology, Charing Cross & Westminster Medical School, London, U.K.

As originally described by Armstrong, Huxley & Julian (J. Physiol. 1966. 186:26P), striated muscle that is released to shorten against a high load (approx. 90 % of maximum force) generally undergoes several cycles of damped length oscillation during the shortening phase. We have explored this phenomenon during fused tetani of isolated muscle fibres of R. temporaria (1-3 °C, sarcomere length 2.25 μm). Length changes were recorded both from the fibre as a whole and from marked consecutive segments (ca. 0.5 mm in length) along the preparation. Fibre stiffness was measured by recording the force response to a 1 kHz length oscillation (peak-to-peak amplitude, ca 1.5 nm/half sarcomere) that was applied to one end of the fibre.

The initial length step during the load-clamp manoeuvre is the actual trigger of the length oscillation. The oscillatory behaviour is exhibited by all segments along the fibre, the various regions acting in synchrony. The length oscillations are associated with cyclic changes in fibre stiffness while force is kept constant at the pre-set clamp level. The oscillations continue as long as the various parts of the fibre remain in synchrony. The oscillatory behaviour is explainable by assuming that the cross-bridges, after attachment to the thin filament, require a finite time to develop their maximum force.

Tu-Pos308

EFFECT OF SARCOMERE LENGTH AND MYOFILAMENT LATTICE SPACING CHANGES ON THE ACTIVATION PROPERTIES OF TRITON X-100 SKINNED RABBIT SOLEUS MUSCLE FIBERS. ((Kimberly A. Palmiter, Bo Sheng-Pan, and R. John Solaro)) Department of Physiology and Biophysics, University of Illinois at Chicago, Chicago, IL 60612.

Increasing the sarcomere length of striated myofilaments increases the Ca^{2+} sensitivity of force development over the ascending and descending limbs of the length-tension relation. How these length changes affect Ca^{2+} activation of striated myofilaments remains unresolved. Stretching the sarcomere not only alters the overlap of thin and thick filaments, it also reduces myofilament lattice spacing. In cardiac muscle, changes in overlap and crossbridge attachment have been hypothesized to affect troponin C (TNC) Ca^{2+} affinity. The important question that arises is: What is the effect of myofilament lattice spacing on TNC Ca^{2+} binding, and can this account for the increased Ca^{2+} sensitivity of the myofilaments along the length-tension curve? We measured force production and Ca^{2+} binding to TNC in Triton X-100 skinned rabbit soleus muscle fibers at sarcomere lengths 2.4, 3.0, and 3.8 μm. These increases in sarcomere length caused a significant leftward shift of the pCa-force relation. However, there was no significant increase in TNC Ca^{2+} binding. In fact, we observed a slight decrease in Ca^{2+} binding to TNC at longer sarcomere lengths. When crossbridges were bound to thin filaments under rigor conditions there was a significant decrease in Ca^{2+} bound to TNC at longer sarcomere lengths. This provides further evidence that the significant leftward shift of the pCa-force relation is not due to feedback effects of the crossbridge reaction on Ca^{2+} binding to TNC. In unrestrained Triton X-100 skinned rabbit soleus fibers hypertonic shrinkage of the myofilament lattice with 3% (w/v) Dextran T-70 had no effect on Ca^{2+} binding to TNC. We therefore conclude that the increased Ca^{2+} sensitivity at longer sarcomere lengths is likely to be due to mechanisms other than an increase in TNC Ca^{2+} affinity. Furthermore, the changes in Ca^{2+} sensitivity associated with changes in myofilament lattice spacing, are not due to increased Ca^{2+} binding to TNC.

Tu-Pos309

SELECTIVE REMOVAL OF ACTIN FILAMENTS FROM MUSCLE BY A CLONED GELSOLIN FRAGMENT: IDENTIFICATION OF THIN FILAMENT PROTEINS AND EFFECTS ON SARCOMERE STRUCTURE. ((Granzier, H.L.M., Wright, J., and Wang, K. 1993)). Department of Chemistry, The Biochemical Institute, University of Texas at Austin, Austin, Texas 78712

The selective removal of actin filaments is a powerful approach to explore the functional and structural roles of actin in the muscle sarcomere. We have recently reported the mechanical properties of rabbit skeletal muscle and waterbug indirect flight muscle before and after the removal of actin filaments with a cloned gelsolin fragment (FX45) which does not require calcium for its actin-severing activity (Granzier and Wang, 1993.Biophy. Journal 65 *in press*). Gel electrophoresis showed that FX45 treatment extracted 80-90% of the actin, tropomyosin, troponin of rabbit psoas fibers within 6-7 hr of incubation. Confocal microscopy of rhodamine-phalloidin labeled fibers revealed that the extraction resistant actin was localized in the Z-line region. No other proteins, including titin and nebulin, were extracted by FX45. Similar analysis of Lethocerus flight muscle fibers indicated 80-90% of the actin, arthrin, tropomyosin and troponin were extracted in 2-3 hr. Additionally, an unidentified 100 Kd protein was also extracted and may represent a new thin filament protein. Electron micrographs of extracted fibers revealed that thin filaments of both psoas and insect fibers were removed from the I-band region and the overlap zone, as expected. A new dense zone appeared in the I-band of psoas fibers. We speculate that this zone represents coalesced material and that it underlies the increase in passive tension observed after thin filament removal from psoas fibers. Cross-sections through extracted psoas and insect fibers revealed bundling of the thick filaments. The high degree of order that is normally present in the A-band apparently requires the presence of thin filaments.

Tu-Pos310

Z-LINE PROTEINS DURING FAST-TO-SLOW SKELETAL MUSCLE TRANSFORMATION INDUCED BY CHRONIC ELECTRICAL STIMULATION. ((James C. Baldi[1], Prasarn Tangkawattana[2], Yasuhara Izumisawa[2], Mamoru Yamaguchi[2], and Peter J. Reiser[1,3])). [1]Exercise Science, [2]Veterinary Anatomy and Cellular Biology & [3]Oral Biology, The Ohio State University, Columbus, OH 43210.

Chronic electrical stimulation of rabbit fast tibialis anterior (TA) muscle results in increased Z-line width within the first three wks of stimulation (Salmons et al., J. Anat. 127:17-31, 1978; Eisenberg & Salmons, Cell Tissue Res. 220:429-471, 1981). We have found that the expression of several Z-line proteins, including desmin and vimentin, is altered during this period. The objectives of the present study are to quantify alterations in the expression of Z-line proteins following different periods of electrical stimulation and to determine their relationship to changes in Z-line width. The amount of desmin was normalized relative to actin in control and stimulated muscle samples run on SDS polyacrylamide gels. We find an ~10x increase in the relative amount of desmin after 3 wks of stimulation. Smaller, graded increases are found after 1 and 2 wks of stimulation. Vimentin is not detected in control TA on Coomassie Blue stained gels but is observed in 3 wk stimulated TA at a ratio of ~1:5 relative to desmin. These changes coincide with the shift in isoforms of α-actinin (another Z-line protein) in 3 wk stimulated muscle (Schachat et al., J. Biol. Chem. 263:13975-13978, 1988). Marked differences in myofibril organization including Z-line width also exist between the muscle midbelly and proximal or distal ends. Thus, it appears that each major protein component of Z-lines is up-regulated or changes its isoform expression during fast-to-slow transformation. Supported by NIH grant AR39652.

Tu-Pos311

SELECTIVE DISASSEMBLY OF SARCOMERIC STRUCTURES UPON REACTIVATION OF A TYROSINE KINASE IN QUAIL MYOTUBES. (Germana Falcone, M. Cristina Gauzzi, M. Teresa Ciotti*, Stefano Alemà and Loriana Castellani*). Istituto di Biologia Cellulare and *Istituto di Neurobiologia, C.N.R., 00137 Rome, Italy.

Avian myoblasts transformed by temperature-sensitive alleles of the tyrosine kinase encoded by the v-*src* oncogene ($pp60^{v\text{-}src}$) offer unique advantages to address questions concerning the regulatory mechanisms involved in the maintenance of the differentiated state. Upon shift to the permissive temperature, the reactivation of $pp60^{v\text{-}src}$ in post-mitotic myotubes is characterized by a number of striking alterations in the synthesis, turnover and supramolecular structure of muscle-specific gene products, leaving unaffected house-keeping gene products. Within 1 hour, specific antibodies or rho-phalloidin reveal the apperance in the myotubes of numerous "actin bodies", containing I-Z-I proteins such as α-actin, α-actinin and nebulin as well as adhesion plaque-associated proteins such as talin, and vinculin. Non-muscle cytoskeletal proteins are not affected. Within 12-24 hours, a sequential disassembly of sarcomeric A-band proteins such as skeletal myosin and titin also begins. Experiments on the dissection of the pathways downstream to $pp60^{v\text{-}src}$, by the use of dominant negative mutants of some members of the small GTP-binding protein family such as *ras* , *rac* and *rho* as well as specific inhibitors of PKC, will be discussed.

Supported by AIRC, Telethon, CNR-PF-Biotecnologie and ACRO.

Tu-Pos312

MYOSIN PHOSPHORYLATION, FILAMENT STRUCTURE AND ACTIVATION IN *LIMULUS* MUSCLE. ((J. Wray, I. Morano and R. Levine)) Dept. Biophysics, Max-Planck-Institut fur medizinische Forschung; II. Physiologisches Institut, University of Heidelberg; Heidelberg, FRG, & Dept. Anatomy & Neurobiology, Medical College of PA, Philadelphia, PA. 19129.

Biochemical, physiological and X-ray studies of several vertebrate and invertebrate striated muscles[1], and EM studies of their thick filaments[2], suggest that phosphorylation of myosin regulatory light chains (MRLCs) modulates crossbridge kinetics and disrupts the crossbridge order that is typical of the relaxed muscles. Here we show that in skinned *Limulus* fibers, X-ray reflections characteristic of relaxed thick filaments persist during and after full activation by Ca^{2+}, as previously observed in living muscles[3]. This persistence may indicate that the fraction of myosin heads involved in tension generation is smaller in *Limulus* than in some other muscles. The result, nevertheless, is unexpected if MRLC phosphorylation is required for activity[1] and causes loss of relaxed crossbridge order[2]. The extent of phosphorylation was significant even in relaxed *Limulus* fibers (having highly ordered thick filaments), and did not increase greatly or consistently during or after contraction (cf.[4]). Possibly, only higher levels of phosphorylation (both heads of each molecule) produce changes in crossbridge order. This and other explanations for our results are under study.

[1] Sellers, J. JBC 256:9274, '81; Wang et al. JBC 268:3776, '93; Sweeney & Stull, PNAS 87: 414, '90; Padron et al. J. Mus. Res. Cell Motil. 12: 235, '91. [2] Craig et al. JCB 105:1319, '87; Levine et al. JCB 113:563, '91; Biophys. J. 64:142a '93; [3] Maeda et al. ibid. 50:1035, '86; [4] Kerrick & Bolles, Pflug. Arch. 392:121, '81.

Tu-Pos313

NON-RIGOR CROSSBRIDGES IN SINGLE GLYCERINATED SKELETAL MUSCLE FIBERS PRODUCED BY NEAR STOICHIOMETRIC AMOUNTS OF PHOTO-RELEASED ATP. ((T. Yamada, S. Suzuki, H. Iwamoto, K. Wakabayashi[1], H. Wada, O. Abe and H. Sugi)) Dept. of Physiol., Sch. of Med., Teikyo Univ., Itabashi-ku, Tokyo 173 and [1]Dept. Biophys. Sci., Fac. of Engineer., Osaka Univ., Toyonaka, Osaka 560, JAPAN.

We studied crossbridge configurations in skeletal muscle fibers following photo-release of near stoichiometric amounts of ATP. Single muscle fibers of glycerinated rabbit psoas were first immersed in a rigor solution containing Ca^{2+} and caged ATP without ATP regenerating system. Then the fiber was put in air and light-flashed. When ATP of about half the concentration of myosin head in the fiber was photo-released, the fiber shortened by about 10 nm/half sarcomere in the unloaded condition, and stopped shortening as the released ATP was exhausted (Yamada et al., J. Physiol. 468, 229-243 (1993)). In the isometric condition, on the other hand, the fiber showed development of tension on release of ATP, the tension being maintained after exhaustion of released ATP. The intensity of [1,1] and [1,0] equatorial X-ray reflections from the fibers changed slightly following release of ATP. Conventional electronmicroscopic observation of the fibers fixed after release of ATP showed crossbridge configuration different from that of rigor fibers. These results indicate that a quasi-stable crossbridge configuration different from that of rigor is produced in the fibers following photo-release of near stoichiometric amount of ATP.

Tu-Pos314

COMPUTED VIBRATIONAL SPECTRA OF FILAMENTOUS ACTIN
((Monique M. Tirion and Daniel Ben Avraham)) Clarkson University, Physics Department, Potsdam, NY 13699-5820.

Atomic, three-dimensional models of f-actin permit quantitative assessments of the inherent flexibilities of the filament. Using a phenomenological model that reflects our limited knowledge of the exact orientation of the surface residues, we compute the vibrational modes inherent to f-actin. Considering only the long-lived, f-actin:ADP filament, we determine the complete eigenvalue spectrum of arbitrary-length filaments, restrained by fixed, periodic, or driven boundary conditions. We examine the comparative eigenvalue and eigenvector spectra of the original f-actin model (Holmes *et al.*, Nature, 1990), the Holmes' model with the 262-274 "plug" rebuilt, and the recent Lorentz model (JMB, 1993). We find that the plug and the reorientation of subdomain 2 significantly affect the vibrational spectra of the filament, which is largely dominated by sliding-type motion of the two long-pitched helices.

The dispersion relation is not linear, or Debye, in character, so that both very short and very long wavelength motions are "soft" or readily excitable. At very short wavelengths, angular twists about the filament axis are apparent. Summation over these modes can lead to apparent disordered motion. We extend our calculation to include the effects of internal flexibilities of the monomer (represented as the normal modes of g-actin:ADP:Ca^{++}) to the vibrational character of the filament.

Tu-Pos315

A MONTE CARLO SIMULATION SUGGESTS A MECHANISM FOR THE TRANSITION FROM ISOTROPIC TO BUNDLED ACTIN FILAMENTS .
((P.A. Dufort and C.J. Lumsden)) Department of Medicine, University of Toronto, Toronto, Canada, M5S 1A8. (Spon. by C.J. Lumsden)

The actin cytoskeleton and its associated regulatory proteins possess the ability to dynamically transform cytoskeletal structure and function in response to intra- and extracellular signaling events. We describe a Monte Carlo simulation suited to exploring this remodeling of actin cytogel structure following such signaling events. The new model simulates the diffusion and reaction of all of the cytoskeletal protein molecules and ligands included in our previous model (Dufort, P.A. and Lumsden, C.J. (1993) *Cell. Motil. Cytoskel.* 25:87-104) and extends the previous model by allowing filaments and cross-linkers to possess any orientation and to stretch and bend in response to applied forces. Molecular translation and rotation probabilities are derived in terms of molecular size, shape, and cytoplasmic viscosity and temperature, and reaction probabilities are specified in terms of experimentally determined rate constants. A simulation of actin filament network remodeling in response to changing levels of phosphatidylinositol bisphosphate (PIP_2), Ca^{2+} and cyclic AMP (cAMP) suggests a possible mechanism for the transformation between loose, isotropic actin filament networks and dense, parallel bundles of filaments. This transition has been observed in renal glomerulus mesangial cells exposed to high levels of glucose in cell culture (Whiteside, C.I, *et al.* (1993) *Am. J. Pathol.* 142:1641-1653). The results of the network to bundling simulation are being used to understand how the actin cytoskeleton participates in mesangial cell hypocontractility during exposure to high glucose levels.

Tu-Pos316

STRUCTURAL DYNAMICS OF F-ACTIN. ((A. Orlova and E.H. Egelman)) Department of Cell Biology and Neuroanatomy, University of Minnesota Medical School, Minneapolis, MN 55455.

We have shown that the structural basis for the destabilization of F-actin by phosphate release after ATP hydrolysis is the breaking of a longitudinal bond in the filament made by subdomain-2 (Orlova and Egelman, 1992, JMB **227**, 1043-1053), and also shown that removing all Ca^{2+} from actin, or modifying the nucleotide, results in a filament with a four-fold increase in flexibility (Orlova and Egelman, 1993, JMB **232**, 334-341). We have now extended these results on multiple conformational states of F-actin by studying the N- and C-terminal residues in actin. We have used antibodies to residues 1-7 in actin (Miller *et al.*, 1987, Biochemistry **26**, 6064-6070) and reconstructed in three-dimensions these decorated filaments from electron micrographs. The reconstruction shows that the antibody binds nearly orthogonal to the main myosin binding site on actin's subdomain-1. We have also used three-dimensional reconstructions and biochemical assays to show that the conformation of the C-terminus in F-actin is a function of the divalent cation bound at the high-affinity site. We find for F-actin the opposite pattern of proteolytic susceptibility as a function of bound cation found for G-actin (Strzelecka-Golaszewska *et al.*, 1993, Eur. J. Biochem. **211**, 731-742). Together, these results suggest that the actin filament may be more dynamic than previously believed, and that different conformational states may be regulated by cations and interactions with other proteins.

Tu-Pos317

GELSOLIN - A NEW TOOL TO STUDY DYNAMICS OF ACTIN.
((E. Prochniewicz, Q. Zhang, P. Janmey*, D.D. Thomas)) University of Minnesota; *Harvard Medical School.

Time-resolved phosphorescence anisotropy (TPA) of Cys-374-erythrosin-iodoacetamide labeled F-actin shows that actin filaments are rotationally mobile on the submillisecond time scale. Two alternative models of actin dynamics are rigid body diffusion and intrafilament rotation. To test the rigid body diffusion model, we examined the effects of filament shortening, using the actin-severing protein gelsolin. Shortening of actin filaments increased the observed rate of rotational motion, but this increase was much less than that predicted by the rigid body diffusion model. Glutaraldehyde crosslinking of short actin-gelsolin filaments decreased the rate of rotational motion but did not change filament length. Exchange of Br-ADP for actin-bound ADP increased the bending flexibility of the actin filament, but did not affect the TPA decay. Therefore, we conclude that TPA detects primarily length-dependent **rotational motions within the actin filament**, and these rotations occur primarily about the filament axis. Theoretical modeling suggests that these motions may include rotations of monomers, resulting in variable twist of the actin filament, but the detected motions are more complex than predicted by present models of twisting of a flexible rod.

Tu-Pos318

OBSERVATION OF THE KINETICS OF RHODAMINE PHALLOIDIN BINDING TO ACTIN IN RABBIT SKELETAL AND CARDIAC MYOFIBRILS. ((Xiaolei Ao & Sherwin S. Lehrer)). Boston Biomedical Research Institute, Boston MA, 02114.

Fluorescent phallotoxins bind to actin filaments in skeletal myofibrils in 2 processes, a immediate initial process to both filament ends and a slow process which results in uniform binding only after several hours (Szczesna & Lehrer, J.Musc.Res.Cell Motil., in press). To study the mechanism of the slow process, we imaged the fluorescence intensity distribution within each sarcomere with time after introduction of excess dye to intact and ghost (myosin depleted) fibrils attached to a microscope slide. For intact and ghost skeletal fibrils, after the fast initial process, rhodamine phalloidin slowly bound to actin unidirectionally, from the pointed ends toward the Z-line. Overnight preincubation with phalloidin or coumarin phallacidin resulted in fast uniform binding of added excess rhodamine phalloidin. Similar experiments with intact and ghost cardiac fibrils, in contrast, showed that the slow process was absent and that immediate uniform binding was observed with or without preincubation with phallatoxin. The most likely explanation for the inhibition of binding to the bulk of the actin filaments in skeletal fibrils is that the protein, nebulin, which is bound to actin filaments in skeletal fibrils but is absent in rabbit cardiac fibrils, competes with phalloidin for actin sites. Furthermore, the slow unidirectional binding process from the pointed end is consistent with a mechanism of cooperative competitive binding, i.e., phallotoxins "unzip" nebulin from actin. (Supported by NSF DMB 8817581 and NIH HL 22461).

Tu-Pos319

TWO-STRANDED F-ACTIN AND TROPOMYOSIN BINDING. **((R. Censullo)) Dept. of Physics, Univ. Alabama-Birmingham, Birmingham, AL 35294**

Depending on the relative strength of the diagonal bond versus the longitudinal bond in F-actin, the filament can either be considered to be a one-start, left-handed, genetic helix or two long-pitch, right-handed helices staggered axially by half a subunit. Observations from electron micrograph studies showing axial patterns in the crossover points of the two strands can be accounted for only if the two strands can vary in their relative azimuthal position (rotational offset). This indicates independent strand-based angular movement with very little intrastrand angular disorder. Additionally, interstrand-based actin angular flexibility is wholly consistent with seven concurrent equivalent interactions with the tropomyosin molecule in muscle thin filaments, along one actin strand at a filament radius of ~40 Å. Conversely, it can be shown via computer modelling, that only a small amount of cumulative angular disorder can exist for the diagonal bond that connects the actin monomers along the genetic helix and still make the same seven concurrent equivalent interactions with tropomyosin.

Tu-Pos320

THREE-DIMENSIONAL RECONSTRUCTION OF LIMULUS THIN FILAMENTS
((W. Lehman[1], R. Craig[2], and P. Vibert[3])) [1]Dept. of Physiology, Boston Univ. School of Medicine, Boston MA 02118; [2]Dept. of Cell Biology, Univ. of Massachusetts Medical School, Worcester, MA 01655; [3]Rosenstiel Center, Brandeis Univ., Waltham, MA 02254.

Three-dimensional helical reconstruction of negatively stained troponin-regulated Limulus thin filaments was performed on isolated (native) filaments maintained in EGTA in the "off-state" as well as on those in the Ca^{2+}-induced "on-state." Under both conditions, reconstructions reveal actin monomers whose bilobed shape and monomer-monomer connectivity are similar to those in reconstructions of vertebrate skeletal and smooth muscle thin filaments (Milligan et al., 1990; Vibert et al., 1993). In addition, a longitudinally continuous strand of density which follows the outer domain of successive actin monomers in EGTA and the inner domain in Ca^{2+} is observed; these strands presumably represent tropomyosin possibly in combination with troponin-T or other extended parts of the troponin complex. Statistical tests show that the Ca^{2+}-induced strand movement is significant at greater than the 95% confidence level. Our demonstration of Ca^{2+}-induced tropomyosin movement in a troponin-regulated system is consistent with a steric mechanism of inhibition of actomyosin ATPase in which tropomyosin in the "off-state" could interfere with the transition from weak to strong myosin-crossbridge binding on actin thereby inhibiting ATPase and crossbridge cycling, a mechanism predicted for but not yet demonstrated in skeletal muscle.

Tu-Pos321

REPTATION DYNAMICS OF SINGLE SEMIFLEXIBLE ACTIN FILAMENTS IN ENTANGLED ACTIN SOLUTIONS.
((J. Käs†, H. Strey‡, P. A. Janmey† and E. Sackmann‡)) †Div. of Experimental Medicine, Brigham and Womens Hospital, Harvard Medical School, Boston, MA 02115. ‡Technische Universität München, Physik Department, 85748 Garching, FRG. (Spon. by E. Sackmann)

The tube model and the concept of reptation are basic theories which explain the diffusion of a polymer in an entangled polymer solution. We report the first direct observation of the reptation dynamics of a single polymer. For this purpose we studied fluorescence labeled, single, semiflexible actin filaments (persistence length $L_p \approx 4$ μm) in entangled non-labeled actin solutions. From the restricted thermal undulations of these filaments we measured the diameter of the tube formed around a filament by the surrounding actin. The average diameter $\langle a \rangle$ agrees with previous mesh size measurements and scales with monomer concentration c_A as $\langle a \rangle \propto c_A^{-1/2}$. The reptation motion of the polymer was visualized by video microscopy. The chain self-diffusion coefficient $D_{||}$ along the tube was measured by analyzing the random walk of the fingering chain ends. The diffusion coefficient $D_{||}$ decreases approximately linear with the filament length L_C and the measured reptation time agrees well with rheological data.

Tu-Pos322

THE HYDROLYSIS OF ATP BY Mg-G-ACTIN IS STRONGLY STIMULATED BY INTERACTION WITH MYOSIN SUBFRAGMENT 1.
((Andrzej A. Kasprzak)) *CRBM-CNRS, INSERM-U.249, Univ. Montpellier I, Montpellier, France*

The interaction of myosin subfragment 1 (S1, isoenzyme A2) with Mg-G-actin has been studied. Polarization titrations of 1,5-IAEDANS-Mg-G-actin, and of ε-ATP-Mg-G-actin with S1 have provided evidence that, similarly to Ca-G-actin the proteins form a tight binary complex with a K_d of about 0.1 μM. Significant amounts of oligomeric forms of actin have not been detected either in the presence or in the absence of S1. The rate of *hydrolysis* of the actin-bound ATP in the G-acto-S1 complex has been measured using γ-^{32}P-labeled ATP. The rate of the nucleotide *release* from the complex has been measured for α-^{32}P-labeled ATP in the presence of a large excess of alkaline phosphatase. Comparison of both rates has indicated that the actin nucleotide is hydrolyzed much faster than it is released from the G-acto-S1 complex. Thus in the presence of S1 the hydrolysis is a relatively rapid reaction with $\tau_{1/2}$ of approx. 1 min. The effect is specific for Mg-G-actin and does not occur in Ca-G-actin. The importance of these findings for cellular regulation of actin polymerization is proposed.

Tu-Pos323

ELECTRODYNAMIC PROPERTIES OF ACTIN FILAMENTS IN SOLUTION. ((H.F. Cantiello and E.C. Lin)) Renal Unit, Massachusetts Gen. Hosp., Charlestown, MA 02129, and Dept. Med., Harvard Med. Sch..

Actin forms long linear polymers in solution. The polyelectrolytic state of actin may play an important role on the anomalous Donnan potential and non-ideal electro-osmotic behavior of the polymer in solution (Cantiello et al., BJ, 1991). A technique was developed to assess the ionic currents elicited by electrically-stimulated single actin filaments. Single, rhodamine-phalloidin labeled actin filaments were isolated with myosin-containing patch-pipettes connected to respective patch-clamp amplifiers, one to stimulate the actin filament and the other to collect current signals. Electrical measurements were conducted in both 1 and 100 mM KCl solutions. With two pipettes physically connected to an isolated actin filament, a 117% larger signal, 2.63 ± 0.1 vs. 5.7 ± 0.6 % (n=10, $p < 0.001$), was observed at the collecting pipette as compared to the unattached conditions. The electrical signals revealed the presence of significant non-linear wavetrains long after the input pulse had ended. The wave patterns observed in the electrically-stimulated actin filaments were remarkably similar to recorded solitary waveforms and solitons on electrically-stimulated non-linear transmission lines. In order for linear polyelectrolytes such as actin to behave as molecular wires, the radial dissipation of counterions about the polymer's surface has to be constrained, thus self-screening has to be postulated. Functionally, actin polymers may thus serve as biological "electrical" wires. The data are consistent with the hypothesis that actin filaments can support ionic movements in the form of non-linear electrical currents and thus demonstrate that actin filaments can function as biological "electrical" wires and can therefore be conceptualized as nonlinear inhomogeneous transmission lines. These ionic waves may play a role as a novel intracellular signal transduction mechanism.

Tu-Pos324

C-TERMINAL MODIFICATION OF ACTIN ALTERS ITS STRUCTURE AND FUNCTION. ((R.H. Crosbie[1], C. Miller[1], P. Cheung[1], T. Goodnight[1], A. Muhlrad[2], E. Reisler[1])) [1]Dept. of Chemistry and Biochemistry, UCLA, Los Angeles, CA 90024 [2]Hebrew University, Hadassah School of Dental Medicine, Dept. of Oral Biology, Jerusalem 91010, Israel

In this study, we use fluorescent probes and proteolytic digestions to demonstrate structural coupling between distant regions of actin. We show that modifications of Cys-374 in the C-terminus of actin slow the rate of nucleotide exchange in the nucleotide cleft. Conformational coupling between the C-terminus and the DNaseI loop in subdomain II is observed in proteolytic digestion experiments in which a new C-terminal cleavage site is exposed upon DNaseI binding. The functional consequences of C-terminal modification are evident from S-1 ATPase activity and the *in vitro* motility experiments with modified actins. Pyrene actin, labeled at Cys-374, activates S-1 ATPase activity only half as well as control actin. This reduction is attributed to a lower V_{max} value as the affinity of pyrene actin to S-1 is not significantly altered. The *in vitro* sliding velocity of pyrene actin is also decreased. However, IAEDANS labeled actin (also at Cys-374) enhances the V_{max} of S-1 ATPase activity and the *in vitro* velocity by approximately 25%. These results are discussed in terms of conformational coupling between distant regions in actin and the effects of Cys-374 modification on actin function.

Tu-Pos325

CONFORMATIONAL CHANGES IN SUBDOMAIN 2 OF ACTIN REPORTED BY DANSYL ETHYLENEDIAMINE AT GLN-41.
((E. Kim, A. Muhlrad, and E. Reisler)) Dept. of Chem. & Biochem. and the Molec Biol Inst-UCLA, L.A., CA 90024.

A fluorescent probe dansyl ethylenediamine (DED) was attached with high specificity to Gln-41 on G-actin via the transglutaminase reaction (Takashi, R., Biochemistry 27, 938 [1988]). The quantum yields and λ_{max} of DED emission depended strongly on the divalent cation and nucleotide present in G-actin. λ_{max} values were 536, 511, and 507nm for G-actins in the Ca-ATP, Mg-ATP, and Mg-ADP forms respectively; the quantum yields of these actins increased in that order. Polymerization of actin by $MgCl_2$ and $CaCl_2$ induced spectral shifts and increases in quantum yield showing changes in probe environment. Spectral differences between different F-actins were much smaller than between G-actins. Fluorescence spectra obtained upon excitation of labeled actin at 295nm showed energy transfer from Trp to DED with an efficiency F-actin > G-actin (Mg-ADP > Mg-ATP > Ca-ATP). These results are discussed in terms of structural changes and flexibility in subdomain 2 of actin.

Tu-Pos326

EVIDENCE FOR AN ACTIN NUCLEATING FACTOR ((Lynn A. Selden[1], Lewis C. Gershman[1†‡], and James E. Estes[1†])) [1]Research and [†]Medical Services, Department of Veterans Affairs Medical Center, Albany, NY 12208 and Departments of [‡]Medicine and [1]Physiology and Cell Biology, Albany Medical College, Albany, NY 12208.

We recently observed that column purification of rabbit skeletal muscle actin on Sephacryl S-300 yields fractions from the leading edge of the actin peak which polymerize (nucleate) faster than later fractions in the peak. A more extensive analysis of the column fractions revealed a broad peak of "actin nucleating factor" (ANF) with a maximum just preceding the actin peak. Though we cannot yet quantitate ANF, and the activity varies with the preparation, a typical mid-peak column fraction of ANF mixed 1:50 with 1 μM Mg-ATP-actin roughly doubles the nucleation rate. We have succeeded in enrichment of ANF activity to some extent by modifying preparation procedures. ANF appears to be much more effective with Mg-actin than Ca-actin, possibly due to differential binding to the two types of actin and/or to their different intrinsic nucleation rates. ANF is preserved on freezing and destroyed by incubation with 1 mM EGTA (in the absence of $MgCl_2$) or on heating to 100 °C for 5 minutes, suggesting that ANF may be a protein. If so, the elution profile suggests a molecular weight on the order of 150 KD. Coomassie Blue-stained and silver-stained SDS-PAGE gels show several weak bands in the 150 KD region which are potential candidates for ANF. ANF enhances actin nucleation at very low concentrations without increasing the actin critical concentration; this suggests that it may be a high-affinity actin-binding protein which stabilizes nucleation without blocking barbed-end growth. (This work was supported by the Department of Veterans Affairs).

Tu-Pos327

VISCOELASTIC PARAMETERS FOR GELSOLIN LENGTH REGULATED ACTIN FILAMENTS. ((Jeffrey Haskell[†], Jay Newman[†], Lynn A. Selden[§], Lewis C. Gershman[§¶‡], and James E. Estes[§¶])) [†]Department of Physics, Union College, Schenectady, NY 12309, [§]Research and [‡]Medical Services, Department of Veterans Affairs Medical Center, Albany, NY 12208 and Departments of [‡]Medicine and [¶]Physiology and Cell Biology, Albany Medical College, Albany, NY 12208.

Dynamic viscoelastic parameters G′ and G″ were determined for F-actin samples whose mean polymer lengths were regulated using gelsolin to be between 10-mers and 1000-mers. Column purified Mg-actin samples at a concentration of 10μM were polymerized for 15 minutes with 150 mM KCl and 2 mM $MgCl_2$, after which 0.2 mM $CaCl_2$ and 0.01 to 1.0 μM gelsolin were added. Samples were then placed in a Rheometrics RFS2 cone and plate rheometer and monitored by repeated low shear experiments at a frequency of 1 rad/sec for about 30 minutes until a plateau was reached. A series of frequency and strain sweeps were then carried out with strains varying between 1% and 200%. We find that below a frequency of about 1 rad/sec there is little length dependence of G′ or G″ (with values of ~ 2-4 dynes/cm^2), although the ratio of G″/G′ does increase by about 50% as the mean filament length increases. At higher frequencies (up to 100 rad/sec), there is a more pronounced length dependence, with G″ increasing an order of magnitude more for the longer than the shorter length samples and the ratio of G″/G′ having a maximum as a function of frequency. This maximum occurs, independent of filament length, at about 50 rad/sec at 8% strain and shifts to about 20 rad/sec at 200% strain. (This work was supported by NSF grant DMB 8905906 to JN and the Department of Veterans Affairs).

CALDESMON AND CALPONIN

Tu-Pos328

FUNCTIONAL STUDIES ON RECOMBINANT FULL LENGTH AND MUTANT SMOOTH MUSCLE CALDESMONS EXPRESSED IN A BACULOVIRUS SYSTEM. ((Z. Wang, K.Y. Horiuchi, S. Jacob, and S. Chacko)) Department of Pathobiology, University of Pennsylvania, Philadelphia, PA 19104.

Recombinant full length caldesmon (PvlCaD) and a mutant, with a deletion of 39 amino acid residues from the carboxyl terminus, were constructed using PCR-cloning strategy and introduced into Baculovirus vectors. These recombinant Baculoviruses were made by co-transfection of the Baculovirus vectors into Sf9 cells with wild-type Baculovirus. The recombinant caldesmons were produced in very high levels as cytoplasmic proteins in Sf9 cells. Both full length and mutant caldesmons were heat-stable and could be purified in high yields using conventional methods. The full length caldesmon bound to actin, tropomyosin, tropomyosin-actin, myosin, and calmodulin as did the native caldesmon purified from chicken gizzard. The level of inhibition of the acto-myosin ATPase activity by PvlCaD was similar to that caused by the native caldesmon. Deletion of 39 amino acids from the carboxyl terminus of the PvlCaD lowered its abilities to bind to actin and to inhibit the actin-activated ATPase activity of smooth muscle myosin. Moreover, the amplification of caldesmon-induced inhibition observed in the presence of tropomyosin was also absent when the mutant caldesmon was used to inhibit the actin-activated ATPase activity. Supported by NIH grants DK39740, DK47514, and DK44689.

Tu-Pos329

ROLE OF CALTROPIN IN CALDESMON-HEAVY MEROMYOSIN INTERACTION. ((Rajam S. Mani and Cyril M. Kay)) MRC Group in Protein Structure & Function, Department of Biochemistry, University of Alberta, Edmonton, T6G 2H7, Canada.

The binding of chicken gizzard caldesmon to smooth muscle heavy meromyosin (HMM) was studied using caldesmon-sepharose 4B affinity chromatography, far-ultraviolet circular dichroism (CD) and the fluorescent probe acrylodan. When HMM was applied to a caldesmon-sepharose column in the presence of 40mM NaCl, most of the protein was retained on the column, and HMM could be eluted by increasing the NaCl level to 0.5M; this interaction was not Ca^{2+} dependent. Far-UV CD studies indicated an interaction between caldesmon and HMM and this interaction was not Ca^{2+} sensitive. Addition of HMM to a caldesmon-caltropin complex induced a conformational change suggesting the formation of a ternary complex for which Ca^{2+} was essential. Acrylodan-labelled caldesmon, when excited at 375 nm had an emission maximum at 515 nm. Addition of HMM resulted in a nearly 20% decrease in fluorescence intensity with little or no shift in the emission maximum. Titration of HMM with labelled caldesmon indicated a strong affinity for HMM [K_a was in the order of $(4.5 \pm 0.5) \times 10^7$ M^{-1}] and this interaction was observed both in the presence and in the absence of calcium. When HMM was titrated with labelled caldesmon in the presence of caltropin in a 0.2 mM Ca^{2+} medium, its affinity for caldesmon was lowered nearly 3 fold [$K_a \approx (1.5 \pm 0.5) \times 10^7$ M^{-1}]. Caltropin, which is very potent in reversing the inhibitory effect of caldesmon in the presence of calcium is also able to modulate the interaction between caldesmon and smooth muscle heavy meromyosin, thus making it a potential calcium factor in regulating caldesmon in smooth muscle.

Tu-Pos330

INTERACTION BETWEEN CALTROPIN AND THE C-TERMINAL FRAGMENT OF SMOOTH MUSCLE CALDESMON. ((Shaobin Zhuang[2], Rajam S. Mani[1], Cyril M. Kay[1], and C.-L. Albert Wang[2])) [1]M.R.C. Group in Protein Structure and Function, Dept. of Biochemistry, University of Alberta, Edmonton, T6G 2H7, Canada, and [2]Dept. of Muscle Research, Boston Biomedical Research Institute, Boston, MA 02114. (Spon. by B. Chakrabarti)

Caltropin (CaT) is a Ca^{2+}-binding protein recently purified from chicken gizzard (Mani and Kay, Biochemistry **29**, 1398-1404, 1990). Previous work showed that CaT interacts with caldesmon (CaD) in a Ca^{2+}-dependent manner with an affinity that is higher than that between CaD and calmodulin (CaM). To further characterize the CaD-CaT interactions, we have tried to photo-crosslink CaT with a benzophenone-labeled C-terminal fragment (27K) of chicken gizzard CaD. After brief photolysis, there was clearly appearance of an additional protein band that migrated on the SDS gel with an apparent molecular weight of ~35 kDa, corresponding to the 1:1 adduct between CaT and 27K. The reaction was Ca^{2+}-dependent; in the absence of Ca^{2+}, no crosslinking was obtained. This result was very similar to that obtained with CaM and the CaD fragment. We have also tested the ability of CaT to interact with the synthetic CaM-binding peptide (GS17C) of CaD. It was found that in the presence of CaT, the apparent affinity of GS17C for CaM was much decreased compared to the case where CaT was not present, suggesting that CaT indeed competes with CaM for binding to GS17C. In contrast to CaM, however, CaT alone did not induce any change in the tryptophan fluorescence intensity of the peptide. Thus although the two Ca^{2+}-binding proteins behave quite similarly, there are some differences in their interactions with CaD. Supported by grants from NIH.

Tu-Pos331

SMOOTH-MUSCLE CASEIN KINASE II: PHOSPHORYLATION OF CALDESMON. ((M.P. Walsh and C. Sutherland)) Department of Medical Biochemistry, University of Calgary, Alberta, Canada T2N 4N1.

A caldesmon kinase activity was partially purified from chicken gizzard and identified as casein kinase II by Western blotting; the smooth muscle enzyme consisted of subunits of 43 (α), 39 (α') and 27 kDa (β). Phosphorylation of caldesmon and casein by smooth-muscle casein kinase II was optimal at ~0.1 M NaCl, did not require second messengers, and was inhibited by heparin. The kinase utilized either GTP or ATP as a substrate. Caldesmon was phosphorylated to ~ 1 mol P/mol with a K_m for caldesmon of 4.9 μM. Phosphate incorporation into both serine and threonine occurred with two principal sites of phosphorylation : ser 73 and thr 83. Four synthetic peptides corresponding to this domain of caldesmon were examined as substrates of casein kinase II : A = RRREVNAQNSVAEEE; B = AQNSVAEEE; C = RSTDDEAA; D = SVAEEETKRSTDDE. Only C and D were phosphorylated and both only at threonine. Phosphorylation of intact caldesmon had no effect on the binding of caldesmon to actin or on the caldesmon-mediated inhibition of actomyosin MgATPase activity but completely abolished the interaction of caldesmon with smooth-muscle myosin consistent with localization of the myosin-binding domain near the *N*-terminus of caldesmon and of the actin-binding domain near the *C*-terminus. Casein kinase II may therefore play a role in regulating caldesmon-myosin interaction and the ability of caldesmon to cross-link actin and myosin filaments in smooth muscle.

Tu-Pos332

MONOCLONAL ANTIBODY AGAINST THE CENTRAL REGION OF SMOOTH MUSCLE CALDESMON. ((Yanhua Li, Katsuhide Mabuchi and C.-L. Albert Wang)) Dept. of Muscle Research, Boston Biomedical Research Institute, Boston, MA 02114. (Spon. by P. Graceffa)

Smooth muscle caldesmon contains 10 repeats of a highly charged sequence in the middle portion of the molecule, which is deleted in the non-muscle isoform by alternative splicing. This segment forms a long helix that separates the two end domains of caldesmon. While the functional significance of such a spacer remains to be understood, its unique presence in the smooth muscle form, but not in the non-muscle form, makes it an ideal candidate to produce specific antibodies for distinguishing the two isoforms. The antigenicity of the middle portion, however, seems to be very low, as reflected by the fact that none of the known anti-caldesmon antibodies available to date bind to the central region of the molecule. To generate anti-central antibodies, we have used as an immunogen a 57-residue synthetic peptide corresponding to the sequence of this region (from Glu-268 to Glu-324, see accompanied abstract). After fusion the hybridoma cells were screened with both the synthetic peptide and native caldesmon. We have obtained a clone producing antibody (CD7) that reacted very strongly with chicken gizzard caldesmon; it reacted much more weakly on dot blots with caldesmon prepared from chicken liver. Both Western blots and examination of chicken gizzard section by fluorescent immunocytochemistry confirmed that the reactivity of CD7 toward the short, hepatic caldesmon was very weak, if any at all. Rotary shadowed electron microscopic images showed that CD7 indeed binds to gizzard caldesmon at the middle point of the molecule. We are currently investigating the effect of CD7 on various biochemical properties of caldesmon. Supported by NIH (AR-41637).

Tu-Pos333

CIRCULAR DICHROISM STUDIES OF HELICAL PEPTIDES OF SMOOTH MUSCLE CALDESMON. ((Enzhong Wang and C.-L. Albert Wang)) Dept. of Muscle Research, Boston Biomedical Research Institute, Boston, MA 02114.

The central region of smooth muscle caldesmon contains up to 10 repeats of a 13-residue motif that shows no sequence homology with any known proteins. This region, spliced out in the non-muscle isoform, was predicted to have a very strong α-helical propensity. A 258-residue chymotryptic fragment (CT54) encompassing this repeating region indeed exhibits a relatively high (~60%) α-helical content, which was best explained by a model that involves a single helix stabilized by numerous salt bridges between charged residues at positions i and i+4 (Wang, C.-L.A., Chalovich, J.M., Graceffa, P., Lu, R.C., Mabuchi, K. and Stafford, W.F., J. Biol. Chem. **266**, 13958-13963, 1991). To verify this hypothesis, we have synthesized peptides corresponding to this region (EE60C, from Glu-268 to Glu-324, and EA25C, from Glu-311 to Ala-332), and studied their secondary structures by circular dichroism. As in the case of CT54, we find that in aqueous solution these synthetic peptides assume an α-helical conformation that is stable over a wide range of salt concentration and pH. The helical structure unfolds gradually over a wide temperature range in a reversible fashion. Addition of 2,2,2-trifluoroethanol increases the helical content to nearly 100%, and the secondary structure is clearly better stabilized in longer peptides. Most significantly, scrambled sequences that are unable to form i to i+4 salt bridges have much less helicity, and unfold at lower temperatures, suggesting that the postulated salt bridges are indeed an important determinant for the secondary structure in this region of caldesmon. Supported by grants from NIH (HL-41411 and AR-41637).

Tu-Pos334

IMMUNOELECTRON MICROSCOPIC STUDIES OF LOCALIZATION OF CALDESMON AND CALPONIN IN CHICKEN GIZZARD. ((Katsuhide Mabuchi)) Dept. of Muscle Research, Boston Biomedical Research Institute, Boston, MA 02114

The distribution patterns of caldesmon (CaD) and calponin (CaN) in chicken gizzard were examined with anti-CaD (rabbit polyclonal) and anti-CaN (mouse monoclonal, Sigma C-6047; rabbit polyclonal, a gift of Dr. K. Takahashi). The antibodies were visualized by the indirect immunoglod method (colloidal gold-conjugated anti-antibodies were from Sigma and Electron Microscopy Sciences). In general the two distribution patterns were different although there were areas where they overlapped. Neither matched the pattern of anti-tropomyosin (rabbit polyclonal, Sigma T-3651) or of anti-desmin (rabbit polyclonal, Sigma D-8281). A significant number of anti-CaN, but not of anti-CaD associated with dense bodies (DB: fusiform densities and attachment plaques) which were identifiable with anti-actinin (mouse monoclonal, Sigma A-5044). However, many anti-CaN were also observed in areas where DBs were absent. The localization CaD and CaN were also examined with fluorescent immunocytochemistry. The distribution of these two proteins overlapped with that of actin filaments with a minor discrepancy. These observation indicate that there are three-dimentional actin-based filamentous networks, with which CaD and CaN associate somehow differently (Supported by grants from NIH).

Tu-Pos335

MAPPING THE C-TERMINUS OF CALDESMON FOR ACTIN, TROPOMYOSIN AND MYOSIN INTERACTION

((P.A.J. Huber, I.D.C. Fraser, *D.A. Slatter, *B.A. Levine and S.B. Marston))
Dept. Cardiac Medicine, NHLI, Dovehouse St. London SW3 6LY, UK,
*University of Birmingham, Edgbaston, Birmingham B15 2TT, UK

A cDNA clone coding for the C-terminal 33kDa fragment (H1) equivalent to amino acids 506-793 of human caldesmon (Humphrey et al. 1992. Gene 112:197) was used to construct and express 6 subfragments (H2 - H9). The fragments range from 6.7 to 20 kDa and represent regions of domains 3, 4a and 4b (Marston and Redwood, 1991, Biochem. J. 279:1). They were tested in order to map the interaction sites of caldesmon with actin, tropomyosin and myosin. H9 (726-793), H7 (622-767) and H2 (683-767) showed an affinity to actin only one order of magnitude less than H1 or full length caldesmon, ($k_d \geq 10^7 M^{-1}$). No binding to actin was exhibited by the fragments H6 (506-626), H3 (506-566) and H4 (622-680), whereas weak interaction was found in H5 (506-680). This suggests that the actin affinity of caldesmon consists of at least two distinct sites, one in domain 4a (625-714) and one in domain 4b (715-793). Actin titration broadened nmr signals of trp 749 and 779, val 721 and met 715 in a 10 kDa C-terminal fragment of chicken gizzard caldesmon. No signal change was found on titration with a 28 aa N-terminal actin peptide. H6, representing the troponin-T like sequence increased the fluorescence of pyrene maleimide labeled tropomyosin only slightly (by 7%). 10-15% fluorescence increase was observed on titration with H2, H4, H5 and H7. H9 did not react with tropomyosin. This suggests that tropomyosin binding is located in the region of domain 4a – very close to the actin interaction sites. The strong myosin binding site found in H1 ($k_d \geq 10^6 M^{-1}$) was not found to be represented by any of the expressed subfragments and therefore seems to involve more than one distinct site.

Tu-Pos336

MECHANISM OF CALDESMON-TROPOMYOSIN REGULATION OF THE STRONG ACTOMYOSIN INTERACTION ((S.B. Marston, I.D.C. Fraser, and P.A.J. Huber))
Dept Cardiac Medicine, NHLI, Dovehouse St., LONDON, SW3 6LY, UK.

We have demonstrated that caldesmon does not alter the affinity of weak binding actomyosin complexes when it inhibits actin-tropomyosin activation at physiological ratios (1 per 14 actins) and we proposed that it acts upon the strong binding complexes, in the same way that troponin-tropomyosin does. This was confirmed by measurements of the binding of [14C]-labelled S1.ADP (a strong complex) to smooth muscle actin-tropomyosin in 0.12M KCl, 30oC. Binding was not co-operative and Kd was 0.56 μM. Addition of inhibitory amounts of caldesmon strongly inhibited S1.ADP binding at low S1:Actin ratios (Kd at [S1] < 0.1μM ≥ 6μM) and the binding curve was highly co-operative. The C terminal 150 amino acids of gizzard caldesmon (domain 4) has the same effect. In order to define the mechanism precisely we expressed recombinant human caldesmon peptides corresponding to the N terminal 3/4 (H7, aa622-767), the C terminal half (H9, aa 726-793) and the middle half (H2, aa683-767) of domain 4. Both H7 and H9 are tropomyosin-dependent, Ca-calmodulin regulated inhibitors of actin activation. However H2, which contains the sequence common to H7 and H9, binds to actin and calmodulin but does not inhibit. This suggests that H2 contains the sequence essential for tropomyosin-dependent inhibition but requires flanking sequence on *either* side to attain its inhibitory structure. We investigated the effect of H2 upon caldesmon inhibition. At low ionic strength low concentrations of H2 reversed the inhibition of caldesmon, H7 and H9 in the presence of tropomyosin although in the absence of tropomyosin it had no effect. In fact when the ATPase of actin-tropomyosin was lower than that of actin (tropomyosin in "off" state), H2 potentiated the ATPase up to three fold. We suggest that H2 can switch actin-tropomyosin to the "on" state whilst caldesmon and the fragments H9 and H7 switch actin-tropomyosin to the "off" state.

Tu-Pos337

CALDESMON ISOFORMS IN SMOOTH MUSCLE CELLS IN INTIMAL PROLIFERATION AND ATHEROSCLEROSIS. ((J. Reckless, K. Pritchard, S.B. Marston)) Dept. of Cardiac Medicine, NHLI, Dovehouse St., London SW3 6LY, UK.

Caldesmon ("CD") isoforms exist in two size classes, "CD_s" and "CD_f". We investigated CD isoforms in healthy smooth muscle, in a model of arterial intimal thickening, in human atherosclerosis and in cultured cells.

Rabbit carotid arteries contained 245 ± 6 nmol/g-tissue protein of CD_s and 68 ± 4 nmol/g-tissue protein of CD_f. This corresponds to 1 mol CD_s per 24 actin monomers. Arteries thus contain sufficient CD to regulate F-actin. The ratio of CD_s:CD in rabbit arteries or stomach was 79:11; in sheep aortas CD_s:CD_f = 85:15. Induction of intimal thickening in carotid arteries was followed by the loss of 44% of CD_s at 4d, when histological changes were not apparent. As intimal thickening developed, CD_s fell to 90 ± 18 nmol/g-tissue at 10d, with little further change by 28d. This is consistent with phenotypic change in most medial s.m.c.'s preceding migration and/or proliferation. CD_f levels passed through a peak of 128 ± 6 nmol/g-tissue around 14d when intimal thickening was maximal.

In human arteries showing intimal thickening CD_s-specific immunofluorescence (IF) was strong in all medial s.m.c.'s but less strong in the intima, decreasing towards the lumen. CD_f-specific IF was weak across the wall. Beneath advanced atherosclerotic plaques, CD_s-specific IF in medial s.m.c.'s was weak except in the outermost layers, although the cells appeared normal. Weak CD_s IF was seen in scattered cells in the plaque cap, but cap cells were readily visualized by CD_f-specific serum.

Passaged rabbit aortic s.m.c.'s had much more CD_f than CD_s. In cultured human s.m.c.'s CD_s-specific antibodies revealed a phenotypic heterogeneity that was not seen when antibodies to α-smooth muscle actin were used. Most passaged cells were CD_s-negative but all appeared CD_f-positive.

Tu-Pos338

DIFFERENTIAL mRNA SPLICING CONTROLS CALDESMON ISOFORM EXPRESSION. ((A.M. Payne-Fergar, P. Yue, K. Pritchard and S.B. Marston)) Dept Cardiac Medicine, NHLI, Dovehouse St., LONDON SW3 6LY.

SDS-PAGE and Western blots show three isoforms of caldesmon in all the species we have examined. One is the 80kD non-muscle isoform (CDl), the other two migrate close together, around 120kD (CDh), and are expressed in contractile smooth muscle cells. Hayashi et al. (PNAS 89, 12122, 1992) has shown that the various isoforms may be derived from differential splicing of mRNA transcribed from a single gene. The large isoforms contain exons 1',2,3a,3b,5 to 13, the small isoform contains exons 1',2,3a,5 to 13, exon 4 is present in some isoforms. Hayashi also found evidence for the substitution of the first exon (exon 1') for an alternative exon 1 in the mRNA of some cell lines. mRNA isoform expression was detected using RT-PCR in various tissues from human, rabbit and sheep using primers that amplify exons 1,1',3a,3b and 4. To date CDh with and without exon 4, and CDl without exon 4 have been detected in most tissues from all the species tested. CDl with exon 4 has only been detected on amplification of cDNA clones from a human aorta lambda gt10 library. Exon 1 has not been detected in any sample .The two 120kD CDh isoforms , present in equal amounts in vascular tissue, can be separated on 6% SDS-PAGE gels. Both CDh bands are anti-exon 4 serum immunoreactive and therefore do not correspond to CDh +/- exon 4. Depletive immunoprecipitation with anti-exon 4 serum shows there to be two bands that do not contain exon 4 migrating at the same position as the two bands which do contain exon 4. 2D PAGE has shown there to be 4 major and 2 minor CDh spots. RT-PCR has excluded the possibility of differences occuring within and around exons 2,3a and 5 to 13. It is possible that the 2 CDh isoforms seen on SDS-PAGE have different first exons the sequences of which are yet to be determined or are differentially post-translationally modified, as well as differing in their inclusion of exon 4.

Tu-Pos339

KINETICS OF BINDING OF CALDESMON TO ACTIN. ((Joseph M. Chalovich & Hai Luo)) Dept. of Biochemistry; East Carolina University School of Medicine; Greenville, NC 27858-4354

Knowledge of the kinetics of caldesmon binding to actin is important for understanding the function of caldesmon and for testing models of inhibition of actomyosin ATPase activity by caldesmon. Several fluorescent probes have been placed on actin and caldesmon to monitor actin-caldesmon binding. The fluorescence of an IANBD probe placed in the actin binding region of caldesmon increases by 70% upon binding to actin. The addition of rigor S-1 to actin-caldesmon reverses the increase in fluorescence seen when caldesmon binds to actin; the addition of ATP restores the fluorescence as S-1 disassociates from actin. The fluorescence of IANBD caldesmon changes only slightly upon binding to myosin or to tropomyosin in the absence of actin. Unfortunately, the fluorescence change of this probe does not vary linearly with the fraction of caldesmon bound to actin. A linear signal was obtained by quenching the fluorescence of acrylodan actin with the IANBD probe on caldesmon. The apparent rate of association at 15°C and 50 mM ionic strength increased in a biphasic manner with the free caldesmon concentration, indicating at least a two step binding process. The maximum observed rate of association is about 900/sec in both the presence and absence of tropomyosin. The observed rate of disassociation was also measured and found to be slower in the presence of smooth muscle tropomyosin.

Tu-Pos340

CALPONIN PHOSPHORYLATION STOICHIOMETRY IN INTACT SMOOTH MUSCLE. ((J. Pohl and W.T. Gerthoffer)) Department of Pharmacology, University of Nevada School of Medicine, Reno, NV 89557.

In intact canine tracheal and colonic smooth muscles, we find that ^{32}P incorporation into calponin increases transiently in response to muscarinic stimulation. To evaluate the functional significance of this observation we determined the stoichiometry of calponin phosphorylation in canine tracheal smooth muscle strips radiolabeled with ^{32}Pi (150 - 200 μCi/ml) and stimulated with 1 μM carbachol for 30 sec, 1 min or 5 min. Specific activity of ^{32}P-ATP formed *in vivo* was estimated from ^{32}P incorporation into monophosphorylated 20 kDa myosin light chains. Unphosphorylated and monophosphorylated light chains were isolated by glycerol-acrylamide gel electrophoresis and Western blotting. Calponin was isolated by nonequilibrium pH gel electrophoresis (NEPHGE). Calponin content was determined by densitometry of gels stained with Coomassie Blue using purified chicken gizzard calponin as a standard. Calponin phosphorylation (moles Pi/mole protein) increased from basal levels of 0.46 $\pm$ 0.11 to 1.1 $\pm$ 0.4 within 30 sec. Phosphorylation then declined to 0.57 $\pm$ 0.13 at 1 min and 0.60 $\pm$ 0.09 at 5 min (N = 5). Analysis of calponin isoforms on NEPHGE gels also showed a shift to more acidic isoforms during contraction. The results are similar to previous results showing calponin phosphorylation during tracheal smooth muscle contraction. Supported by NIH (HL48183) and the Pharmaceutical Manufacturers Assoc. Foundation (J.P.).

Tu-Pos341

EFFECTS OF PHOSPHORYLATION OF CALPONIN AND CALDESMON ON ACTIN SLIDING VELOCITY. ((W.T. Gerthoffer, and J.R. Sellers)) Dept. of Pharmacology, Univ. Nevada School of Medicine, Reno, NV 89557 and NHLBI, NIH, Bethesda, MD 20892.

To test the hypothesis that phosphorylation/dephosphorylation of calponin and caldesmon is important in regulating the crossbridge cycle in smooth muscle, actin sliding velocity was measured using an *in vitro* motility assay. Control sliding velocity was determined using phosphorylated turkey gizzard myosin, 1 μM gizzard tropomyosin, 20 mM KCl, 0.7% methylcellulose and 50 mM dithiotrheitol. Unphosphorylated gizzard caldesmon (0.3, 1 and 3 μM) significantly reduced mean sliding velocity. Velocity in the presence of caldesmon phosphorylated to 0.7 moles Pi/mole protein with p44 MAP kinase (UBI, Inc.) was not different from control. One-dimensional peptide mapping of phosphorylated caldesmon produced one major phosphopeptide and several minor bands. Calponin was phosphorylated with protein kinase C to 1.6 moles Pi/mole protein. Calponin (2 μM) caused a profound inhibition of actin sliding with very few filaments moving. In the presence of phosphorylated calponin, velocity was slightly greater than control with nearly all filaments moving. Phosphorylation of calponin also reduced actin binding in a sedimentation assay. The results are consistent with a model of contractile system regulation in smooth muscles in which phosphorylation of both calponin and caldesmon reverses the inhibitory effects of these proteins on crossbridge cycling. Supported by NIH grants DK41315 and HL48183.

Tu-Pos342

UTILITY OF CALPONIN FRAGMENTS TO MAP DOMAINS OF INTERACTION WITH CALCIUM BINDING PROTEINS. ((Fiona L. Wills[1] William D. McCubbin[1] Mario Gimona[2] Peter Strasser[2] and Cyril M. Kay[1])) [1]Dept. of Biochem. MRC Group in Protein Structure & Function, University of Alberta, T6G 2H7, & [2]Institute of Molecular Biology, Austrian Academy of Sciences, A-5020 Salzburg, Billrothstrasse 11, Austria.

Native calponin is able to bind 2 mols of calcium binding protein (CaBP) per mol calponin suggesting 2 distinct sites of interaction. In order to delineate these sites, fragments of calponin have been studied. One fragment comprising residues 2-51 was isolated from a CNBr cleavage of calponin. This amino terminal fragment possesses 1 tryptophan which can be used to monitor interactions. 2-51 interacts with 1 mol of either calmodulin, S-100b or caltropin producing unique fluorescence effects in each case. This is the first example of a differentiation between the interaction of S-100b and caltropin with calponin. The titration of 2-51 with calmodulin and S-100b show both proteins interact with a Kd of 1uM, suggesting this is the low affinity site and does not have selective affinities for different CaBPs. Also, a carboxyl terminal truncated mutant of calponin comprising residues 1-228 has been produced by recombinant techniques. This 1-228 fragment has 2 tryptophans which can be used to monitor interactions with CaBPs. Analytical ultracentrifugation has shown 1-228 is able to bind 2 mols of CaBP per mol of 1-228 in a Ca^{2+} dependent fashion, indicating there is a 2nd site of interaction between residues 52-228. Studies of the tryptophan fluorescence of this fragment again showed a differentiation between the effect of different CaBPs upon the quantum yield and peak wavelength of the spectra. Temperature denaturation of this C-terminal truncated fragment has been compared to the denaturation of whole calponin. These results show that the C-terminal region does not change the temperature at which calponin melts; however there is greater residual secondary structure with whole calponin vs. the fragment. The two identified sites of interaction correspond to two exposed segments of calponin as predicted by surface plot analysis.

Tu-Pos343

ABSENCE OF CALPONIN PHOSPHORYLATION IN RESTING AND CONTRACTED PORCINE CAROTID ARTERIES. ((L.P. Adam, J.R. Haeberle# and D.R. Hathaway)) Krannert Institute of Cardiology, Indiana University, Indianapolis, Indiana, and #University of Vermont, Burlington, Vermont.

Calponin is an abundant thin filament-associated protein in smooth muscle that may modulate contraction. Calponin inhibits actomyosin ATPase activity and actin filament movement in motility assays, and these effects can be reversed by phosphorylation. It has been postulated that phosphorylation is a switch that regulates calponin function. However, it has not been firmly established that calponin is phosphorylated to significant stoichiometries in intact tissue under physiological conditions. To address this problem, we have purified both calponin and caldesmon from the same muscle stips that were pre-incubated with ^{32}P-orthophosphate and measured stoichiometry of phosphorylation. In resting arteries, caldesmon was phospborylated to a level of 0.41 mole PO_4/mole protein, while calponin was phosphorylated to levels less than 0.01 mole/mole. Stimulation by histamine (5 min), KCl (5 or 60 min) or phorbol-12,13-dibutyrate (1 μM PDBu for 15 or 60 min) did not lead to measurable increases in the phosphate content of calponin. Caldesmon phosphorylation, on the other hand, was elevated by prolonged stimulation with PDBu. Because dephosphorylation of calponin during the purification procedure could account for these results, we monitored the dephosphorylation of purified calponin (covalently labeled with $^{32}PO_4$ by protein kinase C), subject to the same purification protocol, in a separate set of experiments. Calponin was not dephosphorylated under these circumstances. This suggests it is unlikely that dephosphorylation of endogenous calponin, during purification from ^{32}P-labeled tissue, is responsible for the lack of detectable phosphate in the protein. Collectively, these data show that calponin is not phosphorylated under conditions where caldesmon phosphorylation is apparent. Thus, it remains to be proven that calponin is a phosphoprotein in intact vascular smooth muscle.

Tu-Pos344

CHARACTERIZATION OF CALPONIN BINDING TO ACTIN.
((F.W.M. Lu, M.V. Freedman and J.M. Chalovich))
Dept. Biochem., East Carolina Univ. Med. Sch. Greenville, North Carolina

The smooth muscle derived actin binding protein, calponin, inhibits actin activated ATP hydrolysis by myosin. Although the binding of calponin to actin has been studied, reported stoichiometries range from 1 calponin per actin to 1 calponin per 3 actin monomers. We now report the results of binding of ^{14}C-iodoacetamide labeled calponin to actin using a cosedimentation assay (Velaz et al, 1989, J. Biol. Chem. 9602-9610). Labeling calponin with ^{14}C-iodoacetamide affects neither its ability to inhibit actin activated ATPase activity nor its binding to actin. At ≈60 mM ionic strength, there is a single class of binding sites with a 1:1 stoichiometry and a dissociation constant of 0.5-1 μM in both absence and presence of smooth muscle tropomyosin. Under the same conditions, the inhibition of ATPase activity by calponin is independent of the presence of smooth muscle tropomyosin. The affinity of calponin for actin is decreased 2-3 fold in the presence of ATP as suggested by Makuch et al. (1991). In addition, binding 1 calponin per 3 actin monomers initiates crosslinking of actin filaments. Similar crosslinking also occurs at ≈150 mM ionic strength. However, at this higher ionic strength there is an indication that the stoichiometry of binding is 1 calponin per 2 actin monomers. Thus, the observed stoichiometry may depend on the conditions of measurement.

Tu-Pos345

STOICHIOMETRIC LEVELS OF CALPONIN PHOSPHORYLATION DURING AGONIST INDUCED CONTRACTION OF SWINE CAROTID ARTERY.
((Aniko Rokolya and Robert S. Moreland)) Bockus Research Institute, Graduate Hospital, Philadelphia, PA 19146. (Spon. by E.H. Murer)

Calponin is a thin filament associated smooth muscle specific protein, the phosphorylation of which has been implicated in the regulation of smooth muscle contraction. We have previously demonstrated a rapid and sustained increase in ^{32}P incorporation in calponin during stimulation by endothelin-1 (ET-1). The present study was designed to determine the stoichiometry of ET-1 induced calponin phosphorylation. Swine carotid medial strips were labelled with [^{32}P]H_3PO_4, exposed to 0.3 μM ET-1, and frozen during contraction. The specific activity of [γ-^{32}P]ATP extracted from the tissue was determined by measuring protein kinase C catalyzed myelin basic protein$_{4-14}$ phosphorylation. Phosphorylated and unphosphorylated calponin were separated by subjecting the labelled tissues to NEPHGE/SDS PAGE. The electrophoretic spots corresponding to phosphorylated calponin were counted by liquid scintillation and the cpm converted to mol phosphate using the specific activity of the ATP determined from the same tissue. A standard curve of various concentrations of purified calponin subjected to NEPHGE/SDS PAGE was used to determine mol calponin in each electrophoresed gel. Using this approach, basal calponin phosphorylation levels were 0.12 ± 0.04 mol P_i/mol calponin and increased to 1.1 ± 0.08 mol P_i/mol calponin during ET-1 stimulation. These data demonstrate that calponin is phosphorylated during stimulation of intact vascular smooth muscle and may therefore be an important step in contractile regulation.
Supported, in part, by funds from NIH grant HL 46704 (RSM) and a fellowship from AHA SEPA (AR).

Tu-Pos346

BINDING AND DIFFUSION OF CALMODULIN IN SMOOTH MUSCLE CELLS
((Douglas Won and Katherine Luby-Phelps)) UT Southwestern Medical Center at Dallas, Dallas, TX 75235-9040.

Fluorescence recovery after photobleaching (FRAP) was used to study the binding and diffusion of fluorescent calmodulin derivatives in early passage bovine tracheal smooth muscle cells in primary culture. Data obtained with three different derivatives agreed within experimental error and were not fit well by least squares analysis assuming a single recovering species. Fifteen to 25% of the calmodulin was immobile on the 30 sec timescale of the measurement. We estimate the mobility of the fastest recovering species to be 2.18 x 10E-9 cm^2/s. In comparison, 10 kDa fluorescein-dextran could be fit to a single recovering species with a mobility of 2.67 x 10E-8 cm^2/s ± 0.1 SEM (n=10). Assuming that the difference was due to transient binding of the calmodulin to intracellular sites, we calculate that only 10% of the injected calmodulin was freely diffusible. Treatment with 10 μM ionomycin in culture medium increased the immobile fraction of calmodulin but did not alter the recovery kinetics for dextran. The small fraction of freely diffusible calmodulin in smooth muscle cells at resting calcium levels has important implications for understanding the mechanism of activation of myosin light chain kinase.

SR-Ca ATPase, PHOSPHORYLATION

Tu-Pos347

EFFECTS OF LOCAL AND VOLATILE ANESTHETICS ON THE Ca-ATPase IN SKELETAL AND CARDIAC SR. ((Brad S. Karon, Howard Kutchai[†], and David D. Thomas)) Dept. of Biochemistry, University of Minnesota Medical School, Minneapolis, MN 55455 and [†]Dept. of Physiology, University of Virginia, Charlottesville, VA 22908.

Lidocaine and halothane influence the function and oligomeric state of the Ca-ATPase. **Lidocaine inhibited and aggregated** the Ca-ATPase in both skeletal and cardiac sarcoplasmic reticulum (SR), but to a greater extent in cardiac than in skeletal SR. Lidocaine inhibition was calcium dependent in both systems, with μM calcium having a protective effect. The phospholamban (PLB) antibody 2D12 (mimics PLB phosphorylation, provided by L. Jones) had little effect on lidocaine inhibition of cardiac SR. **Halothane activated and disassociated the Ca-ATPase in skeletal SR, but inhibited and aggregated the Ca-ATPase in cardiac SR.** Halothane inhibition of cardiac SR was much greater in the presence of PLB Ab, indicating a protective effect of PLB on halothane inhibition. These results indicate that the action of lidocaine is similar in skeletal and cardiac SR, but distinct from the action of halothane in either system. The PLB-dependence of halothane inhibition of cardiac SR may explain differences between halothane action in skeletal and cardiac SR. These effects underscore the crucial role of protein-protein interactions on Ca-ATPase regulation and anesthetic perturbation.

Tu-Pos348

OXIDATIVE DAMAGE IN SR MEMBRANES: MECHANISM OF PROTECTION BY MEMBRANE PROTEINS. ((A.G. Krainev[*], R.I. Viner[*], C. Schöneich[+], and D.J. Bigelow[*])) Depts. of [*]Biochem. and [+]Pharm. Chem., Univ. of Kansas, Lawrence, KS, 66045 (Spon. by T.C. Squier)

We have employed reverse-phase C_{18} HPLC to quantify 2,4-dinitrophenylhydrazone derivatives of four different products of oxidative degradation of skeletal sarcoplasmic reticulum (SR) membranes from rabbits and in vesicles, prepared from extracts of SR lipids: (a) malondialdehyde (MA), (b) formaldehyde (FA), (c) acetaldehyde (AA) and (d) acetone (Ac). Lipid peroxidaton (LPO) was initiated by 40 mM of thermally unstable 4,4'-azobis-(4-cyanovaleric acid). SR proteins convey an apparent protective effect on the SR lipids, shown by the 4-10 fold decrease in formation of LPO products in SR membranes than in vesicles of SR lipids. Essentially the same behavior was observed in the presence of 75 mM water-soluble initiator, 2,2'-azobis-(amidopropane) hydrochloride, when LPO was studied in SR vesicles, reconstituted with different amounts of Ca^{2+}-ATPase. The production of MA correlated with the lipid abundance in vesicles. In contrast, the production of FA, AA and Ac was dependent on the protein content. In the model oxidation of single amino acids, e.g. cysteine, tyrosine, tryptophan, glycine, and leucine, FA and AA were detected. Only the reaction of azo-initiator with leucine produced Ac. The roles of amino acids in the oxidative damage of SR membranes are discussed.

Tu-Pos349

PROXIMITY OF NUCLEOTIDE BINDING SITES IN THE Ca-ATPase FROM SARCOPLASMIC RETICULUM.

((Shaohui Huang, Linda T. Chen, and Thomas C. Squier)) Department of Biochemistry, University of Kansas, Lawrence, KS, 66045-2106.

We have used fluorescein 5-isothiocyanate (FITC), eosin 5-isothiocyanate (EITC), and erythrosin 5-isothiocyanate (ErITC) to investigate the proximity of nucleotide binding sites on the Ca-ATPase. All three probes label the cytoplasmic domain of the Ca-ATPase. In contrast to FITC, which specifically labels a single saturable binding site that blocks nucleotide binding; EITC and ErITC react with multiple binding sites (i.e., no saturation). We observe a biphasic inactivation of Ca-ATPase activity as a function of FITC and EITC labeling stoichiometries. This is consistent with a dimeric functional unit of the Ca-ATPase. At low stoichiometries of ErITC incorporation, the inactivation profile is virtually identical to that observed using FITC and EITC, and the average lifetime is constant, indicating a homogenous binding site. ErITC incorporation results in a maximal inhibition of 50% of Ca-ATPase activity. Fluorescence depolarization measurements indicate that unlike FITC, ErITC binding sites are far apart. This suggests that one subunit on each homodimer can be specifically labeled with a large probe like ErITC, and argues for a close proximity between nucleotide binding sites.

Tu-Pos350

CONFORMATIONAL TRANSITIONS OF THE SARCOPLASMIC RETICULUM Ca^{2+} PUMP STUDIED BY RAPID MIXING AND TIME-RESOLVED EPR.

((James E. Mahaney, Jeffrey P. Froehlich and David D. Thomas)) Department of Biochemistry, University of Minnesota Medical School, Minneapolis, MN 55455, and National Institute on Aging, NIH, Baltimore, MD 21224.

Time-resolved EPR spectroscopy and rapid mixing kinetic measurmements were used to investigate the dynamic behavior of Ca-ATPase conformational changes involved in Ca^{2+} pumping in sarcoplasmic reticulum (SR) at 2°C. The Ca-ATPase was labeled with an iodoacetamide spin label, and required NEM pre-treatment for site-selective attachment of the label to the enzyme. Rapid mixing of 100 μM ATP with spin-labeled SR vesicles in 100 mM KCl produced a monophasic phosphorylation time course with an apparent rate of 40 s^{-1}. Addition of 0.9 mM caged ATP prior to ATP (to approximate the conditions of the EPR experiment) produced an initial lag in the phosphorylation time course while decreasing the apparent rate to 30 s^{-1}. The EPR spectrum of spin-labeled Ca-ATPase is sensitive to conformational changes during ATP-induced enzymatic cycling. Following laser flash-photolysis of caged ATP, which produced 100 μM ATP in the sample, the EPR signal intensity displayed a similar time-dependent lag and an exponential rise with an apparent rate of 20 s^{-1}. Addition of non-hydrolyzable ATP analogs to the SR vesicles produced the same EPR signal change as ATP, while phosphorylation with P_i gave no change. These results suggest that the time-resolved EPR signal monitors the formation of a conformational state that is activated by ATP binding and disappears upon conversion of E_1P to E_2P. Correlation of this data with the quench flow data suggests that relaxation of the ATP-induced conformation is associated with the rapid transfer of Ca^{2+} to an internal occluded compartment which slowly releases Ca^{2+} to the intravesicular space.

Tu-Pos351

H_{II}-PRONE LIPID INDUCE DISSOCIATION OF RECONSTITUTED CA-ATPASE

((Răzvan L. Cornea and David D. Thomas)) Dept. of Biochemistry, University of Minnesota Medical School, Minneapolis, MN 55455.

We studied the effects of the H_{II}-prone lipid dioleoyl phosphatidylethanolamine (DOPE) on the function and molecular dynamics of reconstituted Ca-ATPase of sarcoplasmic reticulum (SR). The reconstituted Ca-ATPase suffered increased inhibition as the mole fraction of DOPE increased in a mixture with dioleoyl phosphatidylcholine (DOPC). In transient phosphorescence anisotropy (TPA) experiments on similar preparations, DOPE decreased the residual anisotropy of the labeled Ca-ATPase, implying decreased protein association, closer to the values obtained in native SR, which contains 25-30% PE. Lipid EPR spectra indicated that bilayer fluidity decreases with DOPE content. It has been suggested previously that the transport efficiency of the Ca-ATPase is maximized by DOPE (Navarro et al., 1984 *Biochemistry 23*, 130-135). We propose that increased lateral stress introduced in the bilayer by DOPE (Chen et al.,1992 *Biochemistry 31*, 3759-3768) optimizes protein-protein association to maximize Ca-transport efficiency, whereas ATPase activity is inhibited because of decreased bilayer fluidity and a perturbation in the distribution of conformational states caused by lateral stress.

Tu-Pos352

USE OF FLUO-3 TO ASSESS THE EFFECT OF COMPOUNDS ON Ca^{2+} UPTAKE BY CARDIAC SARCOPLASMIC RETICULUM (SR) VESICLES.

((P. Lahouratate, V. Lahouratate and J.C. Camelin)) SmithKline Beecham, Lab. Pharmaceutiques, BP-58, F-35762 Saint Grégoire, France. (Spon. by J. Su)

Fluo-3 (3 μM), added to the exterior of dog cardiac SR vesicles (100 μg/ml), was used to monitor Ca^{2+} uptake in a solution at 30 °C containing (mM) 120 KCl, 6 $MgCl_2$, 20 HEPES (pH 7.02), 1.5 Na_2ATP, 5 NaN_3, 2.5 K-oxalate and 0.15 EGTA with 1 μM $[Ca^{2+}]_{free}$. In these conditions the K_d for fluo-3-Ca^{2+} complex was 422 nM. Changes in fluo-3 fluorescence resulted from the decline in $[Ca^{2+}]_{free}$, owing to active Ca^{2+} accumulation by the vesicles, and allowed the determination of Ca^{2+} uptake velocity. The effects of cyclopiazonic acid (CPA), thapsigargin (THA), gingerol (GIN) and heparin (HEP) on rate of Ca^{2+} uptake were determined and compared with their effects on Ca^{2+} ATPase. CPA and THA inhibited Ca^{2+} uptake with IC_{50} (μM) of 1.5 and 0.048, respectively. The inhibition of Ca^{2+} ATPase was similar with IC_{50} of 0.64 and 0.035, respectively. HEP stimulated Ca^{2+} uptake with a maximum stimulation (E_{max}) of 57% and an EC_{50} (μM) of 0.37. Its effect on Ca^{2+} ATPase was very similar with E_{max} = 57%; EC_{50} = 0.09. GIN stimulated Ca^{2+} uptake and Ca^{2+} ATPase at similar concentrations with EC_{50} of 9.2 and 3, respectively but the maximum stimulation was higher on Ca^{2+} uptake rate with E_{max} = 258% than on Ca^{2+} ATPase with E_{max} = 21 %. In conclusion, this method, which is faster than radioisotopic methods, is very suitable for assessing effects on SR-Ca^{2+} uptake by activators or inhibitors of SR-Ca^{2+} ATPase. Further experiments are required to determine the reason for the different behaviour of GIN in the two assays.

Tu-Pos353

BEAT DEPENDENT KINETICS OF SARCOPLASMIC RETICULUM CALCIUM TURNOVER IN ISOLATED ADULT RAT HEART CELLS

((Robert A. Haworth and Atilla B. Goknur)) University of Wisconsin Department of Anesthesiology, 600 Highland Avenue, Madison, WI 53792 (Spon. by H. Komai)

The isotopic measurement of the small rapidly exchanging cellular pools of Ca which mediate contraction in isolated heart cells is complicated by the presence of much larger, more slowly exchanging pools. We have now been able to measure the rate and extent of beat dependent 45Ca uptake into and release from such a pool, using a dilution method which we developed previously to measure cellular Na. Cells in suspension with 0.2mM Ca, 5µM ruthenium red and 1µM isoproterenol took up an extra 0.132 +/- 0.023nmol Ca/mg protein after 30sec electric field stimulation at 2Hz, compared with unstimulated cells. This uptake was prevented by verapamil (10µM), thapsigargin (2µM, 4min preincubation) or ryanodine (0.1µM, 30min preincubation). On dilution of cells so loaded into unlabelled medium, efflux from this pool was relatively slow (0.90 +/- 0.15%/sec), unless the cells were stimulated or caffeine (10mM) was present. From the rate dependence of the rate of efflux of label we calculate that each beat results in the loss of only 5.18% of label remaining in this pool. A similar figure was calculated from the frequency dependence of the rate of uptake. We conclude that this rapidly exchangeable pool is the sarcoplasmic reticulum, and that pool turnover per beat is relatively slow.

Tu-Pos354

ENHANCEMENT BY INORGANIC PHOSPHATE (Pi) OF Ca^{2+} UPTAKE INTO THE SARCOPLASMIC RETICULUM (SR) CAN AFFECT ESTIMATES OF FORCE PRODUCION IN SKINNED MUSCLE FIBERS.

((T.M. Nosek, R.T.H. Fogaça, I. Kassouf-Silva, and R.E. Godt)) Dept. of Physiology & Endocrinology, Medical College of GA, Augusta GA 30912

Some agents used to chemically skin muscle fibers are detergents (e.g., Triton X-100) which disrupt membranes of the sarcolemma and organelles. However, other agents (e.g., saponin) disrupt the sarcolemma but leave the SR membrane intact permitting study of Ca^{2+} metabolism by the SR. We have found that, after skinning with either Triton or saponin, maximum Ca^{2+} activated force (Fmax) of lobster striated muscle is the same in the absence of added Pi. Fmax of Triton skinned fibers is quite insensitive to Pi; 30 mM Pi has no effect while 100 mM Pi only decreased Fmax by 16%. However, in fibers skinned with saponin, 30 mM Pi decreased F_{max} by 75% and 100 mM Pi by 95%. When saponin-skinned fibers were treated with ionomycin to prevent the SR from accumulating Ca^{2+} or subsequently skinned with Triton to destroy the SR membranes, the enhanced response to Pi was reversed. Similar results were observed in frog and rabbit skeletal muscle. We have previously demonstrated in heart muscle that Pi is able to enter the SR and augment its ability to sequester Ca^{2+}. Therefore, the overestimation of Pi sensitivity of Fmax in saponin-skinned fibers appears to be due to the ability of the SR in the presence of Pi to maintain a lower $[Ca^{2+}]$ in the immediate vicinity of the contractile proteins than is present in the solution bathing the fiber. (Support: NIH AR40598 & AR31636)

Tu-Pos355

FUNCTIONAL DEFECT OF CARDIAC SARCOPLASMIC RETICULUM (CSR) IN DIABETES MELLITUS. ((Hae Won Kim[1], H.R. Lee[2], Y.J. Jang[3], H. Park[1], S.Y. Park[1])) Depts. of Pharmacol.[1], Physiol.[3], Univ. Ulsan Coll. Med.; Div. of Pharmacol. and Toxicol., AILS[2], Seoul 138-040, Korea

Oxidative modification of cellular proteins and lipids may play a role in the development of diabetic complications. Diabetic cardiomyopathy has been suggested to be caused by the intracellular Ca^{2+} overload in the myocardium, which is partly due to the defect of Ca^{2+} transport of the CSR. In the present study, the possible mechanism of the functional defect of CSR in diabetic rats was studied. To investigate whether the functional defect of the CSR in streptozotocin-induced diabetic rat is associated with the oxidative changes of CSR proteins, the carbonyl group content and glycohemoglobin levels were determined. The increases in carbonyl group content of CSR (3.69 nmols/mg prot., DM; 2.91, control) and in glycohemoglobin level (12-16%, DM; 3-5%, control) were observed in the diabetics. The extent of increase in Ca^{2+} transport by phospholamban (PLB) phosphorylation was greater in the diabetic CSR than that in the control. The decrease of norepinephrine levels in the diabetic heart was observed (3.57 ng/mg prot., DM; 6.68, control). The phosphorylation levels of PLB, as determined by SDS-PAGE and autoradiography, were increased in diabetic CSR. These results suggest that the impaired CSR function in diabetic rat could be a consequence of the less-phosphorylation of PLB in the basal state, which is partly due to the depleted NE stores in the heart. Furthermore, the oxidative damages in CSR membranes might be one of additional factors leading to the diabetic cardiomyopathy. (Supported by a grant from AILS 93-10-002).

Tu-Pos356

REST POTENTIATION OF TWITCHES IN MYOCARDIUM
((H.S. Banijamali, H.E.D.J. ter Keurs)) Medical Physiology, University of Calgary, Alberta, Canada

Twitch force (Ft) of contraction of mammalian myocardium is determined by Ca^{++} released from the sarcoplasmic reticulum and the interval from the last contraction. In most species, Ft increases to a peak at intervals up to 1-2s and it declines with longer intervals (rest depression). In rat myocardium Ft increases to a second peak at intervals up to 100s (rest potentiation). Rest depression occurs at intervals >100s and has been attributed to a net Ca^{++} loss from the sarcoplasmic reticulum. Rest potentiation has been proposed to be due to Na^{+}-Ca^{++} exchange-mediated Ca^{++} entry into the sarcoplasmic reticulum. We studied Ft- and Fc-interval relations (Fc: force of cold contracture) in rat cardiac trabeculae (n=50) (Krebs-Henseleit solution, pH 7.4, 26 °C or 0 °C) at varied $[Ca^{++}]_o$. We used $NiCl_2$, and ruthenium red and high $[NaH_2PO_4]$ to block sarcolemmal Ca^{++} transport (Isi and Na^{+}-Ca^{++} exchange) and mitochondrial Ca^{++} transport, respectively. Isoproterenol was used to stimulate sarcoplasmic reticulum Ca^{++} uptake. Ca^{++} transient-interval relation was also studied in iontophoretically fura-2 loaded trabeculae. Rest potentiation of Ft and Fc was 70% and 20%, respectively, suggesting that an increase in the sarcoplasmic reticulum Ca^{++} content can not by itself explain twitch rest potentiation. $NiCl_2$ reduced Ft, but it increased rest potentiation of Ft and Fc and eliminated rest depression suggesting that: Na^{+}-Ca^{++} exchange only extrudes Ca^{++} during rest, and there is an intracellular source that provides Ca^{++} to enter the sarcoplasmic reticulum during rest. Mitochondria is not a likely candidate for this source since ruthenium red and high $[NaH_2PO_4]$ did not alter rest potentiation. Isoproterenol that stimulates sarcoplasmic reticulum Ca^{++} pump reduced twitch rest potentiation. Ca^{++} transient of a control rest potentiated twitch relaxed slower than control steady state. These results are consistent with the hypothesis that rest potentiation of twitch is in part explained by inactivation of the sarcoplasmic reticulum Ca^{++} pump which will favor Ca^{++} binding to myofilaments following Ca^{++} release.

Tu-Pos357

CALSEQUESTRIN IN RAT SMOOTH MUSCLE: VARIABLE CONTENT AND RATIO OF THE SKELETAL AND CARDIAC MUSCLE ISOFORMS. (A. Martini, S. Furlan, J. Meldolesi* and P. Volpe). Centro di Studio per la Biologia e la Fisiopatologia Muscolare del CNR, Universita' di Padova, Padova, and * Dibit, Istituto Scientifico San Raffaele, Universita' di Milano, Milano, Italy.

Expression by smooth muscle cells of calsequestrin (CS), the low affinity-high capacity calcium binding protein of striated muscle sarcoplasmic reticulum (SR), has been investigated in recent years with conflicting results (see Milner et al., J. Biol. Chem. 266: 7155-7166, 1991, and Villa et al., J. Cell Biol. 121:1041-1051, 1993). Here we report the purification and characterization from rat vas deferens of two CS isoforms, the first deemed skeletal muscle, the second cardiac type on account of their NH_2-amino acid termini and other relevant biochemical and molecular properties. Compared to vas deferens, the smooth muscle from the stomach and aorta were found to express lower amounts of CS (aorta > stomach), whereas CS in uterus and bladder was virtually undetectable. The ratio between the two CS isoforms was also variable, with the stomach and aorta expressing predominantly the skeletal muscle type, and the vas deferens expressing the two CSs in roughly similar amounts. Because of the property of CSs to localize within the SR lumen not uniformly, but according to the distribution of their anchorage membrane proteins, the expression of the protein in at least some smooth muscle suggests the existence of discrete SR areas specialized in the rapidly exchanging calcium storage and release, and thus in the control of a variety of functions, including smooth muscle contraction.

Tu-Pos358

THYROID HORMONE ENHANCES Ca^{2+} PUMPING ACTIVITY OF THE CARDIAC SARCOPLASMIC RETICULUM BY INCREASING Ca^{2+} ATPase AND DECREASING PHOSPHOLAMBAN EXPRESSION.
((Y. Kimura, K. Otsu, K. Nishida, T. Kuzuya, and M. Tada)) Osaka University Medical School, Osaka, Japan. (Spon. by Y. Kijima)

Phospholamban is a putative suppressor of the Ca^{2+} ATPase of the cardiac sarcoplasmic reticulum (SR). Thyroid hormone has been shown to increase the level of mRNA encoding the Ca^{2+} ATPase, whereas to decrease the level of phospholamban mRNA *in vivo*. The present study was designed to examine whether these effects of thyroid hormone are exerted directly on cardiac myocytes and whether the resultant incoordinate expression of these proteins alters Ca^{2+} pumping activity. We investigated the levels of phospholamban and Ca^{2+} ATPase mRNA in primary isolated neonatal rat myocardial cells incubated with triiodothyronine (T_3), and also measured the Ca^{2+} uptake activity of the microsomes prepared from the cells. Northern blot analysis showed that T_3 decreased phospholamban mRNA levels to about a half of control in 24 h. On the other hand, Ca^{2+} ATPase mRNA gradually increased with time. EC_{50} for phospholamban mRNA expression was 250 pM, which was approximately 10 times higher than that for the Ca^{2+} ATPase. T_3 increased V_{max} of Ca^{2+} uptake with significant reduction of $K_{0.5}$ for Ca^{2+} (0.43 μM to 0.34 μM), indicating that thyroid hormone stimulates Ca^{2+} pumping activity not only by increasing the number of the transporter units but also decreasing the amount of its suppressor, phospholamban. From these results, we postulated a novel regulation mechanism of the Ca^{2+} ATPase by phospholamban, in which relative expression levels of these two proteins can modulate the Ca^{2+} pumping activity of SR.

Tu-Pos359

CHARACTERIZATION OF NATIVE, CHEMICALLY SYNTHESIZED, AND RECOMBINANT PHOSPHOLAMBAN. ((Edward McKenna, Ernest J. Mayer, Victor M. Garsky, Carl J. Burke, Mohinder Sardana, Loren D. Schultz, Marlene A. Jacobson, Jeffrey S. Smith, and Robert G. Johnson, Jr.)) Merck Research Laboratories, West Point, Pennsylvania 19486

Phospholamban(PLB) is a 52 amino acid protein which modulates the cardiac sarcoplasmic reticulum calcium pump. The hydrophobic nature of PLB has made its isolation difficult and limited its biophysical characterization. A monoclonal antibody affinity column has been prepared which allows for rapid purification of milligram quantities of PLB. In addition, large quantities of PLB were obtained by solid-phase chemical synthesis as well as expression in yeast followed by immunoaffinity chromatography. Direct comparisons of synthetic and recombinant PLB were made with native PLB. All of the proteins migrated as homopentamers in SDS-PAGE (which dissociated to monomers and other smaller oligomers upon boiling), were detectable by Western blot analysis using polyclonal antibody directed against the amino terminus(residues 1-25) of PLB, and were phosphorylated by cAMP-dependent protein kinase. Each protein had an approximate molecular mass of 6.1 kDa as determined by mass spectroscopy, had amino acid compositions consistent with PLB, and yielded internal PLB fragments upon CNBr digestion as verified by microsequencing.

A cys-to-ser PLB analog in which the three cysteine residues (C36,41,46) were substituted by serines was synthesized using solid phase techniques. This cys-to-ser PLB migrated exclusively as a monomer in SDS-PAGE, was phosphorylated by cAMP-dependent protein kinase, and was detectable on Western blot analysis using anti-PLB antibodies. The yeast expression/immunoaffinity chromatography system will be exploited to obtain other forms of PLB for structural and reconstitution studies.

Tu-Pos360

FUNCTIONAL RECONSTITUTION OF RECOMBINANT PHOSPHOLAMBAN WITH RABBIT SKELETAL CA^{2+}-ATPASE. ((L.G. Reddy, R.C. Pace, L.R. Jones, D.L. Stokes)) Dept. of Molecular Physiology and Biological Physics, Univ. of Virginia Health Science Center, Charlottesville, VA 22908 and Krannert Inst. of Cardiology, Indiana Univ. School of Medicine, Indianapolis, IN 46202.

The effect of recombinant phospholamban (PLB) expressed from Sf 21 insect cells infected by bacculovirus has been studied with the purified Ca^{2+}-ATPase from rabbit skeletal sarcoplasmic reticulum (SR) in a reconstituted system. PLB was purified in β-octylglucoside on a monoclonal antibody affinity column; gel electrophoresis indicated that this expressed, purified protein is able to self-associate into heat-sensitive pentamers, similar to native PLB. Ca^{2+}-ATPase was purified in $C_{12}E_8$ by Reactive Red 120 affinity chromatography. For reconstitution, we tested three nonionic detergents (β-octylglucoside , $C_{12}E_8$, Triton X-100) and, after complete solubilization of lipid together with protein (80:1 weight ratio), detergent was removed by SM2 biobeads over a period of 3 hrs at 20°C. When PLB was reconstituted along with purified Ca^{2+}-ATPase (10:1 molar ratio), the Ca^{2+} uptake rates were 67% of control, i.e., Ca^{2+}-ATPase reconstituted in the absence of PLB (avg. of 6 experiments with control uptake = 0.5 I.U. at 25°C). A monoclonal antibody to PLB has previously been shown to mimic the physiological effect of phosphorylation on cardiac SR. When preincubated with this antibody, the inhibition in Ca^{2+} uptake of PLB-containing proteoliposomes was almost completely relieved (92.7% of control). These results indicate that the recombinant PLB is comparable to native PLB in its functional effects on Ca^{2+}-ATPase.

Tu-Pos361

DEVELOPMENTAL REGULATION OF PHOSPHOLAMBAN EXPRESSION AND SARCOPLASMIC RETICULUM FUNCTION IN MURINE HEARTS

((Judy M. Harrer and Evangelia G. Kranias)) Department of Pharmacology & Cell Biophysics, University of Cincinnati, Cincinnati, OH 45267-0575. (Sponsored by L. Lane)

Phospholamban (PLB) is an important phosphoprotein in cardiac SR that regulates the affinity of the Ca^{2+}-ATPase for Ca^{2+}. To determine whether PLB expression is developmentally regulated in mice and if such regulation reflects changes in the SR Ca^{2+}-pump activity, hearts from mice during different stages of development were processed for molecular biological and biochemical studies. Northern and dot blot analyses of cardiac RNA indicated that the PLB mRNA remained low (30%) until 7 days post birth and subsequently increased to adult levels (100%) by day 18 of development. These changes in mRNA levels were indicative of PLB protein levels as determined by quantitative immunoblot analysis. The functional significance of alterations in PLB expression during development was examined using $^{45}Ca^{2+}$-uptake assays in the presence of 5 μM ruthenium red. The initial rates of SR Ca^{2+}-uptake were assayed over a range of physiological $[Ca^{2+}]$ in homogenates from the developing hearts. Analysis of the data indicated that over the course of development: 1) maximal uptake rates remained unchanged (90 nmol/mg/min); and 2) the affinity of the SR Ca^{2+}-pump for Ca^{2+} decreased with increasing PLB levels. These findings suggest that PLB expression is developmentally regulated in the mouse heart. Such regulation may reflect alterations in SR Ca^{2+}-ATPase activity and thus, myocardial relaxation.

(Supported by HL26057, HL22619, and HL07382)

Tu-Pos362

USING PHOSPHOLAMBAN ANTIBODY TO STUDY THE PHYSICAL REGULATION MECHANISM of CARDIAC Ca-ATPase.

((Ming Li, Larry R. Jones, and David D. Thomas)) Department of Biochemistry, University of Minnesota, Minneapolis, MN 55455. (Spon. by Richard E. Poppele).

Voss et al. (Biophys. J. 61:A431, 1992) showed that phospholamban (PLB) phosphorylation, which activates the cardiac Ca-ATPase, also disaggregates the Ca-ATPase protein in the plane of the membrane. PLB antibodies (2D12) activate cardiac Ca-ATPase to a similar extent as phosphorylation does, but the mechanisms of activation are not understood. In the present study, we have used PLB antibody and its F_{ab} fragment, in comparison with phosphorylation, to provide insight into the physical mechanism of regulation in this system. We first showed that the **F_{ab} fragment has the same effect as either the intact antibody or phosphorylation** in activating Ca uptake and Ca-ATPase activity. The physical interaction of the antibody and F_{ab} fragment with PLB was demonstrated by western blot. The physical effects were studied by **time-resolved phosphorescence anisotropy (TPA)** of erythrosin isothiocyanate bound to the Ca-ATPase, which measures the microsecond rotational mobility and protein-protein interactions of the enzyme, and fluorescence of fluorescein isothiocyanate, which measures the E_1-E_2 conformational change of the enzyme. Intact antibody, F_{ab}, and phosphorylation all perturb both the protein-protein interactions and the conformational state of the enzyme, but the results are not identical, indicating differences in the precise physical mechanism of action.

Na CHANNELS II: MODULATION

Tu-Pos363

μ1 ADULT SKELETAL MUSCLE Na CHANNELS EXPRESSED IN HEK 293 CELLS: REGULATION BY ACTIVATORS OF PROTEIN KINASE C

S. Bendahhou, T.R. Cummins* & W.S.Agnew, Depts. of Physiology and Neuroscience, Johns Hopkins University School of Medicine, Baltimore, MD 20205 and *Interdepartmental Neuroscience Program, Yale University School of Medicine, New Haven, CT, 06510

The μ1 skeletal muscle Na channel may be transiently expressed at high efficiency in human embryonic kidney (HEK 293) (Ukomadu et al.(1992), Neuron,8,663-676): the μ1 α-subunit may be phosphorylated by endogenous Protein Kinase A and Protein Kinase C. This channel exhibits multi-modal gating, including fast-inactivating (mode 1), slow inactivating (mode 2) and silent (mode 0) states. μ1 channels expressed in 293 cells exhibit primarily (95-97%) fast inactivating (mode 1) gating. We find that activators of Protein Kinase C markedly alter both peak current and channel gating kinetics. Incubation with 1,2-dioctanoyl-sn-glycerol (DOG) (10 μM) resulted in rapid decrement of peak Na current amplitude by ~50%. This decrease is accompanied by a speeding of inactivation due to elimination of the small (3-5%) slow-inactivating current component. Voltage-clamp analysis reveals a ~13 mV hyperpolarizing shift of steady-state inactivation, but essentially no shift in conductance activation. No change in the time to peak or in peak current vs. voltage relationships were seen. These results differ from the effects of Protein Kinase C on neuronal channels, or those previously reported form muscle channels expressed in cultured muscle cell lines in which Protein Kinase C decreased peak currents but slowed inactivation gating. The distinct effects of Protein Kinase C agonists on kinetics and peak current amplitude may result from multiple sites of phosphorylation or phosphorylation induced changes in the relative stabilities of distinct intrinsic gating modes.

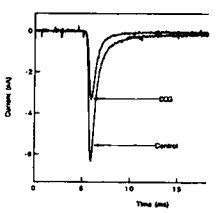

Tu-Pos364

MULTIPLE EFFECTS OF PROTEIN KINASE C ACTIVATORS ON Na^+ CURRENTS.

((C.M.G. Godoy, and S. Cukierman)) Department of Physiology, Loyola University Medical Center, 2160 South First Avenue, Maywood, IL, 60153-5500.

The effects of externally applied different protein kinase C (PKC) activators on Na^+ currents in mouse neuroblastoma cells were studied using the nystatin variation of the whole cell voltage clamp technique. Two diacylglycerol-like compounds, OAG and DOG attenuated Na^+ currents without affecting the time course of activation or inactivation. The reduction in Na^+ current amplitude caused by OAG or DOG was more intense at positive voltages. The steady-state activation curve was unaffected by these substances. Both OAG and DOG shifted the steady-state inactivation curve of Na^+ currents to hyperpolarized voltages. Phorbol esters did not affect Na^+-currents. *Cis*-unsaturated fatty acids (linoleic, linolenic, and arachidonic) attenuated Na^+ currents without modifying the steady-state activation. *Cis*-unsaturated fatty acids shifted the steady-state inactivation curve to more negative voltages. Curiously, inward currents were more effectively attenuated by *cis*-fatty acids than outward currents. Oleic acid, another *cis*-unsaturated fatty acid, enhanced Na^+ currents. This enhancement was not accompanied by changes in kinetic or steady-state properties of currents. Enhancement of Na^+ currents caused by oleate was stronger at negative voltages. The multiple effects caused by the PKC activators were totally prevented by pretreating cells with conventional PKC inhibitors. By themselves, PKC inhibitors did not affect membrane currents. Trans-unsaturated or saturated fatty acids, which do not activate PKC's, did not modify Na^+ currents. Taken together, the experimental results suggest that PKC activation modulates the behavior of Na^+ channels by at least three distinct mechanisms. Because qualitatively different results were obtained with different PKC activators, it is not clear how Na^+ currents would respond to activation of PKC in physiological conditions.

Tu-Pos365

MODULATION OF CARDIAC SODIUM CHANNEL α-SUBUNITS BY PROTEIN KINASE C.

((L. Weigl, B. Frohnwieser, B. Spreitzer, R. Kallen* and W. Schreibmayer)) Institute for Medical Physics and Biophysics, University of Graz, Graz A-8010, Austria. *: Department of Biochemistry and Biophysics, University of Pennsylvania, Philadelphia PA 19109. (Spon. by H. A. Tritthart)

The pore forming α_{IIA}-subunit of the brain sodium channel is a prominent target for phosphorylation by protein kinase C (PKC) and protein kinase A (PKA). It has been shown in addition, that phosphorylation of the neuronal isoform by serine/threonine protein kinases leads to a reduction of sodium inward current through this ion channel. At least six isoforms of sodium channel α-subunits exist, different mostly in their cytosolic and hence likely modulatory regions.

We have investigated the effects of PKC activation on the cardiac isoform (α_{SkM2}) from rat heart, expressed in *Xenopus laevis* oocytes. When 5-Hydroxytryptamine (5-HT) was applied to oocytes coinjected with cRNA encoding α_{SkM2} and the 5HT1C receptor, an inhibition of peak sodium inward current (I_p) of 60 % was observed. 5-HT application to oocytes injected with α_{SkM2} cRNA only, as well as injection of inositol tris-phosphate (IP_3) were ineffective in reducing I_p. Extracellular application of phorbol myristate acetate (PMA) mimicked the effects of 5-HT. Steady-state inactivation and recovery from inactivation were not effected by this modulation. Voltage dependent activation of α_{SkM2} subunits was shifted by 5.7 mV towards more positive membrane potentials.

From our experiments we conclude that PKC modulates cardiac sodium channel activity and kinetics leading to a reduced excitability upon PKC stimulation.

Tu-Pos366

MODULATION OF CARDIAC Na^+ CHANNELS EXPRESSED IN A MAMMALIAN CELL LINE AND IN VENTRICULAR MYOCYTES BY PROTEIN KINASE C

((Y. Qu, Y. Wang, J. Rogers, T. Tanada, T. Scheuer, W.A. Catterall)) Dept. of Pharmacology, U. of Washington, Seattle, WA 98195

Cardiac rH1 Na^+ channel α subunits were stably expressed in Chinese hamster lung 1610 cells (SNa-rH1 cells). We used whole cell and cell-attached patch clamp recording to characterize the voltage-dependent properties of these channels and determine how they were modulated by activation of protein kinase C (PKC). Similar experiments were performed in primary cultured neonatal ventricular myocytes. Mean Na^+ current in SNa-rH1 cells was 2.2 ± 1.0 nA which corresponds to a cell surface density of 1-2 channels per μm^2. The expressed cardiac Na^+ current was TTX resistant (Kd = 1.8 μM) and had similar voltage-dependent properties to the Na^+ current in neonatal rat ventricular myocytes. In cell-attached patches the PKC activator 1-oleoyl-2-acetyl-sn-glycerol (OAG) (10 μM) decreased this current 33% at a holding potential of -114 mV and 56% at -94 mV. This reduction in peak current was accompanied by an 8-14 mV negative shift of steady-state inactivation without any change in activation. Effects of OAG in SNa-rH1 cells and in neonatal rat cardiac myocytes were similar, except that it slows macroscopic Na^+ current inactivation only in myocytes bathed in low Ca^{2+} (1 μM) or Ca-free solution. The effects of OAG on cardiac Na^+ current were blocked in cells that had been previously microinjected with a peptide inhibitor of PKC but not with a peptide inhibitor of cAMP-dependent protein kinase indicating that PKC is responsible for the effects of OAG. Single-channel recordings from SNa-rH1 cells showed that OAG decreased the ensemble average current without inducing late openings observed with PKC modulation of neuronal and skeletal muscle Na^+ channels. Such Na^+ current reductions may have profound effects on cardiac cell excitability.

Tu-Pos367

cAMP-DEPENDENT PROTEIN KINASE INDUCES A DEPOLARIZATION-DEPENDENT POTENTIATION OF RAT BRAIN Na^+ CHANNELS
((M. Li, W.A. Catterall and T. Scheuer)) Dept. of Pharmacology, U. of Washington, Seattle, WA 98195. (Spon. by S.D. Critz)

Na^+ channels normally recover from inactivation within a few ms of returning to the holding potential. We found that Na^+ currents due to rat brain type IIA Na^+ channel subunits expressed in Chinese hamster ovary cells (CNaIIA cells) were actually potentiated up to 2-fold after recovering from inactivation and that this potentiation required cAMP-dependent protein kinase (PKA). Whole cell Na^+ currents were studied using a 50-200 ms long conditioning pulse to between -20 and +60 mV, a 15 ms interval at -100 mV to allow recovery from inactivation and then a test pulse to potentials between -30 and -10 mV. Test pulse currents were potentiated by conditioning prepulses when the pipet solution contained 50 nM of the catalytic subunit of PKA (cA-PK) and 1 mM ATP but not when the pipet contained 10 M of a specific peptide inhibitor of PKA (PKI). Likewise, potentiation was observed in cell-attached macro-patches on control CNaIIA-1 cells but not in similar cells co-expressing a dominant negative mutant of the regulatory subunit of PKA which prevents activation of PKA. Potentiation was strongest for test pulses between Na^+ current threshold and 0 mV and was not seen in test pulses positive to +20 mV, consistent with it being due to a 5-6 mV transient negative shift in the voltage-dependence of activation after the conditioning pulse. Potentiation increased with conditioning pulse depolarization and duration and decayed slowly after a conditioning pulse with a half time of 150 ms at -100 mV. The PKA-dependent potentiation described here would strongly increase Na^+ current, particularly near threshold, and thus favor excitability during repetitive activity.

Tu-Pos368

MOUSE SOLEUS MUSCLE FIBERS EXHIBIT AN INCREASE IN NA CHANNEL DENSITY FOLLOWING INNERVATION BY A FOREIGN NERVE.
((R.L.Milton and M.Behforouz)), Indiana University School of Medicine, Muncie Center for Medical Education, Ball State University, Muncie, IN 47306.

The superficial peroneal nerve in the mouse hind limb was cut and transplanted on to the proximal dorsal surface of the soleus muscle. Two weeks later the limb was reopened and the soleus muscle denervated. These surgical procedures have been shown to induce the formation of new foreign endplates on soleus muscle fibers, many of which exhibit morphological characteristics similar to those innervating fast twitch muscle fibers (Waerhaug et al., Anat. Embryol., 151, 1-15, 1977). Four months after denervation the soleus muscle was dissected out of the animal and the formation of foreign endplates confirmed by the use of fluorescently labeled α-bungarotoxin. The loose patch voltage clamp technique was then used to measure peak Na current density in the region of the muscle receiving foreign innervation. These measurements revealed an approximate doubling of peak current density in these regions (34.0 ± 2.5 mA/cm^2, mean $\pm$ SEM, from foreign innervated muscles versus 17.9 ± 2.1 mA/cm^2 from normal muscles). These results suggest that motoneurons can exert considerable control over Na channel density in the muscle fibers they innervate.

Supported by NIH grant AR40801.

Tu-Pos369

SODIUM CHANNEL CYTOPLASMIC DOMAIN STRUCTURE PROBED USING A SOLUTION PHASE ANTIBODY COMPETITION ASSAY
((Weijing Sun, Robert L. Barchi, and Sidney A. Cohen)) University of Pennsylvania School of Medicine, Philadelphia, PA. 19104

We investigated the spatial relationships among cytoplasmic segments of the sodium channel by examining the interactions between antibodies to defined epitopes within these regions. Anti-peptide polyclonal antibodies directed against epitopes in the N- and C-termini and each of the three interdomain regions were examined for interactions with monoclonal antibodies with epitopes in the proximal N-terminus or interdomain 2-3 regions. Measurements were performed using a solution-phase assay in which solubilized channel protein retains the ability to bind ^{3}H-STX. Except for distal C-terminal polyclonal antibodies (which inhibited proximal N-terminal monoclonal antibody binding with an unusually steep concentration dependence), polyclonal antibody binding to each intracellular region (including the N-terminus) had no effect on N-terminal monoclonal antibody binding. However, interdomain 2-3 monoclonal antibody binding was uniformly inhibited by polyclonal antibody binding to each intracellular region. Our results confirm the localization of each of these segments to the same surface of the channel (cytoplasmic) and indicate: 1) that the N-terminus assumes a rigid, folded structure; 2) that the interdomain 2-3 region assumes a flexible conformation capable of interacting with each cytoplasmic segment; and 3) that the proximal N- terminus and distal C-terminus have a unique spatial relationship which may help to stabilize the quaternary structure of the channel.

Tu-Pos370

HETEROGENOUS PROPERTIES OF VOLTAGE-DEPENDENT CARDIAC Na^+ CHANNELS IN THE CELL-ATTACHED PATCH CONFIGURATION
((Th. Böhle and K. Benndorf*)) Zentrum für Physiologie, Universität zu Köln, 50924 Köln, Germany. *Heisenberg-fellow of the Deutsche Forschungsgemeinschaft. (Spon. by C. Methfessel)

Giga-seal formation may alter the characteristics of Na^+ channels (Kimitsuki et al., Am. J. Physiol. 258, H247-H254, 1990). In cardiac ventricular cells isolated from adult white mice Na^+ channels were investigated in the cell-attached patch configuration at low noise using short, thick-walled pipettes sealed at the rear end with oil (Benndorf, Pflügers Arch. 422, 506-515, 1993). In 29 patches (118799 sweeps, pipette resistance 4-97 MΩ, seal resistance 0.3-1000 GΩ) steady-state inactivation (20 ms prepulse duration) and steady-state activation were determined. In multi-channel experiments the inactivation curve was initially shifted up to 40 mV to more negative potentials. The activation curve was shifted to negative potentials only by up to 20 mV. Independently of the initial shift, in part of the experiments an additional time-dependent shift of up to 60 mV in the same direction was observed for both curves. Neither of the shifts was correlated to the tip diameter of the patch pipettes. In extraordinarily small patches containing one and only one channel, a slow switch between at least two gating modes with different open probabilities was investigated by the perpetual measurement of the mean current per time interval. It is concluded that in single channel experiments steady-state activation and inactivation strongly depend on the actual mode of operation. A possible role of the different gating modes for the shifts of steady-state activation and inactivation is discussed.

Tu-Pos371

MODULATION OF THE NUMBER OF ACTIVATABLE Na^+ CHANNELS BY $[Ca^{2+}]_i$ AND A PHOSPHATASE BLOCKER.
((M. Egger and N.G. Greeff)) Physiologisches Institut, Universität Zürich, Winterthurerstr. 190, CH-8057 Zürich, Switzerland.

We show that $[Ca^{2+}]_i$ in N1E115 cells modulates the peak Na^+ current density (I_{Na}). Approximate doubling in the peak Na^+ current densities was found for intracellular perfusion media with free $[Ca^{2+}]_i$ varying between 1 nM and 100 nM . This Ca^{2+} mediated effect on Na^+ current acts independently from the Ca^{2+} buffer system (Ca^{2+}/EGTA or Ca^{2+}/BAPTA) used. We show that this effect is not correlated with changes in the steady- state inactivation and activation process. In order to study further the $[Ca^{2+}]_i$ induced modulation of I_{Na} the phosphatase blocker ocadaic acid was used. Ocadaic acid (30 nM) in the pCa 9 and 7 (EGTA buffered) perfusion media increased I_{Na} to an equal level which is about 50% higher than in pCa 9 alone. In addition, using non- stationary fluctuation analysis of I_{Na} we could demonstrate the single channel conductance (about 0.58 pA) to be the same under all conditions. Therefore, the significantly higher current densities at pCa 7 and under ocadaic acid could be explained in terms of an increased number of activatable sodium channels. This significant increase of I_{Na} induced by the phosphatase inhibitor and/or high internal free Ca^{2+} compared with pCa 9 alone suggests a strong crosstalk between $[Ca^{2+}]_i$ and phosphorylation processes which results in a functional modulation of the number of activatable Na^+ channels in the cellular membrane. (Supported by Swiss National Fund 31-27788.89)

Tu-Pos372

VOLTAGE-GATED SODIUM CHANNELS IN CULTURED HUMAN AORTIC SMOOTH MUSCLE CELLS.
((R. H. Cox, Z. Zhou and T. N. Tulenko.)) Bockus Res. Inst., Grad. Hosp., Dept. of Physiol., Univ. of PA, and Med.Col. of PA., Phila., PA.

Cultured human aortic smooth muscle cells were used to investigate ion channel properties by whole cell, voltage clamp methods. Cells were plated on glass coverslips, cultured in supplemented M199 media at low serum (1%), and studied at passages 4-6. Inward currents were measured with a Cs^+/TEA^+ pipet solution and with 2.5 mM $[Ca^{2+}]_o$ in the perfusate. Inward currents activated at about -50mV, peaked at about 0mV, and reversed at about +40mV. These currents activated and inactivated rapidly; time to peak current = 2.4±0.3 s, and rate of inactivation = 1.8±0.2 s (@ 0mV test potential, holding potential = -80mV). With a cAMP-free pipet solution, maximum inward current averaged 4.9±0.9 pA/pF. With 10μM cAMP in the pipet solution, maximum inward currents averaged 14.7±3.3 pA/pF. Nisoldipine (10μM) had no effect while 0.1mM Cd^{2+} had only small effects (decreased amplitude and increased inactivation rate) on these currents. The currents were decreased with a reduction in extracellular Na^+ and they were completely inhibited by 10nM TTX, suggesting they represented voltage-gated Na^+ currents (I_{Na}). Lowering external $[Ca^{2+}]_o$ to zero, increased the maximum I_{Na} and greatly increased its rate of inactivation. Increasing external $[Mg^{2+}]_o$ decreased I_{Na} and slowed the rate of inactivation. These studies demonstrate the presence of voltage-gated Na^+ channels with high TTX sensitivity in cultured human aortic smooth muscle cells. These channels are modulated by external divalent cations and may be regulated by cAMP.

Tu-Pos373

MODULATION OF CARDIAC I_{Na} BY ACIDOSIS. ((C.L.Watson, M.R.Gold)) University of Maryland, Baltimore, MD 21201

Conduction slowing is a critical element of reentrant ventricular arrhythmias. Since acidosis is an early consequence of ischemia, we hypothesized that pH could cause changes in I_{Na} that would affect cardiac conduction. To test this hypothesis the whole cell patch clamp method was used to measure I_{Na} in neonatal rat ventricular myocytes exposed to an extracellular pH(pHe) of 7.4, 7.2, 6.9 or 6.4 while perfused at an intracellular pH(pHi) of 7.2, 7.0, 6.7 or 6.2, respectively. Standard protocols were used to evaluate activation, inactivation and reactivation kinetics. Repetitive 200ms depolarizations from -90mV to 0mV were delivered to assess phasic and tonic block of I_{Na}. Stimulation rates of 0.5 to 3 Hz caused a frequency dependent decline in I_{Na} (26% at 3 Hz) that was not significantly affected by acidosis. Trains of 200ms pulses at 2 Hz and holding potentials from -110mV to -70mV caused a 40% decrease of I_{Na} at -70mV, independent of pH. While phasic block was not affected, there was a significant decrease in initial peak I_{Na} during acidosis (24.4 ± 2.7 vs 17.1 ± 2.9 pA/pF), an increase in time to peak current, and a depolarizing shift in half inactivation. Independent changes of pHe and pHi indicate that both the reduction in peak I_{Na} and the shift in steady-state inactivation are a function of pHe, while recovery from inactivation is modulated by pHi. Time to peak I_{Na} appears to depend on both pHe and pHi. We conclude that acidosis has important effects on I_{Na} amplitude and kinetics in cardiac myocytes.

Tu-Pos374

EFFECTS OF TIME AND H_2O_2 ON SLOWLY INACTIVATING SODIUM CHANNELS OF FELINE MYOCARDIAL CELLS. ((P.L. Barrington, R.L. Martin, and K. Zhang)) Dept. of Pharmacology, Northwestern University, Chicago, IL 60611.

Tetrodotoxin (TTX) blocks the effects of H_2O_2 on the action potentials of rat and guinea pig ventricular myocytes (Beresewicz and Horackova, 1991). Voltage clamp experiments on frog myocytes exposed to *tert*-butyl hydroperoxide suggest reduced peak sodium current (I_{Na}) and shifts in activation and inactivation curves that predict an increased Na window current (Bhatnagar, et al., 1990). Evidence for an increased Na window current or slowly inactivating I_{Na} was sought using whole-cell voltage clamp techniques. I_{Na} was monitored in feline ventricular myocytes isolated by collagenase perfusion. Substitution of Cs^+ for K^+ in internal and external solutions blocked K currents while F^- in internal solutions prevented Ca currents. Cells were exposed to either 1 mM H_2O_2 for 30 min or left untreated. Voltage ramps from -100 to 0 mV run at 10 to 100 mV/s and a transmembrane Na gradient of 135 mM (19-20 °C) were used to elicit a TTX-sensitive, slowly inactivating I_{Na}. A reverse ramp, 0 to -100 mV at 2 mV/s, failed to elicit a true "window" current. In untreated cells peak I_{Na} amplitude during voltage ramps increased for 20 mins after membrane rupture, then decreased. A time-dependent shift of peak current to more negative voltages was seen. Current-voltage relationships (IV) and steady-state inactivation curves (h_∞) were determined at 12-15 °C with a transmembrane Na gradient of 10 mM. In untreated cells, peak IV increased and shifted to more negative potentials with time; a similar negative shift in h_∞ was seen. The time courses of slowly inactivating I_{Na}, IV and h_∞ changes in cells exposed to H_2O_2 were the same as those for untreated cells. Thus, no evidence of a H_2O_2 induced increase in slowly inactivating I_{Na} was found. These results suggest that H_2O_2 induced changes in cellular action potentials do not occur by direct action on Na channel proteins or supporting lipids.

Tu-Pos375

Rapid Onset of Lysophosphatidylcholine Effects on Sodium Current in Rat Ventricular Myocytes

Gregg S. Shander, Albertas I. Undrovinas and Jonathan Makielski
The University of Chicago, Chicago, Illinois

Lysophosphatidylcholine(LPC), an ischemic metabolite, may be responsible for some of the electrophysiological changes in acute ischemia. Recently, effects of LPC upon Na current(I_{Na}) kinetics have been reported. Here we expand these observations to include effects on steady-state inactivation(h_∞), recovery from inactivation and detailed timing of onset. We studied I_{Na} by the whole cell voltage clamp technique at 23 °C with reduced Na(45mM out, 5mM in) from a holding potential of -150mV. Changes in electrophysiological parameters were measured after LPC 10μM was added to the bath(n=5) and compared to cells for which no LPC was added(time controls, TC, n=4). Normalized peak I_{Na} at -30mV declined 19.6%±10.1% as compared to an increase of 1.1%±9.2% for (TC)(p=.05 t-test). The decay of I_{Na} was best fit with two time constants. (τ_{fast}) increased from 0.75±.03ms to 1.13±.10ms(p<.01) and (τ_{slow}) decay prolonged from 2.47±.36 to 3.63±.13ms (p<.01) both significant with respect to (TC)(p=.02,p<.01) respecitively. The rate of shift of the midpoint of the h_∞ relationship (250ms conditioning) increased after addition of LPC from .32±.08mv/min to .73±.09mv/min(p<.01) as compared to a decrease in the rate of shift of (TC). The time constant of slow recovery from inacativation (conditioning step -30mV, 1000ms) was also prolonged by LPC from 111.1±36.56ms to 228.69±29.84ms(p<.01) again significant with respect to (TC) (p<.01). The ratio of the amplitudes were not effected by LPC with slow τ contributing = 20%. The onset of effects occured between 12 and 16 minutes after adding LPC to the bath. Effects on decay and recovery from inactivation were partially reversed in two cells and cell survival was less than 20 minutes if LPC was not removed from the bath. We conclude that the whole-cell I_{Na} changes further implicate LPC as a deleterious ischemic metabolite.

Tu-Pos376

CONCENTRATION-DEPENDENT ENHANCEMENT OF SODIUM CHANNEL CONDUCTANCE BY LACTATE IN GUINEA-PIG VENTRICULAR MYOCYTES

((H. Guo, J.A. Wasserstrom, J.E. Rosenthal)) Reingold ECG Center, Northwestern University Medical School, Chicago, IL 60611

We have previously reported that Na lactate increases Na^+ current (I_{Na}) in isolated guinea-pig ventricular myocytes. We investigated (1) the potency of the lactate induced effect on I_{Na}, and (2) if the lactate effect on the Na^+ channel is direct or indirect (e.g. due to a change in intracellular pH or removal of the inhibitory effect of divalent cations due to chelation by lactate). Assessment of the dose-response relationship of the lactate effect (using cesium lactate) showed a sigmoidal, concentration dependent increase in I_{Na}, with apparent K_d=1.8 mM and Hill coefficient of 1.8. The maximal response occurred at 10 mM. The effects of lactate on I_{Na} were qualitatively similar with internal solutions containing low (5 mM) and high (20 mM) concentrations of HEPES buffer; with lactic acid, the Na^+ and the Cs^+ salts of lactate; and when Mg^{2+} (1.0 mM) was omitted from all solutions. Ca^{2+} sensitive electrode measurement showed that lactate (1-10 mM) did not significantly alter the Ca^{2+} activity in the test solutions. **Conclusions:** (1) lactate increases I_{Na} conductance in a sigmoidal, concentration-dependent manner. (2) This increase occurs by a mechanism that involves neither chelation of Ca^{2+} or Mg^{2+} by lactate nor changes in intracellular pH resulting from lactate influx, but rather appears to be a direct action on the Na^+ channel.

Tu-Pos377

STRUCTURAL AND FUNCTIONAL ASPECTS OF TNF-α and TNF-β ION CHANNEL ACTIVITY. ((William A. Ernst, Tajib Mirzabekov*, Bruce L. Kagan* and Bernadine J. Wisnieski)) Dept. of Microbiology and Molecular Genetics and *Dept. of Psychiatry, UCLA, Los Angeles, CA 90024.

Having ascertained that TNF-α exhibits acid-enhanced membrane binding, insertion, and ion channel formation, as well as acid-enhanced killing of human U937 histiocytic leukemia cells and induction of Na^+ uptake in these cells, we have now demonstrated that the related protein called TNF-β or lymphotoxin also exhibits intrinsic ion channel activity. With the free protein, this activity is most readily observed when the pH of the solution in the *cis*-compartment of a planar bilayer chamber is acidified. However, when TNF-α and TNF-β are added in a DMPC vesicle-embedded formulation prior to planar bilayer construction from azolectin, channel activities are readily detected solely upon application of a membrane potential. Thus, the low pH-requirement for optimal channel activity seen when the free forms of the proteins are used reflects a requirement for membrane binding and insertion and not for channel opening, which remains voltage-dependent. We have also analyzed the effects of various channel modulators (e.g., monoclonal antibodies, Ca^{2+}), and the relationship between the structure of acid-treated and membrane-inserted TNF and channel activity. Among the methods employed, native gel electrophoresis and crosslinking studies were conducted to assess the structures of the larger-sized but apparently discrete channels that appear after 30 to 60 min with free TNF and almost immediately with vesicle-embedded TNF. [Grants USPHS GM22240 (BJW) & NIMH MH43433 (BLK)]

Tu-Pos378

THYROID HORMONE ENHANCES AVAILABILITY OF SINGLE SODIUM CHANNEL IN GUINEA-PIG VENTRICULAR MYOCYTES

((Yoshihide Sakaguchi, Luyi Sen)) VAMC/West LA and UCLA School of Medicine Los Angeles, CA 90073

It has been reported that thyroid hormones play an important role on cardiac electrophysiological properties. Previous study from our laboratory has shown that thyroid hormone enhances whole-cell cardiac sodium currents.

To estimate the detailed mechanism for enhancement of sodium channel current(I_{Na}) by thyroid hormones, single I_{Na} was recorded in guinea-pig ventricular myocytes before and 25 min after superfusion of T_3(3,5,3'-triiode-L-thyronine) using cell-attached single channel recording technique (holding potential = -140mV). T_3 10^{-8} M caused an increase in ensemble I_{Na} from 344 ± 31 to 570 ± 73 pA(1000 sweeps) at test potential(TP) = -30mV (n = 8, $p<0.005$). T_3 also significantly increased ensemble I_{Na} at TP = -40, -50 and -60mV. Probability of null sweeps was significantly reduced by T_3 at each TP (Figure). However mean open duration, channel unit amplitude and averaged number of openings per sweep with openings did not change at each TP. These results demonstrate that T_3 enhances I_{Na} by reduction of null probability without any changes in open behavior. As we know, nulls are considered to be transition to inactivated state directly from the closed state(C) without entering the open state(O). Thus, reduction of null probability by T_3 could result from acceleration of transition from C to O.

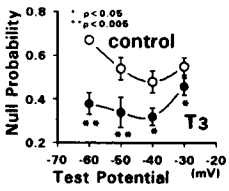

Tu-Pos379

A NEW LOW-VOLTAGE-ACTIVATED CA CURRENT THROUGH NA CHANNELS IN HUMAN ATRIAL MYOCYTES ?

S. Lemaire, C. Piot, J. Seguin, J. Nargeot and S. Richard (spon. by C. Malécot)
CRBM, CNRS, Route de Mende, BP 5051, 34033 - Montpellier - France.

The present report characterizes the electrophysiological and pharmacological properties of a Low-Voltage-Activated Ca^{2+} current (I_{Ca}) evidenced in human atrial myocytes. I_{Ca} were recorded using the whole-cell patch-clamp technique (20-22 °C) in enzymatically dispersed myocytes obtained during cardiac surgery. All recordings were obtained using Na^+-free extracellular solutions (in mM: TEACl: 136, $CaCl_2$: 2, $MgCl_2$: 1.1, 4-AP: 4, HEPES: 25, dextrose: 22; adjusted to PH 7.4 with TEAOH). Recording pipettes contained (in mM) : Cs-aspartate (120), EGTA (10), HEPES (20), (Mg) ATP (3), (Mg) GTP (0.4) ; adjusted to PH = 7.2 with CsOH. During depolarizations from a HP of -100 mV, the LVA I_{Ca} begins to activate at ~-50 mV and peaks at ~-35 mV. This current shares many properties of T-type I_{Ca} including a transient waveform, availability only from negative HPs (< -60 mV), dependence upon extracellular Ca^{2+} or Ba^{2+} and blockade by inorganic divalent cations such as Co^{2+} (2 mM) and Cd^{2+} (100 µM). However, it was insensitive to La^{3+} (which blocks T- and L-type Ca^{2+} currents at 10 µM) but was suppressed by tetrodotoxin (10 µM) and was potentiated by veratridine (veratrine 0.5 mg/ml) which are specific for the Na channel. This current is not linked to pathology and seems specific of the atrium since it was also observed in atrial, but not in ventricular, myocytes from adult rats. We suggest therefore that this LVA Ca^{2+} current reflects the presence and activation of Na channels markedly altered in their selectivity for Na^+ ions in atrial myocytes. We are currently investigating its physiological relevance.

Tu-Pos380

ON PHYSIOLOGICAL ROLE OF BACKGROUND NA CHANNELS.

((Y. I. Zilberter, C. F. Starmer and A. O. Grant)) Duke University Medical Center, Durham, NC 27710.

Properties of two types of late Na channel openings,burst and background, and their contribution to a steady-state Na conductance in rabbit ventricular cells were studied using single channel recordings.The existence of this conductance in the range of cell resting potential was confirmed by application of TTX in the whole-cell configuration. In 5 cells,the average steady-state inward current decreased by 2 3±12.4 and 15.3±9.1 pA at -70 and -80 mV respectively. After step depolarization, burst Na channels could be active for more than 3 seconds but then underwent inactivation.Busts also terminated promptly on repolarization to -80 mV.We conclude that the bursting mode of channel gating does not contribute to resting Na conductance.Background channel openings were recorded at constant potentials in the range of -120-0 mV.At step depolarization, background channels underwent incomplete inactivation.We used the channel mean open time as a criterion for distinguishing background channel openings and openings related to the initial transient current.Voltage dependency of the mean open time for each channel type was bell shaped with maxima separated by 20-30 mV. In 5 patches, the mean open time for early Na channels was: 0.89-±0.15 ms at - 40 mV and 0.66±0.12 ms at -70 mV; for background Na channels it was: 0.34±0.061 ms at -40 mV and 0.49±0.082 ms at -70 mV.Analysis showed that after step depolarization to potentials in the range of activation threshold and more negative, e.g. to -70 and -80 mV, a significant fraction of Na currents is carried through background channels.We suggest that background channels represent a special type of Na channels which can play an important role in the initiation of cardiac action potential and in the resting Na conductance.

Tu-Pos381

ONTOGENY OF VOLTAGE-GATED CHANNEL EXPRESSION DURING MURINE EMBRYONIC STEM CELL CARDIOGENESIS.

((T.D. Bahnson, S.J. Fuller, J. Schnee, and K.R. Chien)) University of California San Diego, La Jolla, CA 92093-0636. (Spon. by J.W. Covell)

Little is known about the ontogeny of voltage-gated ion channels during mammalian cardiogenesis. Accordingly, we purified spontaneously beating muscle cells from 12-14 day murine embryoid bodies. To determine whether these cells represent cardiac progenitor cells, and to characterize the currents responsible for spontaneous excitability, whole-cell patch-clamp recordings were made within 1-2 days of purification. Cells had a spontaneous beating frequency (@22°C) of 59 ± 11 per minute (mean ± S.E.M., n=9). Current-clamp records revealed a V_m of -56 ± 7 mV (n=8, maximum negative diastolic potential). Beating was dependent on extracellular Na^+ and Ca^{2+}. The predominant voltage-activated current was inward and reversed at 66 ± 4 mV (n=7), consistent with a Na^+ current (E_{Na} = 66.7 mV). This current was insensitive to 10 µM tetrodotoxin. Current density was 75 ± 9 pA/pF, the voltage for ½ maximal activation was -33 ± 3 mV (n=7), and steady state voltage for ½ maximal inactivation was -46 ± 3 mV (n=7). Typical voltage-activated outward currents were not apparent at this developmental stage using standard intracellular and extracellular salines. Thus, these cells demonstrate Na^+ currents similar to those recently described in developing heart cells from chick, mouse, and hamster. Since mouse embryonic stem cells are amenable to genetic manipulation via homologous recombination, this represents an ideal system to study the ontogeny of voltage-gated channels during cardiogenesis.

K CHANNELS II: REGULATION AND BLOCK

Tu-Pos382

TREMORGENIC INDOLE ALKALOIDS ARE POTENT BLOCKERS OF MAXI-K CHANNELS.

((O.B. McManus, H.-G. Knaus, S.H. Lee, L.M.H. Helms, M. Sanchez, K.M. Giangiacomo, W.A. Schmalhofer, G.J. Kaczorowski and M.L. Garcia)) Departments of Membrane Biochemistry and Biophysics, and Natural Product Chemistry, Merck Research Labs, PO Box 2000, Rahway, NJ 07065

We describe a class of indole alkaloids that are potent inhibitors of high-conductance calcium-activated potassium (maxi-K) channels. Tremorgenic indole alkaloids produce neurological disorders in ruminants whose food supply is contaminated with these mycotoxins. Their mode of action is not understood, but may be related to their known effects on neurotransmitter release. To determine whether these effects could be due to inhibition of potassium channels, we examined the interactions of various indole diterpenes with maxi-K channels from bovine aortic smooth muscle. Aflatrem, paspalitrem C, penitrem A, and paspalitrem A inhibited binding of [^{125}I]charybdotoxin (ChTX) to maxi-K channels with half-maximal effects occurring at 0.2 to 2 uM. In contrast, two structurally related compounds, paxilline and verruculogen enhanced toxin binding by about two fold with a half-maximal effect occurring at 170 nM. As predicted from the binding studies, covalent incorporation of [^{125}I]ChTX into the 31 kDa subunit of the maxi-K channel was blocked by compounds that inhibit [^{125}I]ChTX binding and enhanced by compounds that stimulate [^{125}I]ChTX binding. Modulation of [^{125}I]ChTX binding was due to allosteric mechanisms. Despite their different effects on binding of [^{125}I]ChTX to maxi-K channels, all compounds potently inhibited maxi-K channels in electrophysiological experiments. When applied the internal side of the channels, 10 nM of the various indole diterpenes blocked the channels by 70 to 100%. Other types of voltage-dependent or Ca-activated K channels examined were not affected at these concentrations. These data suggest that indole diterpenes are the most potent non-peptidyl inhibitors of maxi-K channels identified to date. Some of their pharmacological effects may be due to inhibition of maxi-K channels.

Tu-Pos383

STEREOSELECTIVE BUPIVACAINE BLOCK OF THE HUMAN CARDIAC DELAYED RECTIFIER Kv1.5 CHANNEL.

((C. Valenzuela, E. Delpón, O. Pérez, M.M. Tamkun, J. Tamargo, D.J. Snyders)). Dept. Pharmacology, Univ. Complutense, Madrid, SPAIN and Vanderbilt Univ., Nashville, TN 37232.

The effects of bupivacaine (B) enantiomers on a cloned human cardiac potassium channel (hKv1.5) expressed in a stable Ltk$^-$ cell line were studied using the whole-cell configuration of the patch-clamp technique. Neither S(-)-bupivacaine (SB) or R(+)-bupivacaine (RB) modified the initial activation time course of the hKv1.5 current at 20 µM, but both induced a subsequent fast decline to a lower steady-state current level with time constants of 18.7±1.1 ms (SB) and 10.9±0.9 ms (RB). Steady-state block (250 ms depolarization to +60 mV) was significant less for SB compared to RB (31±2% vs. 80±3%, n=12, $p<0.001$). SB and RB inhibited hKv1.5 with an apparent K_D of 27.3 and 4.1 µM, respectively. Block by both enantiomers displayed a similar voltage dependence consistent with a binding reaction sensing 16% of the applied electrical field (δ=0.16±0.01, from inside). Compared to control, both SB and RB reduced the tail current amplitude upon return to -40 mV, and slowed the deactivation time course resulting in a "cross-over" phenomenon. The results indicate that 1) both isomers act as open channel blockers of hKv1.5, 2) binding occurs most likely at the same site presumably in the internal mouth of the ion pore, 3) block is stereoselective with a 1.2 Kcal/mole difference in binding energy between both enantiomers. The latter may derive from the relatively rigid configuration of aromatic and amine moieties around the chiral center.

Supported by CICYT SAF92-0157, Salud 2000 and NIH HL47599.

Tu-Pos384

EFFECTS OF THE ENANTIOMERS OF A NEW BRADYCARDIC AGENT ON HKV1.5 CHANNELS. ((E. Delpón, C. Valenzuela, O. Pérez, D.J. Snyders, J. Tamargo)). Dpt. Pharmacology. School of Medicine. Univ. Complutense, Madrid, SPAIN and Vanderbildt Univ. Nashville, TN 37232.

S-16257-2 (S57) and S-16260-2 (R60) are the (S) and (R) enantiomers of a new benzazepin-2-on derivative which exhibits bradycardic effects. We have characterized the effects of S57 and R60 on cloned human cardiac potassium channels (hKv1.5) expressed in a stable Ltk$^-$ cell line using the whole-cell configuration of the patch-clamp technique. During the application of 250 ms pulses to +60 mV the block increased progressively, reaching similar values with S57 and R60 (64.0 ± 2.0% vs. 64.0 ± 1.3%, respectively) (n=5, P > 0.05), resulting in a fairly similar apparent K_D (24.3 μM and 31.6 μM, respectively). However, the time course of the decline was faster for R60 than for S57. The blockade induced by both enantiomers was voltage-dependent, and the voltage dependence indicated that both enantiomers act from the inside of the membrane and move about 19% (δ= 0.19 ± 0.004) into the membrane electrical field. Relative to control, both S57 and R60 reduced and slowed the tail currents recorded on return to -40 mV, resulting in a "crossover" phenomenon. These results indicate that both enantiomers interact primarily with the open state of the channel and that they must dissociate from the channel before it can close. Although there was no stereoselectivity in the apparent affinity, the blocking rate for R60 was faster. Supported by CICYT (SAF92/0157), Salud 2000 and NIH HL 47599.

Tu-Pos385

BLOCK OF THE CARDIAC DELAYED RECTIFIER (I_K) BY THE 5-HT$_3$ ANTAGONISTS, ONDANSETRON AND GRANISETRON. ((F. de Lorenzi, T. Bridal and W. Spinelli)) Wyeth-Ayerst Research, Princeton, NJ 08543.

Antagonists of the 5-HT$_3$ receptors have been shown to alter cardiac repolarization. This action may explain adverse cardiac effects observed in animal models and humans. We have studied the effects of two clinically used 5-HT$_3$ antagonists, Ondansetron (O) and Granisetron (G), on the delayed rectifier (I_K) of cat ventricular myocytes using whole-cell current recordings at 36°C. Tail current amplitude on repolarization to -45 mV was used to estimate the effects on I_K. O and G fully blocked I_K with IC_{50}=1.2±0.3 μM and 3.6±0.1 μM (S.E.), respectively. The block was reversible and independent of the duration of the depolarizing steps (250-2500 ms). Activation curves (-45 to +45 mV) were well described by the Boltzmann distribution: neither drug affected $V_{1/2}$ or k. The percentages of block between -25 and +45 mV were well fitted by the normalized activation curve, suggesting open state block. Fractional electrical distance (δ) associated with block of I_K by the charged form of each molecule was 0.08 and 0.11 for O and G, indicating a weak dependence on the transmembrane electric field. The block of I_K was accompanied by a significant increase in APD. O (1 μM) and G (3 μM) prolonged APD_{90} by 37±10 % and 37±11 % (0.5 Hz; n=3) without altering resting potential or other parameters. In conclusion, our data are consistent with an open state block of I_K at a site close to the inner opening of the channel. Block of I_K by the 5-HT$_3$ antagonists O and G might underlie the reported abnormalities of repolarization.

Tu-Pos386

COMPLEX REGULATION OF K^+ CONDUCTANCE BY OPIOID RECEPTOR LIGANDS IN DRG NEURONS AND F11 CELLS. ((S.F.Fan[1,2] and S.M. Crain[2])) [1]Dept. Neurosci. AECM, Bronx, NY 10461 and [2]Dept. Physiol. Biophys. SUNY, Stony Brook, NY 11794.

The effects of opioid ligands on the whole-cell K^+ currents (I_K) of cultured mouse DRG neurons and neuroblastoma x DRG neuron hybrid F11 cells were studied. (1) The effects of μ, δ and κ selective opioid receptor agonists (DAGO, DPDPE, Dyn A[1-13], U-50,488H and morphine) were dose-dependent. Low conc. (<nM) usually elicited a transient increase in I_K (< 1 min) followed by a sustained decrease in I_K, whereas μM conc. rapidly elicited a sustained increase in I_K. After brief treatment with cholera toxin subunit B, low conc. of opioids elicited only a sustained increase in I_K. In contrast, after chronic treatment with pertussis toxin, more than half of cells responded with a sustained decrease of I_K when tested with uM as well as nM opioids. (2) The opioid receptor antagonist, naloxone (NLX) alone had no effect on I_K in naive cells when tested in regular saline with or without 5mM Ba^{2+}. After acute treatment with GM1 ganglioside (1 μM for 20-30 min), nM NLX decrease I_K. Ba^{2+} was not required. In contrast, after chronic opioid treatment (1μM DADLE for 3-7 days) NLX decrease I_K in most cells, but only when Ba^{2+} was presented. These results indicate that more complex signal transduction systems are involved in the regulation of K^+ channel activities via opioid receptors than that suggested by us previously. (Supported by NIDA Grant DA-02031 to S.M.C.)

Tu-Pos387

MODULATION OF AN INWARD RECTIFYING K^+ CURRENT EXPRESSED FROM RAT BRAIN RNA. ((L. DiMagno, N. Dascal*, N. Davidson, H.A. Lester, W. Schreibmayer#)) Caltech, Pasadena CA 91125, *Tel Aviv Univ., Ramat Aviv, Israel, #Univ. of Graz, Graz, Austria

We are investigating an inwardly rectifying K^+ channel which can be expressed following injection of rat brain poly A^+ mRNA into *Xenopus* oocytes. When the perfusion solution is changed from ND96 (2 mM K^+) to high K^+ (HK; 96 mM K^+) solution an inward rectifying K^+ current (I_{HK}) is observed (1.14 +/- 0.07 μA at -80mV; 5 oocytes). Native oocytes in HK solution do not show sensitivity to the neurotransmitter serotonin (5HT), but in oocytes injected with rat brain mRNA application of 2-10 nM 5HT produced two inward current responses. The first 5HT response is the usual transient, inward oscillatory Cl^- current. In the second phase, the I_{HK} is inhibited on average by 30%. Experiments using antisense oligonucleotides specific for the 5HT1c, 5HT2, and 5HT3 receptors showed that inhibition of I_{HK} by 5HT is mediated by the 5HT1c receptors. Exogenously expressed 5HT1c receptors are known to couple to an oocyte G-protein, then to hydrolyze a membrane phospholipid, PIP_2, producing lipid-soluble diacylglycerol (DAG), which activates protein kinase C, and water-soluble inositol-1,4,5-triphosphate (IP_3), which releases Ca^{2+} ions from internal stores. When IP_3 (6 pmol) is injected into oocytes only the transient response is observed. Subsequent application of 5HT inhibits I_{HK}. Application of 5HT to oocytes injected with the PKC antagonists staurosporine (1μM) and chelerythrine (1μM) reproduces the transient response, while I_{HK} is inhibited by only 20%. The PKC agonist phorbol 12-myristate 13-acetate (PMA; 40 nM) mimics the inhibition of I_{HK}. In summary, rat brain mRNA expresses an inwardly rectifying K^+ current I_{HK} in oocytes which can be inhibited by activation of 5HT1c receptors. This inhibition is mediated by the PKC pathway either by phosphorylation of the K^+ channel directly or by an intermediate regulatory protein. (Support: NIH, U.S.-Israel BSF, MDA, ARF)

Tu-Pos388

STIMULATION OF A POTASSIUM-SELECTIVE CURRENT IN RABBIT CORNEAL EPITHELIUM BY CARBON MONOXIDE. ((A. Rich, G. Farrugia, and J.L. Rae)) Mayo Foundation, Rochester, Minnesota 55905.

Carbon monoxide (CO) has been shown to stimulate a K^+ current (I_K) in human intestinal smooth muscle cells and is a putative intercellular messenger in brain slices. The effects of CO on a K^+ conductance in freshly dispersed rabbit corneal epithelial cells were measured using the perforated patch whole cell voltage clamp technique. Perfusion with NaCl-Ringer's solution containing 1%CO resulted in a 126±46% (mean± SE, n=15) increase in I_K, and a membrane hyperpolarization from -40±4mV to -49±4mV. The current that is specifically stimulated by CO, obtained by subtracting control I_K from CO-stimulated I_K, reversed at -60±6mV (E_K= -87mV). Application of quinidine or diltiazem, agents which selectively inhibit I_K, after CO stimulation resulted in complete inhibition of the stimulated I_K (360±207%, n=3 and a 100±25%, n=4 reduction of I_K, respectively). The mechanism by which CO stimulates I_K was further examined at the single channel level. Steady-state open probability increased from 0.003 to 0.156 at a holding potential of -40mV in the cell-attached configuration. Single channel conductance measured from -40 to +40mV was unaffected. CO did not affect K^+ channel gating in excised patches. These results show that CO specifically activates the K^+ conductance in corneal epithelia cells through an increase in single channel open probability. (supported by grants EY03282, EY06005, DK08677-03)

Tu-Pos389

ACTIVATION OF PROTEIN KINASE C ENHANCES THE CALCIUM-DEPENDENT POTASSIUM CURRENT IN RAT BASILAR SMOOTH MUSCLE CELLS. ((C.J. Kim, H. Zhang and B. Weir)) Univ. of Chicago, Chicago, IL 60637. (Spon. by R. Josephs)

A large conductance, voltage-dependent calcium-sensitive potassium channel was identified in freshly isolated rat basilar arterial smooth muscle cells by using both whole-cell, inside-out and cell-attached single-channel recordings. This conductance was reduced by bath application of charybdotoxin (100 μM) and TEA (3-10 mM) but not by glibenclamide (6 μM). Activation of protein kinase C by bath application of phorbol 12-myristate 13-acetate (PMA; 1-100 nM) and phorbol 12, 13-dibutyrate (PDBu; 10-100 nM) dose-dependently enhanced the calcium-dependent potassium current in whole-cell studies. Subsequent bath application of TEA (10 mM) reduced the potassium current activated by the phorbol esters. Washout with bath solution reversed the block of the potassium channel by TEA, but did not reduce the potassium current enhanced by the phorbol esters. In cell-attached studies, PMA and PDBu, at same concentrations, increased potassium channel activity and open time, but did not change the channel conductance. We suggest that activation of protein kinase C either increases internal calcium by promoting calcium entry and release, or increases the sensitivity of channel to calcium following its phosphorylation.

Tu-Pos390

REGULATION OF THE GATING AND CONDUCTIVITY OF THE CARDIAC SARCOPLASMIC RETICULUM K^+ CHANNEL BY H^+ ((Q-Y. Liu and H.C. Strauss)) Duke University, Durham, NC 27710.

Changes in intracellular pH are known to alter contractility and Ca^{++} homeostasis in the heart. The pH sensitivity of the canine cardiac sarcoplasmic reticulum potassium channel (SR-K^+) was studied using the planar lipid bilayer technique. When the pH was decreased from 7.2 to 5.2 both the conductance and the mean open time of the SR-K^+ channel decreased. However, single channel conductance was insensitive to a change in pH from 7.2 to 9.0. In contrast, the open probability (P_o) of the channel increased greater than 10 fold for the same pH increase at a holding potential of +20 mV measured from cis (cytoplasmic) to trans (lumenal). Changes in pH from 7.2 to > 7.8 shifted the potential dependence of gating equilibrium strongly in the negative direction. The apparent affinity for these two effects at 0 mV (100 mM symmetric KAc) differs by approximately an order of magnitude, suggesting that H^+ binding alters gating at a site(s) which is distinct from the site(s) which alters conductance. Since alterations in P_o were insensitive to whether pH was changed in either cis alone, trans alone or both cis and trans simultaneously, we speculate that this effect may be mediated through residues which reside within the channel pore, and which can be reached by H^+ from either side of the membrane. The broad pH range over which a P_o sensitivity was observed, suggests that this effect was not mediated through titration of a single amino-acid residue. It seems likely that multiple binding sites exist for H^+ which alter the free energy of SR-K^+ channel gating. (Supported in part by NIH grant HL-19216)

Tu-Pos391

NEUROPEPTIDE Y INHIBITS Ca^{2+}-ACTIVATED K^+ CHANNELS IN VASCULAR SMOOTH MUSCLE CELLS. ((Z.G. Xiong and D.W. Cheung)) University of Ottawa Heart Institute, Ottawa, K1Y 4E9. (Spon. by B. Huang)

The effects of neuropeptide Y (NPY) on Ca^{2+}-activated K^+ channel in smooth muscle cells from the rat tail artery were studied by whole-cell and single channel patch-clamp recording technique. In the presence of nifedipine (1 μM), outward currents through Ca^{2+}-activated K^+ channels were elicited by depolarizing pulses from a holding potential of -40 mV. NPY inhibited the outward currents in a dose-dependent manner from 20 to 200 nM. A maximum inhibition to about 48% of the control current could be achieved. Recording from outside-out patches showed that the open probability of Ca^{2+}-activated K^+ channels were similarly inhibited by NPY. At 200 nM, the open probability was reduced to about 36% of control. NPY did not affect the open times or current amplitude, but increased significantly the short and long close times. Inhibition of Ca^{2+}-activated K^+ channels by NPY may contribute to its excitatory action on vascular smooth muscle cells.

Tu-Pos392

UNSATURATED FREE FATTY ACIDS ACTIVATE A DISTINCT CLASS OF K CHANNELS IN CULTURED NEURONAL CELLS FROM MESENCEPHALIC AND HYPOTHALAMIC AREAS OF RAT BRAIN. ((D. Kim, C.D. Sladek, C. Aguado-Velasco, J.R. Mathiasen)) Department of Physiology and Biophysics, Chicago Medical School, North Chicago, IL 60064.

Certain free fatty acids such as arachidonate have been shown to activate a K-selective ion channel in cardiac and smooth muscle cells. We examined whether free fatty acids could also activate a similar type of channel in neuronal cells. In cultured neuronal cells, arachidonate (50 μM) in the pipette or applied to the cytosolic side of the membrane caused a slow activation of a K-selective channel with either a linear or inwardly rectifying I-V relationship (symmetrical 140 mM KCl). Linoleic and docosahexanoic, but not palmitic, stearic and myristic, acids also caused a concentration-dependent, reversible activation of the K channels. The K channels were not affected by second messengers such as Ca, cAMP or ATP. Once activated by a fatty acid, the K channel activity could be increased by intracellular acidosis (pH 6.8). The K channels were also sensitive to stretch; applying negative pressure to the pipette (10-50 mmHg) caused a pressure-dependent increase in channel open probability. The K channels were not blocked by glybenclamide (inhibitor of ATP-sensitive K channel), TEA or gadolinium (blocker of certain stretch-activated channels). These properties of the fatty acid-activated K channel in neurons resemble those in cardiac cells. Thus, the K channels activated by certain unsaturated free fatty acids also exist in neuronal cells and belong to a new family of K-channels with distinct channel properties.

Tu-Pos393

ACTIVATION OF MAXI K CHANNEL OF HUMAN MYOMETRIAL CELLS BY THE HORMONE RELAXIN ((P. Meera*, K. Anwer§, B. Sanborn§, and L. Toro*)) *Baylor College of Medicine and §Univ. Texas, Houston, TX 77030.

Relaxin , a peptide hormone promotes relaxation of uterus by suppressing its contractility. We have investigated the underlying mechanism in an immortalized myometrial cell line derived from pregnant human uterus. Fluorescence measurements showed that relaxin causes membrane hyperpolarization and prevents the rise of $[Ca^{2+}]i$ induced by oxytocin, suggesting a role of K channels. In agreement, cell-attached patch clamp recordings revealed an increase in the activity of large conductance (≈230 pS), calcium-activated K channels (K_{Ca}) on addition of 200 nM human relaxin. Channel open probability (Po) increased 10 to 100 fold at all potentials (n=7) (*e.g.* at +40 mV, $NP_{o\text{-before}}$=0.0017±0.001, $NP_{o\text{-after}}$=0.017±0.01, n=3), due to an increase in open time ($\tau_{o\text{-before}}$=0.73 ms; $\tau_{o\text{-after}}$=2.9 ms) and a decrease in closed times ($\tau_{o\text{-before}}$=2.3 s; $\tau_{o\text{-after}}$=1.0 s). On excision of the patch (inside-out) the channels were sensitive to $[Ca^{2+}]i$, and were blocked by TEA (50 mM, n=2). We have observed that in cell-attached patches relaxin induced multiple channel openings even at very low NPo < 0.01, indicating that relaxin may alter the Ca^{2+}-sensitivity of K_{Ca} channels resulting in an increase in the number of active channels in the patch. The stimulatory effect of relaxin was diminished by the cAMP antagonist, Rp-cAMP[S] (0.1-0.5 mM), both prior (20 min) or after the addition of relaxin (n=6). Our results suggest that one mechanism of relaxin action on the uterus is through the activation of K_{Ca} channels possibly via an increase in their Ca^{2+} sensitivity after phosphorylation by PKA. This activation of K_{Ca} channels by relaxin that leads to hyperpolarization would be responsible for smooth muscle relaxation.

Tu-Pos394

REGULATION OF A SMOOTH MUSCLE DELAYED RECTIFIER K^+ CHANNEL BY PROTEIN KINASE A. ((S.D. Koh, A.Carl and K.M. Sanders)) Department of Physiology, University of Nevada School of Medicine, Reno, NV 89557. (Sponsored by J.D. Campbell)

Cyclic AMP hyperpolarizes and relaxes smooth muscle tissue from the canine colon. To identify and characterize protein kinase A (PKA) mediated regulation of delayed rectifier K^+ channels, single channel current was recorded from excised inside-out patches of freshly dispersed smooth muscle cells from the canine proximal colon. Symmetrical 140/140 mM KCl was used and 200 nM charybdotoxin was included in the pipette solution to suppress 260 pS Ca^{2+}-activated K^+-channels. Three delayed rectifier K^+ channels (20 pS, 100 pS and 150 pS) were identified under these conditions. The catalytic subunit of PKA (10 U/ml, bovine) increased open probability NP_o of the 100 pS K^+ channel from 0.05 ± 0.02 to 0.18 ± 0.01 in the presence of 1.2 mM Mg^{2+} and 1 mM ATP. This increase was mainly due to an increase in mean open time from 39 ± 5 ms to 82 ± 8 ms (n=3). PKA had no effect on 10 pS, 4-aminopyridine sensitive K^+ channels. The activation of 100 pS K^+ channels was likely due to phosphorylation since PKA had no effect on the open probability of these channels in the absence of Mg^{2+}-ATP. These data suggest that cAMP-dependent activation of protein kinase A may hyperpolarize colonic muscle and/or reduce electrical slow waves by selectively activating the 100 pS K^+ channels. Supported by NIH-DK 41315.

Tu-Pos395

EXPRESSION OF KV1.5 IN THE RAT TISSUES AND THE MECHANISM OF CELL SPECIFIC REGULATION OF KV1.5 GENE BY CAMP
((H. Wang, Y. Mori and G. Koren, Brigham and Women's Hospital, Boston, MA))

Kv1.5 is a Shaker-like delayed rectifier K^+ channels. Using RNase protection assay in combination with immunoblotting, we found that Kv1.5 is expressed in the adult rat aorta, heart, small intestine, uterus, skeletal muscle and brain. We used in situ hybridization and immunofluorescence to investigate the cell-type specific expression of Kv1.5 in the cardiovascular system in general and in smooth muscle cells in particular. The results demonstrate that Kv1.5 is exuberantly expressed in the vascular smooth muscle cells of the adult rat heart and small intestine as well as in the smooth muscle cells of adult uterine myometrium. Intermediate level expression of Kv1.5 mRNA was also detected in the adult atrium but not in the 3 days old neonatal atrium. In addition, we have cloned and analyzed promoter region of Kv1.5 gene. A cAMP response element ($CRE^{Kv1.5}$) was identified in 5'-non coding region of the gene. The effect of cAMP on Kv1.5 expression was tested using myogenic cells as well as GH3 cells (rat pituitary tumor-derived cells). In primary culture of rat neonatal atrial cells, cAMP increases the steady state levels of Kv1.5 transcript. Transient transfection experiments in C2C12 myotubes using a Kv1.5 promoter-CAT reporter gene reveal that cAMP increases the promoter activity. Furthermore, the mutation of $CRE^{Kv1.5}$ sequence abolished the effect of cAMP. In contrast, steady state levels of Kv1.5 transcript in GH3 cells is decreased by cAMP.The half-life of Kv1.5 transcript in GH3 cells was 36.5±5.4 min., and was not significantly altered by cAMP(35.3±4.3 min.). Nuclear run-on experiment confirmed that cAMP decreased the transcription rate of Kv1.5 gene in GH3 cells. Our studies show that Kv1.5 is expressed in vascular smooth muscle cells and cardiac myocytes. Furthermore, in GH3 cells the $t_{1/2}$ of transcript is very short and transcription rate of this gene can be rapidly modified by cAMP.

Tu-Pos396

DIACYLGLYCEROL INDUCES FAST INACTIVATION IN SLOWLY INACTIVATING VOLTAGE-GATED POTASSIUM CHANNELS.
((M.R. Bowlby and I.B. Levitan)) Department of Biochemistry and Center for Complex Systems, Brandeis University, Waltham, MA 02254

Diacylglycerol (DAG) is a common intracellular second messenger which activates protein kinase C (PKC). We are examining the direct effects of DAG on gating kinetics in cloned voltage dependent potassium channels. Potassium channels are studied by expression of their cRNA's in *Xenopus* oocytes and recording macroscopic currents from membrane patches. When applied internally, DAG produces a 13 fold increase in the inactivation rate of Kv 1.3 and a 3 fold decrease in the peak current. This effect has an IC_{50} of 0.2 μM and a fast time course, with a maximal effect occurring within 1 min. and a reversal to control within several minutes. The action of DAG is independent of PKC activation, as it is not blocked by the PKC inhibitor peptide 19-36 or by staurosporin, nor do the PKC activators OAG or PMA have a similar effect. DAG alters the kinetics and current amplitude of several voltage-gated potassium channels, as similar effects are observed in *Shaker*-IR and Kv 1.6. It appears that DAG interacts directly with the channel, as it interacts competitively with internally applied TEA. The binding site for DAG, however, is different than that for TEA, as the *Shaker* mutant T441S is insensitive to internal TEA, yet remains sensitive to DAG.

Tu-Pos397

OXYGEN MODULATES K^+ CHANNEL ACTIVITY VIA A MEMBRANE-DELIMITED MECHANISM IN NEURONS.
((C. Jiang & G. G. Haddad)) Departments of Pediatrics (Respir. Med.) and Cellular and Molecular Physiology, Yale Univ. Sch. Med., New Haven, CT 06520.

K^+ channel modulation is an important integral cellular response to O_2 deprivation. Although part of this modulation results from changes in concentrations of several cytosolic factors such as ATP and Ca^{++}, our previous studies have suggested that mechanisms other than those originating in the cytosol may be involved. To test this hypothesis, we performed experiments using patch clamp techniques and dissociated neurons from rat neocortex and substantia nigra. In voltage clamp mode, whole-cell outward currents showed an initial transient increase followed by a pronounced decrease during O_2 deprivation. In cell-free excised membrane patches, we found that a specific K^+ current (large conductance, inhibited by glibenclamide, μM concentration of ATP and activated by Ca^{++}) was reversibly inhibited by lack of O_2. This inhibition was characterized by I. a marked decrease in channel open state probability (P_{open}) with selective suppression of the longer period of openings leading to rapid channel flickering, and II. a slight reduction in unitary conductance. P_{open} was ~0 with $PO_2 < 1$ Torr, while there was no change in P_{open} at $PO_2 \geq 20$ Torr. PO_2 at $P_{open} = 0.5$ (K_D) was ~10 Torr. In sharp contrast, low PO_2 had no effect on another K^+ current that had a much smaller conductance and was Ca^{++}-independent. These results therefore demonstrate that a cytosol-independent, membrane-delimited O_2-sensing mechanism plays a role in the modulation of K^+ channel activity in central neurons.

Tu-Pos398

ACTIVATED AND DEACTIVATED STATE BLOCK OF A CLONED TRANSIENT K^+ CHANNEL BY 4-AMINOPYRIDINE.
((R.L. Rasmusson, Y. Zhang, D.L. Campbell, M.B. Comer and H.C. Strauss)) Duke University, Durham, NC 27710.

4-Aminopyridine (4-AP) shows complex state dependent interactions with many voltage gated K^+ channels. We studied the action of 4-AP on an inactivating K^+ channel isolated from ferret ventricle (FK1) expressed in *Xenopus* oocytes and an N-terminal deletion mutant (ΔNco) which lacks fast inactivation. The following properties were observed for both FK1 and ΔNco: 1) Blockade required channel activation. 2) Blockade accumulated from pulse to pulse and was sensitive to the applied potential during deactivation, indicating trapping of 4-AP in deactivated channels. 3) For long trains of pulses, (50 mV; HP -90; 0.1 Hz) blockade increased with decreasing pulse duration. 4) Enhanced blockade during trains of brief (<50 msec) pulses took many pulses to accumulate and was relieved by 2 or 3 pulses of 500 msec duration. The mechanisms underlying this behavior were further elucidated by the following observations in ΔNco: 1) Application of 4-AP produced inactivation-like behavior (0.1 Hz to +50 mV, HP -90 mV). 2) Application of 4-AP did not cause crossover of deactivation tail currents. 3) Blockade during a 500 msec pulse to varying potentials followed by a second pulse to +50 mV for 500 msec revealed that blockade developed with time and increased above -40 mV. 4) The effective electrical distance for 4-AP binding at positive potentials was approximately zero. This data can be explained by a model in which 4-AP binding is most stable when the channel has a symmetric arrangement of voltage sensors (i.e. four subunits in a fully activated or deactivated conformation), has a lower affinity for asymmetric arrangements (i.e. transition states) and has a binding site which is occluded by conformational changes in the vestibule region associated with deactivation.

Tu-Pos399

BLOCK BY 4-AMINOPYRIDINE OF A $K_v1.2$ DELAYED RECTIFIER K^+ CURRENT EXPRESSED IN *XENOPUS* OOCYTES
((S.N. Russell, N.G. Publicover, P.J. Hart, A. Carl, J.R. Hume, K.M. Sanders and B. Horowitz.)) Department of Physiology, University of Nevada School of Medicine, Reno NV 89557.(Spon. by J. Kenyon)

The blocking action of 4-aminopyridine (4-AP) on a smooth muscle delayed rectifier K^+ channel ($K_v1.2$) (CSMK1) expressed in oocytes was investigated at room temperature (22 - 24°C) and physiological temperature (34°C) using the double electrode voltage clamp and patch clamp techniques. At room temperature 4-AP (100 μM) inhibition occurred only after activation of current. The rate of onset of block was dependent upon the length of time current was activated by a depolarizing step. Similarly, removal of block required current activation. The degree of block by 4-AP was not reduced by increasingly more depolarized step potentials nor did the amount of block change over the duration of a 1 s step. When channels were nearly fully inactivated addition of 4-AP produced no block of the following depolarizing step suggesting that 4-AP did not bind when channels were in the inactivated state. In single channel experiments, 4-AP decreased the mean burst duration, mean open time and the number of openings per burst in a dose dependent manner but did not alter the mean single channel current amplitude. At 34°C the I-V relationship and inactivation curve shifted to more negative potentials. However increasing the temperature to 34°C did not alter the degree of block by 4-AP although the rate of onset of block was greatly enhanced. Results suggest that 4-AP binds to the open state of the $K_v1.2$ channel and can be trapped when the channel closes. 4-AP cannot bind when the channel is closed or inactivated prior to the addition of drug. Inactivation and 4-AP binding to the channel are mutually exclusive. A model for the mechanism of action of 4-AP on the $K_v1.2$ channel is proposed based on experimental data. Supported by NIH DK42505 and DK41315.

Tu-Pos400

LOCALIZATION OF THE 4-AMINOPYRIDINE BINDING SITE ON A $K_v1.2$ K^+ CHANNEL THROUGH CHIMERA CONSTRUCTION AND SITE-DIRECTED MUTAGENESIS
((S.N. Russell, K.E. Overturf, P.J. Hart and B. Horowitz)) Department of Physiology, University of Nevada, Reno NV 89557-0046.

CSMK1, a $K_v1.2$ class K^+ channel cloned from canine colonic smooth muscle (Hart et al., PNAS 90:9659,1993), has a high sensitivity to 4-aminopyridine (4-AP) relative to other K^+ channels of this class (IC_{50}; CSMK1 = 74.7 μM, RK2 = 600 μM, RCK5 = 800 μM). Of the 8 amino acid differences between CSMK1 and these 2 other $K_v1.2$ K^+ channels, 2 lie in or near the pore region while the remaining 6 are in the amino terminal end of the protein. We have constructed chimeras which have paired the amino or carboxy terminal domains of RK2 and CSMK1 through the use of a common *Sac I* restriction site (Fig 1 shows a schematic of the constructs). These recombinant cDNA constructs were then expressed in *Xenopus* oocytes and their relative sensitivities to 4-AP steady state block was determined. Using a 100μM dose of 4-AP the CSMK1 current was reduced by 60 ± 3% while the RK2 current was only inhibited by 11 ± 4%. The chimera constructed with CSMK1 as the amino terminal domain of the RK2 clone was relatively insensitive to 4-AP block with 100μM reducing current by 29 ± 4%. The opposite chimera was reduced by 35 ± 2%. The results suggest that while the amino terminal domain may influence the binding of 4-AP to the $K_v1.2$ channel clone the actual binding site lies outside this area. Alteration of individual amino acids through site-directed mutagenesis is proceeding. Supported by NIH DK42505 and DK41315.

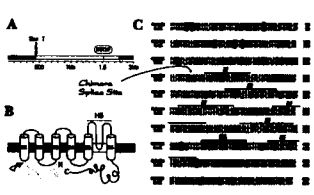

Tu-Pos401

BARIUM-INDUCED ASYMMETRIC OCCURRENCE OF A SUBCONDUCTANCE LEVEL IN BK CHANNELS FROM RAT SKELETAL MUSCLE.
((W. B. Ferguson, R. A. Bello, L. Song, and K. L. Magleby)) Univ. Miami School of Medicine, Miami, FL 33101-6430.

Ba^{2+} can block the passage of K^+ through BK channels by binding in the pore of the channel (Miller et al. 1987, Biophysical J. 90:427.) While studying Ba^{2+}-block we have observed an asymmetry in the number of transitions to a subconductance level immediately preceeding or following bursts in BK channels. Outward single channel currents were recorded from excised patches of muscle membrane held at 30 mV (normal intracellular surface (i) positive). The solutions contained 5 mM TES (pH = 7), 150 mM $NMDG_o$ or 50 mM KCl_o, and 150-500 mM KCl_i. High $Ca^{2+}{}_i$ (50 μM) was used to activate the channel so that the majority of gaps between bursts were due to Ba^{2+} blockade. In three experiments with 50-500 μm $Ba^{2+}{}_i$, typically about 10 % of the first openings of each burst were immediately preceeded by a transition to a subconductance level of 26 ± 2 % of the maximum single channel conductance, while none of the last openings of each burst were followed by such a transition. The mean duration of the preceeding subconductance levels was 0.8 ± 0.2 ms. This effect was readily reversed by removing $Ba^{2+}{}_i$ or by replacing Ba^{2+} with Mg^{2+}. Raising $Ca^{2+}{}_i$ to 5 mM in the absence of $Ba^{2+}{}_i$ did not produce an effect similar to that produced by Ba^{2+} (tested in one experiment). Two possible explanations for these observations are: 1) Open-channel block by Ba^{2+} may occasionally induce the channel protein to assume a partially open (subconductance) conformation that is not apparent because of the block. After Ba^{2+} exits the channel the partially open conformation exists for about 0.8 ms before assuming a normal open conformation. 2) Ba^{2+} may bind sequentially to at least two sites as it passes through the open channel. The first binding produces a complete block that lasts several seconds and the second binding produces a partial block that lasts about 0.8 ms. Supported by Grants from the NIH and the Muscular Dystrophy Association.

Tu-Pos402

EFFECTS OF CLOFILIUM AND NE-10064 ON IKs, THE SLOW COMPONENT OF THE CARDIAC DELAYED RECTIFIER.
((Mark A. Smith, Mary Lee Conder, Karnail S. Atwal and John R. McCullough)) Bristol-Myers Squibb Pharmaceutical Research Institute, Princeton, NJ 08543-4000.

The electrophysiological effects of clofilium and NE-10064, (E)-1-[((5-(4-chlorophenyl)-2-furanyl]methylene]amino]-3-[4-(4-methyl-1-piperazinyl)-butyl-2,4-imidazoldinedione di-HCl, a novel Class III antiarrhythmic agent, on the slow component of the cardiac delayed rectifier current (IKs) were studied in freshly dissociated guinea pig ventricular myocytes by using whole cell patch-clamp techniques. Experimental conditions were selected to isolate IKs from other ionic currents and electrogenic processes. IKs was activated in a time- and voltage-dependent manner. Significantly more IKs was activated after a train of depolarizing pulses given at a rate of 4 Hz than after a train of 0.5 Hz ($\Delta IKs = 0.48 \pm 0.12$ nA, $p<0.005$, $n=10$), suggesting that IKs can contribute to the cardiac action potential shortening observed at faster rates. Clofilium inhibited IKs in a concentration-dependent manner with an IC_{50} of 20 μM. NE-10064 also inhibited IKs with an IC_{50} of 1.7 μM. Clofilium (3-30 μM) did not exhibit a rate-dependent block of IKs. Rate-dependent inhibition of IKs was observed in the presence of 1 and 3 μM NE-10064: significantly greater inhibition was observed with stimulation at 4 Hz compared to stimulation at 0.5 Hz (1 μM = 9.25 ± 2 % vs. 4.66 ±1.24 %, $p<0.05$, $n=6$ and 3 μM = 28.52 ± 5.92 % vs. 18.02 ± 3.33 %, $p<0.05$, $n=4$, respectively). Preliminary data suggests that NE-10064 inhibits IKs in a voltage- and time-dependent manner. These results indicate that NE-10064 is a potent rate-dependent inhibitor of IKs in cardiac cells.

Tu-Pos403

THE ROLE OF CHANNEL OPENING IN TRANSIENT OUTWARD CURRENT BLOCK BY QUINIDINE, FLECAINIDE, AND 4-AMINOPYRIDINE IN HUMAN ATRIAL MYOCYTES.
((S. Nattel, Z. Wang, B. Fermini)) Montreal Heart Institute, Montreal, Quebec, Canada, HIT IC8.

The transient outward current (I_{to}) is an important repolarizing current in human atrium and ventricle. To assess the determinants of I_{to} block by flecainide (F), quinidine (Q), and 4-aminopyridine (4AP), isolated human atrial myocytes were studied at 36°C with whole-cell voltage clamp techniques. F, Q and 4AP inhibited I_{to} in a concentration-dependent fashion. Q block was unaltered by inactivating prepulses (IPP), but increased with voltage of the depolarizing test pulse (TP) in parallel with I_{to} activation ($r=0.98$). F block was weakly affected by TP voltage, but was enhanced by IPP, tracking the inactivation variable ($r=0.99$). 4AP block was relieved by depolarization to inactivate I_{to}, and restored by returning to the holding potential. These results are consistent with contrasting state-dependent block: F is inactivation-dependent, Q activation-dependent, 4AP rested-state dependent. However, for all 3 drugs, fractional I_{to} block (ΔI_{to}/control I_{to}) was 0 at the onset of a depolarizing pulse, but appeared over time following channel opening (figure). All drugs accelerated apparent I_{to} inactivation, compatible with open-channel blocking. Conclusion: Activation of I_{to} channels appears necessary for blockade irrespective of the favored binding state for each drug. I_{to} blockers may act by mimicking the "inactivation particle," binding to a high-affinity site upon channel opening.

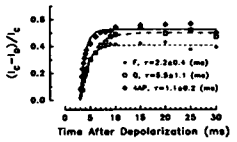

Tu-Pos404

QUINIDINE BLOCK OF THE HUMAN CARDIAC hKv1.5 CHANNEL IN INSIDE-OUT PATCHES.
((T.C. Rich, D.J. Mays, M.M. Tamkun, and D.J. Snyders)) Departments of Biomedical Engineering, Molecular Physiology and Biophysics, and Pharmacology, Vanderbilt University, Nashville, TN.

We have recently shown that hKv1.5, a human cardiac potassium channel, is sensitive to clinically relevant quinidine concentrations. To further examine the mechanism of quinidine binding we used cell-attached and inside-out patches obtained from L-cells expressing wild type and mutant hKv1.5 channels. The charge neutralization E524Q+D526N (just beyond S6) did not modify hKv1.5 currents, and did not change the kinetics or the apparent affinity for quinidine binding when assessed with whole cell voltage clamp after extracellular application. One clonal cell line expressed currents in excess of 20 nA (at +50 mV); inside-out patches of this cell line yielded total patch currents between 20 and 80 pA. In these inside-out patches, the activation kinetics were similar to wild type (τ ~1.6 ms at +50 mV). After application of quinidine (2 - 20 μM) to the intracellular face, a time-dependent reduction (τ ~6 ms for 20 μM) of outward current to less than 30% of control was observed. These results extend previous observations and strongly support the proposed intracellular action of quinidine. Supported by NIH grants GM08452, HL46681 and HL47599.

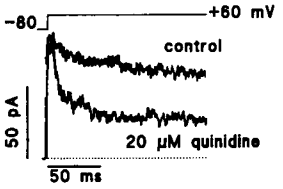

Tu-Pos405

EFFECTS OF RYANODINE ON A HUMAN CARDIAC DELAYED RECTIFIER.
((M. L. Bhattacharyya, S. Sarker, K. Seth)) Department of Physiology, Meharry Medical College, Nashville, TN.

Effects of ryanodine (Ry) on cardiac potassium channels have usually been attributed to be secondary to Ry effects on sarcoplasmic reticulum calcium release. We examined whether Ry could have effects on a potassium channel that does not depend on calcium for activation and gating. Therefore effects of Ry were studied on the human hKv1.5 channel with the whole cell voltage clamp technique using a L-cell line which stably expresses this channel. Experiments were performed at 23 °C with 5 mM BAPTA in the intracellular solution. A dose-dependent inhibition of hKv1.5 current was observed for both initial peak current and late steady-state (250 ms) current, as illustrated by the data below for depolarization to +70 mV.

Concentration	Peak (%reduction)	250 ms (%reduction)
10^{-7} M	11.3±4.8	14.1±6.3
3×10^{-7} M	21.5±9.6	24.9±7.2
10^{-6} M	30.0±14.0	33.3±12.5
10^{-5} M	43.6±12.5	46.8±15.5

Dose response data could be fitted to a Hill equation with an IC_{50} of 1.2 μM. Block by Ry did not display any voltage dependence. The inhibition was only partially reversible at concentrations below 1 μM. These results suggest that Ry may interact directly with sarcolemmal potassium channels.
Supported by NIH grants GM08037 and HL02480.

Tu-Pos406

PROBING THE SITE OF Zn^{2+} ACTION USING CLONED AND MUTANT VOLTAGE-GATED K^+ CHANNELS.
((G. Talukder, S. J. Gibbons, M.M. Tamkun* and N. L. Harrison.)) Anesthesia & Pharm/Phys, The University of Chicago, Chicago Il 60637. *Dept. of Mol. Phys. and Biophys., Vanderbilt University, Nashville TN.

Zn^{2+} modulates the gating of cloned rat and human voltage- activated K^+ channels (Harrison et al. 1993 Mol. Pharm. 43 482-486). We are attempting to locate the binding site for Zn^{2+} by comparing the effects of Zn^{2+} on several cloned K^+ channels (rKv1.1, hKv1.4, hKv1.5, rKv2.1) as well as two channels with single point mutations (rKv1.1 N207Q, hKv1.5 R484Y) expressed in mouse L cells. Whole cell recordings were made at 25°C, using intracellular solutions based on K gluconate and continuous extracellular perfusion with HEPES-buffered saline containing 3mM K^+. All *Shaker* sub-family homologues studied showed a characteristic shift in activation gating towards more positive potentials in extracellular Zn^{2+} (2-1000μM). Addition of 200μM Zn^{2+} to the intracellular solution had no effect on the gating of hKv1.4, or on its modulation by extracellular Zn^{2+}. Gating of rKv2.1 was insensitive to extracellular Zn^{2+} (1mM). Mutation of a probable glycosylation site (N207Q) on rKv1.1 did not affect channel gating or sensitivity of the channel to Zn^{2+}. A pore mutant (hKv1.5 R484Y), which has an increased sensitivity to extracellular TEA ions had the same sensitivity to Zn^{2+} as the wild type. On the basis of these data we suggest that a discrete Zn^{2+} binding site exists on certain K^+ channels. The Zn^{2+} binding site appears to be located on the extracellular aspect of the channel and to be distinct from the binding site for TEA.
SJG is supported by DHHS training grant #DA07255-02.

Tu-Pos407

CLOTRIMAZOLE, A BLOCKER OF CALCIUM-ACTIVATED K^+ CHANNELS.
**((A.R. Rittenhouse, C. Brugnara, and S.L. Alper))
Molecular Medicine and Renal Units, Beth Israel Hospital;
Clinical Laboratories, The Children's Hospital;
and Depts. of Cell Biology and Pathology, Harvard Medical School.**

Clotrimazole (CLT) blocks Ca^{2+}-activated K^+ transport in human erythrocytes and is currently being tested as an oral treatment for the prevention of sickle cell dehydration. The actions of CLT in erythrocytes appear specific for the Gardos pathway, thought to be a Ca^{2+}-activated K^+ channel of mid-range conductance, as CLT competitively displaces binding of ^{125}I-charybdotoxin with an ID_{50} of 10 nM (*J. Clin. Invest.* 1993. 92:520). We used standard whole cell patch clamp techniques in order to verify that CLT blocks K^+ conductance. In murine erythroleukemia cells stimulated by the Ca^{2+} ionophore A23187, CLT inhibited whole cell K^+ current by 72 ± 2%. However, CLT is also known to be an inhibitor of cytochrome P450 epoxygenases, the products of which have been shown to alter activities of many types of ion channels. We therefore tested the specificity of CLT as an ion channel inhibitor. Exposure of PC12 cells to 100 nM CLT inhibited whole cell K^+ current by 47 ± 9%, a value similar to the extent of inhibition produced by 30 nM iberiotoxin, whereas L-type Ca^{2+} current was inhibited by only 13 ± 4%. In contrast, CLT at concentrations as high as 1 μM had no inhibitory effect on Na^+ currents in neonatal rat superior cervical ganglion neurons. Since CLT can potently displace ^{125}I-charybdotoxin from erythroid binding sites, we initiated experiments to determine whether CLT also blocks the channel pore. Preliminary experiments suggest that in addition to diminishing whole cell K^+ current in PC12 cells, CLT changes the I-V relationship. Moreover, CLT appears to be capable of blocking K^+ channels in the closed state.

Tu-Pos408

EFFECT OF 4-AMINOPYRIDINE ON SLOW INACTIVATION OF Kv1.1 AND SHAKER K⁺ CHANNELS ((N.A. Castle, S. Fadous, G.K Wang, *D.E. Logothetis,)) Anesthesia Research Labs, Brigham and Women's Hospital, Boston, MA 02115; *Dept. of Physiol. and Biophys., Mount Sinai School of Medicine, NY, NY 10029.

In the present study we have used two electrode voltage clamp of *Xenopus* oocytes expressing either Kv1.1 or Shaker B Δ6-46 (ShB) K⁺ channels to examine the effect of 4-AP on the process of slow inactivation. Neither of these channels exhibit fast inactivation. 4-AP was found to produce open channel block of both channel types with IC_{50}s ranging between 0.1-0.2 mM. In the absence of drug, inactivation of Kv1.1 and ShB channels at 0 mV was biexponential (see table for time constants). In the presence 4-AP the rates of inactivation of Kv1.1 and ShB were markedly reduced resulting in a crossover phenomenon where in the presence of drug the outward current is less than control at the beginning of the depolarizing pulse but crosses over during the pulse to become greater than the control. The most obvious change induced by 0.2 mM 4-AP was a 2-fold slowing of the slow phase of inactivation. In addition, there was a significant increase in the contribution of the slower phase of inactivation of ShB channels in the presence of 4-AP. These results are consistent with an inability of 4-AP bound open channels to undergo slow inactivation.

		τ_{FAST} (s)	τ_{SLOW} (s)	$A_{slow}/(A_{fast}+A_{slow})$
Kv1.1	Control	7.8 ± 0.3	33.9 ± 0.9	0.79 ± 0.02
	0.2 mM 4-AP	3.9 ± 1.1*	67.1 ± 3.6*	0.85 ± 0.04
ShBΔ6-46	Control	3.5 ± 0.4	13.1 ± 1.8	0.35 ± 0.06
	0.2 mM 4-AP	3.5 ± 0.4	23.7 ± 2.6*	0.75 ± 0.02*

* Significantly different from control, $p < 0.05$

Tu-Pos409

INTERACTION BETWEEN TWO DIFFERENT OPEN CHANNEL BLOCKERS OF Kv1.1 K⁺ CHANNELS ((N.A. Castle, G.K Wang, *D.E. Logothetis)) Anesthesia Research Labs, Brigham and Women's Hospital, Boston, MA 02115; *Dept. of Physiol. and Biophys., Mount Sinai School of Medicine, New York, NY 10029.

In the present study we have used whole cell patch clamp to compare the block of Kv1.1 K⁺ channels (stably transfected into Sol-8 cells) by 4-aminopyridine (4-AP) and the local anesthetic agent, bupivacaine. When channels were activated by depolarization after drug concentrations were allowed to reach steady state, both 4-AP and bupivacaine produced a time dependent inhibition of Kv1.1 currents, exhibiting IC_{50}s of 90 μM and 46 μM at 0 mV for 4-AP and bupivacaine, respectively. However, whereas 4-AP became "trapped" upon return to a holding potential of -80 mV (channel in closed state) bupivacaine was found to unbind during channel closure. While 4-AP had no measurable effect on Kv1.1 deactivation kinetics, the rate of current deactivation (at -60 mV) decreased from 10.4 ms in control to 28.3 ms in the presence of 100 μM bupivacaine. The slowing of deactivation resulted in a "crossover" of tail currents. Such a phenomenon suggests that channel closing may not occur until bupivacaine dissociates from its binding site. We utilized the trapping of 4-AP upon channel closure and the absence of trapping of bupivacaine to show that when these functionally distinct open channel blocking agents were applied together, binding of 4-AP was reduced. Indeed, in the presence of 1 mM bupivacaine little or no binding of 4-AP (0.3 mM) was evident (as assessed by the proportion of channels that remain blocked in the closed state following washout of both agents). These results suggest that despite their functional differences, 4-AP and bupivacaine may share the same or overlapping binding sites, or alternatively, their respective binding sites are allosterically coupled.

Tu-Pos410

LINOPIRDINE (DUP 996), A NEUROTRANSMITTER RELEASE ENHANCER, BLOCKS M-CURRENT IN RAT CA1 HIPPOCAMPAL NEURONS. ((S.P. Aiken and B.S. Brown)) The DuPont Merck Pharmaceutical Co., Wilmington, DE 19880. (Spon. by S.L. Brenner)

Linopirdine, which has been shown to enhance the release of acetylcholine, dopamine and glutamate in the mammalian CNS and to improve performance in animal models of learning and memory, may be useful in the treatment of Alzheimer's disease. To study its mechanism of action, the single electrode voltage-clamp technique was used to determine the electrophysiological effects of linopirdine on CA1 neurons in rat hippocampal slices. At a concentration previously found optimal for *in vitro* release enhancement (10μM), linopirdine consistently caused a 2-5mV depolarization and blocked the M-current in tetrodotoxin (500nM)-treated slices. After 30 minutes exposure to linopirdine, M-current amplitude had declined to 43.2±4.7% of the pretreatment value (215±35pA; n=8). Linopirdine-induced block of M-current was: 1) unaffected by atropine (10μM); 2) not accompanied by a block of I_{AHP}; and 3) reversible upon washout. Therefore, it is likely that this effect involved a site distal to the muscarinic receptor and did not result from the release of endogenous acetylcholine. These results suggest that membrane depolarization and the block of M-current, which have been associated with enhanced neuronal excitability and reduction of spike frequency adaptation, may, in part, account for the mechanism whereby linopirdine enhances neurotransmitter release.

Tu-Pos411

SALICYLALDOXIME BLOCKS THE TRANSIENT OUTWARD K⁺ CURRENT IN RAT VENTRICULAR MYOCYTES. ((S. Karhu[1,2], M. Weckström[2], T. Kivistö[1], and L.C. Sellin[1])). Depts. of Biophysics[1] and Physiology[2], University of Oulu, 90570 Oulu, Finland. (Spon.by J.McArdle)

The mechanical uncoupling agent 2,3-butanedione monoxime (BDM) has multiple biological effects including blockade of voltage-gated ion channels. To study the molecular basis for such multiple actions, we tested a number of oxime "analogues" of BDM. Action potentials (AP) and transient outward currents (I_{to}) were recorded from single, isolated rat ventricular myocytes after addition of salicylaldoxime (SAL). AP duration at 90% repolarization ($APD_{90\%}$) increased by 32±40%, 130±90%, 120±80% and 80±100% (mean±SD, n=3) in 0.1, 0.5, 1.0 and 2.0 mM SAL, respectively. Control peak I_{to} was 3.19±0.60 nA with a maximum sustained current of 1.53±0.31 nA at 255 ms for voltage steps from -80 to +60 mV (n=5). SAL in 0.1, 0.5 and 2.0 mM concentrations significantly ($p<0.05$) reduced I_{to} peak current by 12±4%, 27±4% and 64±5%, and sustained current by 6±3%, 22±4% and 56±10%, respectively (n=5). The K_d for SAL was 1.46 mM. At 2.0 mM and above, SAL probably affects other ionic currents because $AP_{90\%}$ and AP amplitude decreased and E_m became more negative. SAL is over 10x more potent than BDM in prolonging rat cardiac AP duration and blocking I_{to}. It may provide a structural basis for new anti-arrhythmic agents. (Supported by the Finnish Heart Disease Foundation).

Tu-Pos412

PHARMACOLOGIC DISSECTION OF DELAYED RECTIFIER CURRENT (iK) IN CANINE VENTRICULAR MYOCYTES BY E-4031 AND TERFENADINE; iKr & iKs "Swap" ((Gary A. Gintant)) Cardiol. Div., Wayne State Univ. School of Med., Detroit MI. 48201

Deactivation of delayed rectifier current (iK) in canine myocytes (tail currents) has previously been described as the sum of a rapid (iKe1, tau= 150-300 msec) and slow (iKe2, tau=2.5 sec @-40 mV) exponential components. As guinea pig iK is subdivided into two components (iKr,iKs) based on sensitivity to E-4031 (Sanguinetti et al., 1990), the effects of this agent were examined in canine ventricular myocytes using whole cell patch clamp techniques (37oC). In canine myocytes, E-4031 (5 uM) blocked the *slower* tail component (iKe2), leaving the faster component (iKe1) unaffected (depolarizing pulse range -20 to +60 mV, holding potential = -40 mV). This effect is opposite to that in guinea-pig, where E-4031 blocks the *rapid* tail component iKr. The voltage-dependence of E-4031 insensitive tail component in canines is similar to that of E-4031 sensitive component in guinea-pigs, suggesting an iKr/iKs tail current "swap" across species. In contrast, the E-4031 sensitive component during activation of iK is comparable for both species. In a similar pattern, reducing [K+]o to 0 mM blocks the slower tail component in canines (vs.rapid tail component in guinea-pigs). Pharmacologic dissection of canine iK was also possible with the antihistamine terfenadine (5 uM) which blocked the slower tail current component with minimal effects on iK activation. The results demonstrate i) two iK components can be defined pharmacologically in canine ventricular myocytes, ii) E-4031 sensitive iK is similar to guinea-pig iKr during activation but not deactivation, and iii) iKr tail current behavior is species-dependent.

Tu-Pos413

DIFFERENTIAL EFFECTS OF QUINIDINE ON VOLTAGE-GATED K CHANNEL CLONES. ((G-N Tseng, B Zhu, J-A Yao)) Pharmacology, Columbia University, New York, NY 10032

We studied the effects of quinidine (Q, 100 uM) on different K channel clones expressed in oocytes: a fast-activating delayed rectifier channel (RAK), a fast-inactivating channel (RHK1), and its mutant form in which the fast-inactivation process had been disrupted (DelA). External application of Q had a dual effect on RAK: block at strong depolarization (DEP) [equivalent electrical distance (δ)=0.06±0.02, n=7] and negative shift in the voltage-dependence of activation ($V_{0.5}$ shift 9.8±3.4 mV, n=13). Thus Q increased RAK at -20 mV by 50.4±14.3% (n=14), but decreased it at +40 mV by 26.4±16.7% (n=7). Intracellular injection (INJ) of Q blocked RAK without causing voltage shift, suggesting two sites of Q actions. Q blocked RHK1 and DelA at all voltages without enhancement. Q was more potent in blocking DelA than RHK1 (at +20 mV, block > 50% vs < 20%). Q slowed RHK1 decay during DEP while accelerated DelA decay, suggesting an interaction between Q and the inactivation gate of RHK1. Block of DelA by Q was accentuated by DEP (δ=0.26). INJ of Q blocked DelA, consistent with Q blocking DelA from cytoplasm at a site within the membrane electrical field. We are currently studying the residues involved in Q actions by site-specific mutagenesis in the S4 and deep-pore regions of DelA and RAK. In conclusion, the actions of Q on K channels may be influenced by structures involved in channel activation, inactivation and permeation.

Tu-Pos414

COMPARISON OF EFFECTS OF QUINIDINE ON CLONED AND NATIVE SLOW DELAYED RECTIFIER K CHANNELS ((J-A Yao, G-N Tseng)) Dept. of Pharmacology, Columbia U., New York, NY 10032.

The actions of quinidine (Q) on slow delayed rectifier channel may contribute to its antiarrhythmic or proarrhythmic effects. We studied the effects of Q on cloned and native slow delayed rectifier channels. The cloned channel from a human genomic library (hI_{sK}) was expressed in oocytes and studied by two-microelectrode voltage clamp. The currents of native channels in dog (DI_{Ks}) and guinea pig (GPI_{Ks}) ventricular myocytes were recorded using the whole-cell configuration of patch clamp. Q (100 μM) blocked hI_{sK} by 16±6 % at +10 mV and 8±3 % at +40 mV (n=3). The ratio of current in the presence of Q (I_d) to the control (I_c) increased upon depolarization to > 0 mV, and decreased during repolarization (-40 mV), suggesting that depolarization relieved Q block while repolarization induced reblock. Intracellular injection of Q (100 μM) did not block hI_{sK}, suggesting an extracellular site of action. Q was more potent in blocking DI_{Ks} and GPI_{Ks} than hI_{sK}. Q (10 μM) blocked DI_{Ks} by 37% at +10 mV and 20% at +40 mV (n=2), suggesting a similar voltage-dependence of Q block in DI_{Ks} and hI_{sK}. This voltage-dependence is opposite to that of actions of Q on GPI_{Ks} (*Circ. Res.* 69:519, 1991). Our data suggest that Q blocked hI_{sK} and DI_{Ks} with a similar voltage-dependence but different potencies.

Tu-Pos415

CHLOROQUINE SELECTIVELY BLOCKS THE INWARD RECTIFYING POTASSIUM CHANNEL IN DOG CARDIAC MYOCYTES. THE INTRACELLULAR EFFECT.

Jorge Cebada and Eduardo M. Salinas . Centro de Ciencias Fisiológicas, Instituto de Ciencias, Universidad de Autónoma de Puebla, Puebla, MEXICO.

Chloroquine (CQ), has been widely used for its antiparasitic action. It has been found that in some cases chloroquine induces severe effects upon cardiac tissue. Reports have appeared that chloroquine decreases cardiac contractility and lengthens the action potential duration. This study describes the effect of chloroquine upon the inward rectifying potassium current (I_{K1}) in dog cardiac myocytes using whole cell patch clamp recording. The currents were elicited from a holding potential of -70mV to -110mV with 10mV steps lasting 1 second, the experiments were performed at room temperature (20-22° C). The drug was applied directly to the internal solution (in mM:aspartic acid 70; K2PO4 0.3; MgSO4 7H2O 0.11; KCl 50; EGTA 5, HEPES-K 5; ATP-Na 10, pH 7.25), for 20 minutes, reaching final concentrations of 10µM (n= 5), .No effect of the drug was found . This result has a contrast with that reported for extracellular application of the drug (J.Mol.Cell.Cardiol, 1993). We can conclude that CQ seems to use an external receptor in the membrane and its blocking effect and not intracelular receptor.

Tu-Pos416

EFFECTS OF HIGH OSMOTIC STRESS ON *SHAKER* K CHANNELS.

((John Starkus[1,2], Thomas Schlief[1], Stefan H. Heinemann[1])) 1: Max-Planck-Insititut für biophysikalische Chemie, Abt. 140, D-37077 Göttingen, Germany; 2: Univ. of Hawaii, Pacif. Biomed. Res. Ctr., Honolulu, HI 96822

Shaker B potassium channels were expressed in *Xenopus* oocytes and currents were recorded in the inside-out and outside-out patch clamp configuration. When bathing media were made hyperosmolar by addition of sucrose (without change in ionic strength) fully reversible effects on channel function were observed. When the osmolarity of the intracellular side is raised, time constants of activation, inactivation (see Fig. a) and recovery from inactivation are slowed down. External application of hyperosmolar solutions (up to 2000 mosm) had only weak effects on channel kinetics (see Fig. b). Peak current amplitude was reversibly reduced by high osmolar solutions in both conditions. These data suggest that the gating of potassium channel involves osmotically sensitive steps whose molecular rearrangements involve protein parts facing the intracellular side.

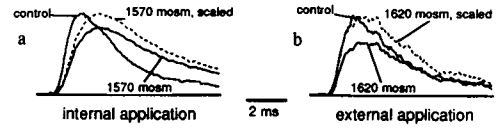

Responses to pulses to +50 mV. a: Inside-out, b: outside-out. Int. sol. (in mM): 115 KCl, 1.8 EGTA; ext. sol.: 115 NaCl, 2.5 KCl, 1.8 $CaCl_2$.

Tu-Pos417

PHOSPHORYLATION BY PROTEIN KINASE A OF RCK1 K^+ CHANNELS EXPRESSED IN XENOPUS OOCYTES.

((T. Ivanina , T. Perez , W.B. Thornhill@, G. Levin , N. Dascal , I. Lotan)) Dep. of physiology, Sackler School of Medicine, Tel-Aviv University, Ramat Aviv 69978, Israel. @Dep. of Physiology and Biophysics, Mount Sinai School of Medicine, The mount Sinai Hospital New York, NY 10029-6574

Phosphorylation-mediated regulation of voltage-gated K^+ channels activity has been implicated in numerous electrophysiological studies; however, complement biochemical studies have been hampered. In this study we have exploited the Xenopus oocyte expression system to demonstrate direct phosphorylation by protein kinase A (PKA) of a rat brain RCK1 (Kv1.1) channel protein. We have studied the biosynthesis and the *in vitro* and *in vivo* phosphorylation of the RCK1 protein in both cytosolic fraction (including intracellular membranes) and in plasma membrane isolated separately from oocytes injected with RCK1 cRNA. We show that the channel protein is expressed in the form of several polypeptides. The 57 kDa polypeptide, usually the major constituent, resides both in cytosolic fractions and in plasma membrane and is N-glycosylated. Its levels were correlated with RCK1 current amplitudes and upon incubation of the cRNA-injected oocytes with tunicamycin its molecular weight was reduced to 54 kDa; concomitantly the RCK1 current amplitudes were reduced by 76%. We conclude that the membranal 57kDa polypeptide represents the functional channel. It can be phosphorylated by the catalytic subunit of PKA (PKA-CS) in the presence of [τ-^{32}P]ATP. We demonstrate that in its basal form in intact oocytes the 57 kDa polypeptide is partially phosphorylated, the extent of phosphorylation varies among different donors. It can be further phosphorylated in oocytes metabolically labeled with ^{32}P by stimulation with a cell permeable cAMP analog (Sp-cAMPS). Using site-directed mutagenesis, we have found that the phosphorylation of a single site on the channel molecule fully accounts for the basal and PKA phosphorylation.

ACETYLCHOLINE RECEPTORS

Tu-Pos418

EFFECT OF POLYCYCLIC AROMATIC COMPOUNDS ON NICOTINIC ACETYLCHOLINE RECEPTORS FROM *TORPEDO CALIFORNICA*.

((Lily Lin and Howard H. Wang)) Department of Biology, University of California, Santa Cruz, California 95064

Polycyclic aromatic hydrocarbons and their metabolites are persistent pollutants in the aquatic environment with major inputs from refining- and transportation-related activities and from urban sources. Acute biological effects of polycyclic aromatic compounds on aquatic organisms are documented, but the mechanisms of action are not well-established. We used the nicotinic acetylcholine receptors from the electric organ of *Torpedo californica*, the Pacific electric ray, as a system to study the effects of potential neural toxins. In the present study, we used the ligand binding property of the acetylcholine receptor to assay for the effect of toxins. The binding of tritiated phencyclidine to the high affinity site in the ion channel of the receptor was used as the control in the absence of toxins. The change in binding affinity for tritiated phencyclidine by the receptor was examined in the presence of the various toxin concentrations. The method has been established by examining the effect of a number of xenobiotic compounds on receptor-ligand interaction. The compounds tested included fluorinated compounds, long chain alcohols and hydroxylated and chlorinated aromatics. The results showed, under equilibrium conditions, a consistent effect of the toxins on receptor affinity at high concentrations of 1 to 10 mM. However, in kinetic studies of receptor-ligand association, the results suggested allosteric changes in the receptor at toxin concentrations from 1 to 3 orders of magnitude lower.

Tu-Pos419

ACETYLCHOLINE RECEPTOR AND CALCIUM LEAKAGE ACTIVITY IN CULTURED NORMAL AND DYSTROPHIC (MDX) MOUSE MYOTUBES.

((Carlson, C.G. and T. Officer)) Dept. Physiology, University of North Dakota School of Medicine, Grand Forks, N.D. 58202.

Cell attached patch clamp recordings from cultured normal myotubes that are obtained with pipette solutions containing 5 x 10^{-7} M ACh exhibit embryonic (E) and adult (A-) Acetylcholine Receptor (AChR) events along with a smaller class of low conductance (3 to 15 pS), short open time (1-3 msec.) events that reverse at a pipette potential more negative than the reversal potential for E- and A-AChR activity. Similar small events are observed in control patches that lack ACh and contain either normal or elevated calcium, or elevated barium concentrations. These results suggest that the small events are produced by calcium leakage activity that can occur in the absence or presence of simultaneous AChR activity. Long term cell attached patches with stable seal resistances (up to 15 min.) that were obtained from cultured mdx muscle exhibited decreases in E-AChR activity that were associated with increases in small channel activity. Subsequent acquisition of an inside-out patch resulted in the re-appearance of E-AChR activity having the same conductance and burst duration characteristics as that originally recorded in the cell attached patch clamp configuration. Acquisition of an inside-out patch from areas of mdx myotube initially exhibiting 100% small channel activity (cell attached configuration) led to the appearance of typical E-AChR activity. Although several long term patches (up to 45 min.) from control myotubes did not exhibit these effects, a proportion of control cell attached patches also exhibited reductions in E-AChR activity associated with increases in small channel activity. The results are currently being examined in order to determine whether alterations in AChR function may be partly responsible for enhanced calcium leakage activity in cultured mdx myotubes. Supported by MDA.

Tu-Pos420

SINGLE CHANNEL KINETIC ANALYSIS OF MOUSE ACHR M2 MUTANTS αL251C and αS248C. ((W. Sigurdson, J. Chen, *M. Akabas, *A. Karlin, and A. Auerbach)) Dept. of Biophysical Sciences., SUNY at Buffalo, NY and *Center for Molecular Recognition, Columbia Univ., New York, NY (Spon. by H. Berman)

Mutations in the M2 (presumptive pore) region of the α subunit of mouse acetylcholine receptors shift the macroscopic ACh dose-response curve. To quantify the effects of these mutations on agonist binding and channel gating, we have studied the single-channel kinetic properties of αL251C and αS248C, mutants that decrease and increase the EC_{50} for ACh, respectively (Akabas et al, Science 258:307, 1992). AChR was transiently expressed in HEK 293 cells and single-channel currents were recorded from cell-attached patches (22 °C). With αL251C, 36 hr after transfection the cells appeared to be more damaged than after tranfection with wt DNA. Currents from cells transfected with αL251C had variable kinetic behavior. Sometimes, at depolarized potentials, discrete single-channel currents were observed but at hyperpolarized potentials no transitions and only excess noise were observed. This suggests that αL251C can assume a conformation that remains ion-conducting for very long periods (>20 minutes). In other patches, clear, long lived single-channel currents, which increased in frequency with increasing ACh (10-100 nM), were seen. These channels had a conductance that was ~70% of the wt ACh, and an apparant open channel lifetime that was ~5 times that of the wt at the same analysis bandwidth. Preliminary kinetic analyses suggest that αL251C closes >10 times more slowly than wt (15 s^{-1} vs 200 s^{-1}), but opens at about the same rate as wt (15,000 s^{-1} vs 20,000 s^{-1}). αS248C AChR produce clusters of inward current at 100 μM ACh (Popen=0.91). Modeling of intracluster intervals (Horn-Lange method; 2 patches) indicates that this mutant AChR closes about twice as fast as do wt receptors. M2 mutations appear to selectively alter closing rates. (Supported by NIH, NSF, MDA, AHA, and Klingenstein)

Tu-Pos421

ELECTROPHYSIOLOGIC ACTIONS OF ADENOSINE MEDIATED BY K_{ATP} CHANNELS IN THE ABSENCE OF INTRACELLULAR ATP DEPLETION. ((G.R. Li, A. Shrier, S. Nattel)) Montreal Heart Institute, McGill University and University of Montreal, Montreal, Quebec, Canada, H1T 1C8.

Adenosine (Ad) is believed to produce cardiac electrophysiological effects by activating acetylcholine (ACh)-sensitive channels. Whole-cell voltage-clamp and cell-attached patch-clamp were used to assess the potential role of K_{ATP} channels in Ad's effects on guinea pig atrial cells. Ad (10 μM) increased holding current at -40 mV from 38±9 pA to 257±29 pA ($p<0.01$), and glyburide (20 μM) restored the holding current to 65±8 pA ($p<0.01$ vs Ad alone). ACh (10 μM) increased the holding current, but ACh's effects were not altered by glyburide. Ad and ACh added an inwardly-rectifying component to the steady-state I-V curve. Glyburide inhibited Ad-induced current, but did not alter ACh's effect. The inclusion of ACh (10 μM) in the pipette of cell-attached patches produced an inwardly-rectifying channel with a conductance of 41±5 pS (Figure). When Ad (10 μM) was included in cell-attached pipettes, two types of channels were elicited, one similar to that induced by ACh, and a higher-conductance channel (72±2 pS) with weaker rectification. Glyburide (20 μM) suppressed the high-conductance channel, leaving a single channel type (37±6 pS). Ad-induced shortening of APD in multicellular preparations was antagonized by glyburide (IC_{50} 31 μM), in both physiologic and low-chloride (7.4 mM) superfusate. These results suggest that Ad and ACh do not have identical signal transduction mechanisms, with K_{ATP} activated by Ad and not ACh under nonischemic conditions.

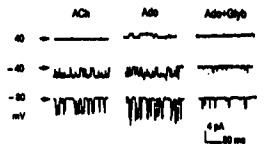

Tu-Pos422

EXPRESSION OF EMBRYONIC AND ADULT FORMS OF NICOTINIC ACH RECEPTOR CHANNELS FROM *XENOPUS* MYOTOMAL MUSCLE ((N. Murray, M.A. Bolinger*, Y.C. Zheng, G. Mandel, P. Brehm and R.W. Kullberg*)) Dept. of Neurobiology and Behavior, SUNY, Stony Brook, NY 11794 and *Dept. of Biological Sciences, Univ. of Alaska, Anchorage, AK 99508.

Nicotinic ACh receptor channels from *Xenopus laevis* myotomal muscle were expressed in *Xenopus* oocytes. Two synthetic RNA combinations, αβδγ and αβδε, were injected into oocytes and functional expression was assayed by two electrode voltage clamp. Two days post injection, application of 100μM ACh activated greater than 10μA at a holding potential of -80mV. Single channel measurements from outside-out patches were made using 300nM ACh at -100mV. Receptors composed of αβδγ subunits exhibited a conductance of 39 pS between -180 mV and -40 mV. Open duration histograms were fit to three exponentials yielding the following time constants (mean ± S.D. (area)): 0.21 ms ± .06 (4.9%); 3.71 ms ± .71 (79%); 19.51 ms ± .67 (14%). Receptors composed of αβδε subunits had a conductance of 56 pS and open duration histograms were fit to two exponentials: 0.45 ms ± .14 (32%) 1.74 ms ± .33 (68%). Comparisons to cell attached recordings from *in-vivo* myotomal muscle support the idea that αβδγ receptors correspond to an embryonic receptor type on the basis of similarity in channel open time and conductance. The conductance of αβδε channels expressed in oocytes is similar to that obtained from cell attached recordings on *Xenopus* myotomal muscle. However, the open time of receptors expressed in oocytes is longer. Ribonuclease protection assays indicate that γ and ε mRNA levels change in concert with the developmental switch between embryonic and adult receptor function. Overall, these data support the idea that developmental changes in ACh receptor kinetics in amphibian muscle result from a gamma to an epsilon subunit switch, as occurs in developing mammalian skeletal muscle.
Supported by NS 24078 (RWK) and NS 18205 (PB).

Tu-Pos423

PROTON-DEUTERIUM EXCHANGE AND INFRARED DICHROISM: PROBES OF THE CONFORMATIONAL CHANGES ASSOCIATED WITH DESENSITIZATION OF THE nAChR. ((N.Méthot and J.E. Baenziger)) Dept. of Biochemistry, University of Ottawa, Ottawa, Canada.

Attenuated total reflection Fourier transform infrared spectroscopy has been used to investigate the conformational changes associated with the desensitization of the nicotinic acetylcholine receptor (nAChR). The solvent accessibility of the secondary structures of the nAChR were monitored by following the rate and extent of the decrease in intensity of the amide II band centered near 1547 cm^{-1} upon exposure of the nAChR to ^2H_2O buffer and by monitoring changes in the shape of the deconvolved amide I band as a function of the progression of H/D exchange. In the presence and absence of the ligands tetracaine and carbamylcholine, which stablize the resting and desensitized states of the nAChR, respectively, both the rate and magnitude of H/D exchange were essentially the same. In addition, spectral deconvolution did not detect significant changes in the accessibilities of individual types of secondary structures. The results indicate that, in agreement with others, the global conformation of the nAChR is not changed by desensitization. Infrared dichroism measurements of the nAChR performed in the presence and absence of the ligands tetracaine and carbamylcholine will be discussed in terms of both structural models of the nAChR and models of nAChR desensitization.

Tu-Pos424

SECONDARY STRUCTURE AND CONFORMATIONAL CHANGES ASSOCIATED WITH DESENSITIZATION OF THE nAChR PROBED USING FTIR SPECTROSCOPY. J.E. Baenziger[1], J.P. Chew[1], M.P. McCarthy[2], and N. Méthot[1]. [1]Dept. Biochemistry, Univ. of Ottawa, Ottawa, Canada, and [1]Dept. Pharmacology, UMDNJ, Piscataway, NJ.

The secondary structure and structural changes associated with the desensitization of the nicotinic acetylcholine receptor (nAChR) have been examined using FTIR spectroscopy. Spectra of the nAChR were recorded in both H_2O and D_2O buffer and were deconvolved to reveal the amide I component bands in the 1600-1700 cm^{-1} region. The number and frequencies of the components bands were used to curve fit the amide I band contour and gave the following estimate of the secondary structure: 39% α-helix, 35% β-sheet, 6% turn and 20% random structures. The α-helical content is sufficient to account for the four putative transmembrane helices of each subunit as well as a sufficient portion of the extramembranous domains. Deconvolved spectra acquired in the presence and absence of the ligands carbamylcholine and tetracaine were essentially identical indicating that no *large scale* conformational changes are associated with desensitization. Subtle secondary structural changes were detected in resting-to-desensitized difference spectra acquired from affinity purified and native nAChR membranes. The nature of the subtle changes in secondary structure associated with desensitization will be discussed.

Tu-Pos425

IDENTIFICATION OF AMINO ACIDS INVOLVED IN THE BINDING OF [^{3}H] TETRACAINE TO THE *TORPEDO* NICOTINIC ACETYLCHOLINE RECEPTOR

((Martin J. Gallagher and Jonathan B. Cohen))
Department of Neurobiology, Harvard Medical School, Boston, MA 02115

Tetracaine (TET, 4-[Butylamino]benzoic acid 2-[dimethylamino]ethyl ester) is a local anesthetic that is bound with 100-fold greater affinity by the *Torpedo* nicotinic acetylcholine receptor (AChR) in the absence of agonist than in the agonist bound, desensitized state. To identify amino acids involved in TET binding, we photoincorporated [^{3}H]TET into the AChR using histrionicotoxin (HTX) to define non-specific labeling. [^{3}H]TET specifically incorporated into each receptor subunit with similar, albeit low, efficiency (~0.1%). Specifically labeled fragments from endoproteinase-lys-C digests of alpha and delta subunits were purified by tricine SDS-PAGE followed by reverse phase HPLC. N-terminal sequence analyses of these purified fragments established that [^{3}H]TET labeled the homologous residues α-Leu-251 and δ-Leu-265 which are located within the M2 hydrophobic regions and which previous photolabeling and mutagenesis studies have implicated in lining the ion channel pore. These results demonstrate that even in the absence of agonist, this region of the pore is accessible to compounds the size of tetracaine.

In addition to specific labeling in the M2 region, sequence analysis revealed HTX-inhibitable labeling of α-Tyr-190 which is associated with the agonist binding site. In view of the sensitivity to HTX and other pharmacological criteria, it appears that labeling of α-Tyr-190 is due to a secondary photochemical mechanism rather than from TET bound to the agonist site.

Tu-Pos426

CHARACTERIZING THE INTERACTION OF THE PHOTOACTIVATABLE HYDROPHOBIC PROBE [^{3}H] DIAZOFLUORENE WITH *TORPEDO* NICOTINIC ACETYLCHOLINE RECEPTOR MEMBRANES

((Michael P. Blanton[1] ,S.K. Raja[2], Anil K. Lala[2], Jonathan B. Cohen[1])) [1] Department of Neurobiology, Harvard Medical School, Boston, MA 02115; [2] Biomembrane Lab, Department of Chemistry, Indian Institute of Technology Bombay, Bombay, India.

When incubated with *Torpedo* Nicotinic Acetylcholine Receptor (AchR) enriched membranes, 2-[^{3}H] Diazofluorene ([^{3}H] DAF) photoincorporates into each AchR subunit in approximately equal abundance, and the pattern of incorporation is the same in the absence or presence of carbamylcholine (100 μM). We have identified the [^{3}H] DAF labeled residues in the M4 region of each of the AchR subunits. The labeled residues are for the most part the same as those identified as being situated at the lipid-protein interface using the photoactivatable probe 3-trifluoromethyl-3-m-[^{125}I]iodophenyl) diazirine ([^{125}I] TID) (Michael P. Blanton & Jonathan B. Cohen, *Biophys. J.* 64: A322). [^{3}H] DAF incorporation into Trp-453 in γ-M4 and into Phe-443 and Phe-444 in β-M4 are two notable exceptions. Interestingly, in the resting state of receptor [^{3}H] DAF incorporates into δ-Val-269 within the M2 region. In contrast, [^{125}I]TID incorporates specifically into both δ-Leu-265 and Val-269. A comparison of the structures of both [^{125}I]TID and [^{3}H] DAF provides important information about the structure of the ion channel in the resting state of the receptor. Finally, in addition to the AchR, [^{3}H] DAF also incorporates into a number of previously unidentified protein bands present in *Torpedo* AchR-enriched membrane preparations, including a 34 Kdal band identified as the *Torpedo* homologue of mitochondrial porin and an 89 Kdal Chloride channel protein (CIC-0).

Tu-Pos427

ACTIVATION AND BLOCK OF ACH RECPTOR CHANNELS BY TMA.

((H.I. Mody, J. Lee and J.P. Dilger)) Dept. of Anesthesiology, SUNY, Stony Brook, NY 11794.

Tetramethylammonium (TMA) is thought to be a partial agonist at the nicotinic acetylcholine receptor (AChR) channel. Like other cationic agonists, TMA may also have a voltage-dependent, channel blocking action on the AChR. To determine the binding affinity, efficacy and blocking affinity of TMA, we measured macroscopic currents activated by rapid application of TMA to outside-out patches from BC3H-1 cells. The peak, absolute open probability, p_o, was calculated by comparison with the current response to 100 μM ACh (p_o=0.9). The p_o vs [TMA] curve at –50 mV (Figure below) is fit to a 5-state model for channel activation and block ($R \leftrightarrow AR \leftrightarrow A_2R \leftrightarrow A_2R^* \leftrightarrow A_2R^*A$). We find an agonist binding affinity of 1.6 mM (equivalent sites assumed), a gating isomerization ratio (β/α) of 1.4 and a blocking affinity of 20 mM. In the absence of block, TMA would open a maximum of 60% of the channels. The efficacy of TMA is less than that of ACh (β/α≥20) and greater than that of decamethonium (β/α=0.016). The channel closing rate determined from single channel analysis is 1100/s. Thus, the channel opening rate for TMA is 1600/s.

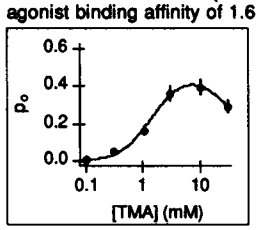

Supported by GM42095 (JPD).

Tu-Pos428

EFFECTS OF ALCOHOLS AND ETHER ON ACTIVATION OF ACH RECEPTOR CHANNELS.

((Y. Liu, A.M. Vidal and J.P. Dilger)) Dept. of Anesthesiology, SUNY, Stony Brook, NY 11794.

The inhibition of nicotinic acetylcholine receptor (AChR) channels by n-alcohols and general anesthetics can be understood in terms of a model in which the drugs bind to and block open and closed channels (J. Physiol. 437:431, '91; Mol. Pharmacol. 41:127, '92). These drugs also have a separate, excitatory effect on the AChR; they increase the frequency of bursts of channels seen at low concentrations of agonists. 10 mM butanol increases the burst frequency induced by 0.2 μM ACh (a full agonist) 1.6-fold and 1 μM decamethonium (Deca, a partial agonist) 2.7-fold. An increase in burst frequency may arise from effects of the drug on agonist binding, channel gating or desensitization. To distinguish among these alternatives, we measured the current response to rapid application of saturating concentrations of agonists. 10 mM butanol increases the current induced by 100 μM Deca by 2-fold. In addition, 20 mM butanol and 3 mM pentanol both decrease the onset time of the current response to 10 mM ACh (by 40% and 25%, respectively). In contrast, ether (as we found for isoflurane, Mol. Pharmacol., in press, Nov. '93) does not significantly change the onset time. We conclude that butanol and pentanol increase burst frequency by increasing the channel opening rate whereas ether does so by increasing the agonist binding affinity of the AChR.

Supported by GM42095 (JPD).

Tu-Pos429

ROLE OF THE VICINAL DISULFIDE BOND BETWEEN CYS-α192 AND CYS-α193 IN LIGAND BINDING TO 18MER FRAGMENTS OF THE NICOTINIC ACETYLCHOLINE RECEPTOR

((Qing-luo Shi and Edward Hawrot)) Section of Molecular and Biochemical Pharmacology,Brown University,Providence, RI 02912

The vicinal disulfide bond between the invariant Cys-192 and Cys-193 in the α-subunit of the nicotinic acetylcholine receptor (nAChR) has been implicated by numerous studies as being involved in the binding domain for nicotinic agonists and antagonists.

We have been studying an 18mer (α181-198) and an 18mer$^{Phe\text{-}190}$ (a modified 18mer containing Phe-190 in place of the invariant Tyr-190), in both reduced and oxidized (S-S) forms, in their interactions with the agonists acetylcholine (ACh), carbamylcholine (carbachol) and with an antagonist, α-bungarotoxin (BGTX). The interactions were monitored by circular dichroism (CD) in both the near (330-250nm) and far UV region (250-190nm). With the 18mer in both reduced and oxidized (S-S) forms, a BGTX-binding induced CD change could be detected both in the near UV and the far UV regions, but the induced CD is slightly more pronounced for the 18mer containing the S-S bond. The 18mer$^{Phe\text{-}190}$ in the reduced form exhibits little if any CD change resulting from BGTX-binding, consistent with its 60-fold decrease in binding affinity for BGTX as compared with the 18mer. The oxidized form, however, shows significant CD change, when combined with BGTX under the same conditions as with the reduced form. Adding ACh or carbachol to each of the four peptides causes some CD increase around 210nm, with the increase being much more distinct for the peptides having a disulfide bond. The pattern of CD change of the 18mer$^{Phe\text{-}190}$, however, is somewhat different than that of the 18mer. (Supported by NIH-GM 32629)

PERMEATION THROUGH MEMBRANE CHANNELS

Tu-Pos430

SELECTIVITY OF VOLTAGE-ACTIVATED K^+ AND Na^+ CHANNELS PROBED BY MULTIMERIC cDNAs AND 3-D MODELLING.

((Ch. Verboven, J. Tytgat, C. De Ranter and E. Carmeliet)) Laboratory of Analytical Chemistry and Medicinal Physico-Chemistry, Laboratory of Physiology, University of Leuven, Belgium.

Deletion mutants of *Shaker* K^+ channels lacking the middlemost 2 residues of the amino acid sequence Gly-Tyr-Gly-Asp in their P-region loose K^+-selectivity and become functionally similar to voltage-activated Ca^{2+} channels (1). To investigate a possible evolutionary connection between voltage-activated K^+ and Na^+ channels, deletion mutants lacking Tyr-Gly residues in the P-region of delayed rectifier RCK1 (Kv1.1) K^+ channels were made. The next residue, Asp, was either left unaffected or mutated to Glu, Lys, or Ala, based on primary sequence alignment with the Na channel. We then have concatenated the mutant monomeric K^+ channel cDNAs into tetrameric constructs with respective P-region sequences: Gly-Asp, Gly-Glu, Gly-Lys, Gly-Ala. In contrast to deletion mutants Gly-Asp and Gly-Glu of *Shaker* K^+ channels, none of the mutant mono- or tetrameric cDNAs from RCK1 K^+ channels yielded functional expression. To gain better insight in these lethal pore-mutants 3-D modelling was performed using Insight & Discover (2). Starting with a model of the wild-type *Shaker* K^+ channel according to Durell & Guy (3), the CVFF force field and the steepest descents algorithm for energy minimization were used to compare the structures of wild-type and mutant RCK1 K^+ channels.

(1) Heginbotham *et al.* 1992 *Science* **258**:1152-1155.
(2) Insight II, Discover. San Diego: Biosym Technologies, 1992.
(3) Durell & Guy 1992 *Bioph. J.* **62**:238-250.

Tu-Pos431

CATION CHANNELS THAT ARE PERMEABLE TO MONOVALENT AND DIVALENT CATIONS.

((Yoshio Oosawa)) International Institute for Advanced Research, Matsushita Electric Industrial Co., Ltd., 3-4-1 Hikaridai, Seika-cho, Soraku-gun, Kyoto, 619-02 JAPAN.

Tetrahymena have been used for the study of membrane excitation by making use of conventional electrophysiological techniques. The ionic mechanisms for membrane excitation in *Tetrahymena* are fundamentally identical to those in its larger relative, *Paramecium*. Cation channels from *Tetrahymena* cilia were incorporated into planar lipid bilayers. The cation channel was permeable to K^+ and Ca^{2+}. The single channel conductance in mixed solutions of K^+ and Ca^{2+} was determined by the Donnan ratio of K^+ and Ca^{2+} ($[K^+]/\sqrt{[Ca^{2+}]}$). For explaining this fact, the binding sites of the channel were considered to be always occupied by two potassium ions or by one calcium ion under the experimental conditions: 5-90 mM K^+ and 0.5-35 mM Ca^{2+}. In solutions of K^+, the channel conductance reached a maximum value as the K^+ concentration was increased. Three-barrier, two-ion channel model can explain the saturation curve in solutions of K^+.

Tu-Pos432

CALCIUM PERMEABILITY OF α-BUNGAROTOXIN-SENSITIVE NICOTINIC ACETYLCHOLINE RECEPTORS IN RAT HIPPOCAMPAL NEURONS. ((N.G. Castro and E.X. Albuquerque)) Dept. Pharmacol. Exp. Therap., Univ. Maryland Sch. Medicine, Baltimore MD 21201.

The calcium permeability of α-bungarotoxin-sensitive, neuronal nicotinic receptor channels (carrying *type IA* currents, as per: *J. Pharmacol. Exp. Ther.* 265:1455, 1993, and presumably containing the α_7 subunit) was investigated and compared to that of NMDA channels. The reversal potentials (V_R) of agonist-induced whole-cell currents were recorded from cultured rat hippocampal neurons under two different $[Ca^{2+}]_{out}$. Permeabilities relative to Cs^+ were estimated using the GHK model. Acetylcholine (ACh) or NMDA (and glycine) was dissolved in the external solutions and applied to the neurons through a U-tube. The test solutions were (in mM): internal, CsCl 60, CsF 60, CsOH 38.5, $MgCl_2$ 5, EGTA 10, HEPES 10, ATP 5, phosphocreatine 20, Tris 52.5, and creatine phosphokinase 50 U/ml (pH 7.3); external, Cs-methanesulfonate 100, CsCl 50, $CaCl_2$ 1 or 10, HEPES 10, D-glucose 10 and N-methyl-D-glucamine-HCl 35 or 20 (pH 7.3). An agar-KCl bridge was used in the reference electrode. The V_Rs were obtained by fitting a 3rd-degree polynomial to the peak current-voltage relationships and were corrected for junction potentials. In 1 and 10 mM Ca^{2+}, the V_Rs of type IA ACh currents were (in mV) -3.1 ± 0.8 (n=6 neurons) and $+2.5\pm0.9$ (n=8), while those of NMDA currents were -2.8 ± 1.4 (n=6) and $+5.6\pm1.1$ (n=5). The V_Rs of both ACh and NMDA currents at 1 mM Ca^{2+} were more negative than would have been expected if Cs^+ and Ca^{2+} were the only permeant ions. After ruling out a significant anion permeability, the ionized Tris buffer, which permeates the muscle endplate channel, was the best candidate to account for the more negative V_Rs. Taking Tris into consideration yielded a good fit of the GHK model. Using ion activities, the fitted P_{Cs}/P_{Cs} and P_{Tris}/P_{Cs} were: for ACh, 5.8 and 0.3; for NMDA, 10.2 and 0.4. Thus, as previously shown for NMDA currents, a large fraction of the type IA ACh currents was carried by Ca^{2+}. For these ACh currents, which show a linear I-V relationship below -20 mV, the Ca^{2+} influx *in vivo* can be maximum at near-resting membrane potentials, as is not the case with NMDA currents. Supported by NIH grant NS25296 and CNPq-Brazil.

Tu-Pos433

HOW DO CARDIAC ANTIARRHYTHMIA DRUGS INDUCE OSCILLATIONS IN REENTRY?

((Teresa Ree Chay)) Department of Biological Sciences, University of Pittsburgh, Pittsburgh, Pennsylvania 15260

It has been demonstrated experimentally that the action potential duration (APD), the diastolic interval (DI), and the cycle length (CL) oscillate either when the reentrant pathway is shortened or when certain types of antiarrhythmic drugs are used. It is a challenge to show theoretically how these drugs may induce the oscillations. Using bifurcation analysis approach, we first show how to locate accurately the critical wave length (CWL), which separates sustained reentry from non-sustained. This wave length is informative in that lengthening of CWL leads to instability and shortening of it leads to stable reentry. We then demonstrate using a cardiac cell model of ventricular myocardium that both sodium and calcium channel blockers decrease the CWL, the former much more effectively than the latter. The potassium channel blockers, on the other hand, increase this length considerably. In addition, we show by means of the numerical simulations why APD, CL, and CV all oscillate in the vincinity of CWL. The period of the oscillation depends on the ring size such that the period becomes shorter as the ring shrinks. This work thus provides theoretical explanation for why Class IC drugs (which exclusively block the sodium channels) can sometimes bring about stable reentry from non-sustained reentry, whereas Class III drugs (potassium channel blockers) can induce complex oscillations in APD, DI, and CL from sustained stable reentry. It also explains that the drugs which block the sodium and calcium channels can exert a proarrhythmic effect while the potassium channel blockers are the most effective drugs for suppressing ventricular reentrant arrhythmias.

Tu-Pos434

CONDUCTANCE REDUCTION AND NOISE OF A SINGLE SYMMETRICAL AMPHOTERICIN B CHANNEL IN THE PRESENCE OF DIFFERENTLY SIZED POLYMERS. ((S.M.Bezrukov[1], R.A.Brutyan[1,2], I.Vodyanoy[3])) [1]NIDDK, NIH, Bethesda, MD 20892; [2]Univ. of Maryland, MD 20742; [3]ONR, Arlington, VA 22217-5000

We studied the effect of polyethyleneglycols (PEGs) of different molecular weights (200 - 20,000 Da) on the conductance and the power spectral density of current fluctuations of an open single ion channel induced by symmetrical addition of amphotericin B to lipid bilayers (L-alpha-phosphatidylserine: cholesterol = 5:1). In the presence of 15 % (w/w) PEG in the membrane bathing solution, channel conductance decreased with decreasing polymer molecular weight to a degree that exceeds the polymer's effect on specific conductivity of the bulk solution. With PEG 200, reduction of the channel conductance is approximately 1.5 times *stronger* than reduction of the bulk solution conductivity, suggesting attractive interactions between polymer and channel. The low-frequency part of polymer-induced current noise shows a non-monotonic dependence on polymer molecular weight with a pronounced maximum at 400 - 600 Da. The results are interpreted in terms of polymer partitioning and dynamics inside the channel. Osmotic stress effects on the channel complex are also discussed.

Tu-Pos435

NOISE INDUCED BY DIFFERENTLY SIZED POLYETHYLENE-GLYCOLS SHOWS INTERACTION OF POLYMER WITH THE α-TOXIN ION CHANNEL

((J.J. Kasianowicz[1], R.A. Brutyan[2,3], I. Vodyanoy[2,4], S.M. Bezrukov[2]))
[1]NIST, Gaithersburg, MD, [2]NIH, Bethesda, MD, [3]U. MD at College Park, [4]ONR, Arlington, VA.
(Spon. by S. Krueger)

We have measured the fluctuations in current through single channels formed by *S. aureus* α-toxin induced by different low molecular weight polyethylene-glycols (PEGs). We find a non-monotonic dependence of the current noise on the PEG MW. Specifically, 2,000 MW PEG (hydrodynamic radius = 1.27 nm, Kuga. 1981. J. Chromat. 206:449) increases markedly the current noise spectral density, whereas smaller (MW ≤ 1,000) and larger (8,000 ≤ MW ≤ 20,000) PEGs do so to a much lesser extent. Interestingly, the degree to which the PEGs induce current noise suggests that the polymer interacts with the pore. This is also supported by our measurements of the low voltage single channel currents and the bulk aqueous conductivities in the presence and absence of PEG. Low MW PEGs, which partition into the pore, decrease the single channel current to a greater extent than they do the bulk conductivity. We discuss our results in terms of previous estimates of the channel pore "radius" by others using PEG or other non-electrolytes and completely different methods (e.g. Füssle, et al. 1981. J. Cell Biol. 91:83; Krasilnikov, et al. 1991. FEMS Microbiol. Immun. 105:90). Supported by a NAS/NRC Research Associateship (JJK) and a grant from the ONR (VA Parsegian).

Tu-Pos436

ANALYTIC AND STOCHASTIC SOLUTIONS TO THE NERNST-PLANCK EQUATION FOR ELECTRODIFFUSION IN ION CHANNELS: FORMALISM AND CORRESPONDENCE TO EXPERIMENTAL DATA. S. Bek, J. Huang, and E. Jakobsson, Dep't of Physiology and Biophysics, Nat'l Center for Supercomputing Applications, Univ. of Illinois, Urbana, IL 61801. The Nernst-Planck electrodiffusion equation for ion permeation of membrane channels may be solved either analytically or by Brownian dynamic simulation. The Brownian dynamics method has the advantage that it naturally, explicitly, and accurately reflects the physical assumptions that the user puts into the calculation. Analytical methods have the advantage that solutions are generally obtained with greater computational efficiency. We compare the properties of analytical solutions to the Nernst-Planck equation for ion permeation with the results of Brownian dynamics simulations of the same process, and with experimental data. By these comparisons we infer features of the underlying physics that are implicit in the analytical solutions and may be features of actual channels. One result is that ion-ion interactions in a channel selective to just one ion tend to cause the open channel I-V curve to become quite linear, even at quite asymmetric bathing concentrations. On the other hand, asymmetric distributions of potential minima, or preferred sites for ions, induce asymmetry in the open channel I-V curve, even in symmetric bathing solutions. In this paper we suggest possible application of these results to understanding I-V relationships observed in particular ion channels. Support by NSF and Nat'l Center for Supercomputing Applications.

Tu-Pos437

Molecular Cloning of A Mercurial-Insensitive Water Channel (MIWC30) Expressed in Selected Water Transporting Epithelia.
((H. Hasegawa, T. Ma, W. Skach, M.A. Matthay and A.S. Verkman)) Cardiovascular Research Institute, U.C.S.F.

A novel water transporting protein (MIWC30, Mercurial-Insensitive Water Channel of 30 kDa) was cloned from a rat lung λgt10 cDNA library with a 360 bp DNA probe prepared by PCR amplification of lung cDNA using degenerate primers. A positive clone with a ~1.2 kb insert encoded a 282-amino acid protein with 30.1 kDa predicted protein size and 41% amino acid homology to CHIP28 and WCH-CD water channels. Sequence analysis showed a hydrophobic protein with multiple membrane-spanning domains, two sites for N-linked glycosylation and three phosphorylation sites for protein kinase A and C. Northern blot and PCR/Southern blot analysis showed MIWC30 expression in brain, eye, lung, kidney, colon, liver and salivary gland with ~5.5 kb mRNA. Interestingly, an alternatively spliced form of MIWC30 (sMIWC) with a 165 bp deletion in the coding sequence, which is nearly equivalent to exon 2 of human CHIP28, was identified in a tissue-specific manner. Expression of transcribed cRNA in *Xenopus* oocytes gave a >10-fold increase in water permeability which was not sensitive to $HgCl_2$; this result is consistent with the presence of alanine (rather than cysteine for CHIP28 and WCH-CD water channels) at position 188, while sMIWC did not function as a water channel. Cell-free translation produced a non-glycosylated 30 kDa protein. MIWC30 did not transport protons or urea. *In situ* hybridization revealed that mRNA encoding MIWC30 was expressed selectively in renal papilla, brain cells lining the subarachnoid space and ventricles, alveolus and a layer of retina. MIWC30 is the first mercurial-insensitive water channel to be identified and probably plays an important physiological role in fluid-transporting cells.

Tu-Pos438

TWO-DIMENSIONAL CRYSTALLIZATION OF THE CHIP28 WATER CHANNEL IN LIPID BILAYER MEMBRANES.
((Alok K. Mitra, Alfred N. van Hoek#, Michael C. Wiener#, A. S. Verkman# and Mark Yeager*)) *The Scripps Research Institute, Dept. of Cell Biology, La Jolla, CA 92037. #University of California at San Francisco, Depts. of Medicine and Physiology, Cardiovascular Research Institute, San Francisco, CA 94143.*

CHIP28 is a CHannel forming Integral Protein of 28 kDa that functions as a water channel in the plasma membranes of erythrocytes and renal tubule epithelial cells. Recent spectroscopic and biochemical studies have revealed that CHIP28 forms tetramers in membranes [Verbavatz *et al., J. Cell. Biol.* in press (1993)] in which individual monomers function independently and contain multiple, putative α-helical, membrane-spanning domains [Van Hoek *et al., Biochemistry*, in press (1993)]. However, the molecular envelope and tertiary folding of CHIP28 are not known. To elucidate the molecular mechanism of water transport through CHIP28, high resolution three-dimensional structural information is required. Membranes enriched in CHIP28 were isolated by treating human erythrocyte ghosts with KI and N-lauroylsarcosine [Van Hoek and Verkman, *J. Biol. Chem.* 267, 18267-18269 (1992)]. The membranes were solubilized in 35 mM β-octylglucoside, and CHIP28 was purified by anion exchange (DEAE sephacel) and size-exclusion HPLC chromatography. Highly purified CHIP28 in β-octylglucoside was mixed with phospholipid micelles, and the detergent was removed by slow dialysis over several days. Reconstituted membranes were stained with uranyl acetate and examined by minimal dose, transmission electron microscopy using 100kV electrons. Images of membrane sheets displayed crystalline areas measuring ~0.5 μm^2 with a tetragonal lattice (a = b ~ 95Å). The membrane crystals diffract to ~20Å resolution and are suitable for analysis by electron microscopy and image processing.

Tu-Pos439

Functional Independence of Monomeric CHIP28 Water Channels Revealed by Expression of Wild-Type-Mutant Heterodimers. ((Lan-bo Shi, W. Skach and A.S. Verkman)) Cardiovascular Research Institute, U.C.S.F.

CHIP28 is a major water transporting protein in erythrocytes and kidney that forms tetramers in membranes (Verbavatz et al., *J. Cell Biol.* 1993; 123, in press). To determine whether CHIP28 monomers function independently, chimeric cDNA dimers were constructed which contained wild-type CHIP28 in series with either a non-water transporting CHIP28 mutant (C189W) or a functional but mercurial-insensitive CHIP28 mutant (C189S). Transcribed cRNAs were injected in *Xenopus* oocytes and plasma membrane expression was assayed by quantitative immunofluorescence and osmotically-induced swelling. CHIP28 homo- and heterodimers were targeted to the oocyte plasma membrane and functioned as water channels. Relative osmotic water permeability (P_f) values (normalized for plasma membrane expression) were: 1.0 (CHIP28 monomer), 0.0 (C189W), 1.1 (C189S), 1.1 (CHIP28-CHIP28 dimer) and 0.6 (CHIP28-C189W). The increase in oocyte P_f was linearly related to plasma membrane expression of wild-type CHIP28 and C189S subunits. $HgCl_2$ (0.3 mM) inhibited channel-mediated P_f in oocytes expressing wild-type CHIP28 monomers and dimers by 80-90%, but did not inhibit P_f in oocytes expressing C189S; $HgCl_2$ inhibition in oocytes expressing CHIP28-C189S dimers was intermediate at 43 ± 5 %. These results indicate that despite its tetrameric quaternary structure, CHIP28 monomers function independently as water channels.

Tu-Pos440

CLONING, EXPRESSION AND FUNCTIONAL STUDIES OF FROG LENS MIP. ((C. Kushmerick, S.J. Rice, G.J. Baldo, H.C. Haspel and R.T. Mathias)) SUNY at Stony Brook, N.Y. 11794

A frog lens MIP clone was isolated from a cDNA library. We modified the clone by inserting a 5' untranslated region from a highly translated viral sequence and adding a poly A sequence to the 3' end. mRNA from this construct was injected into Xenopus oocytes and its expression detected by SDS-PAGE. Immunofluorescence studies localized the expressed protein to the oocyte plasma membrane. MIP RNA-injected oocytes were compared to control (water-injected) oocytes using two-electrode voltage clamping, quantitative video microscopy of osmotically-induced volume changes and measurement of radiolabeled neutral solute uptake.

Current-voltage relationships suggest MIP does not form an ion channel in single oocytes. The average membrane potentials were -42±8.7 mV and -52±7.7 mV (mean±SD, n=23,22) and the input resistances 2.2±0.19 MΩ and 1.0±0.22 MΩ for MIP and control oocytes, respectively. MIP RNA-injected oocytes swelled more rapidly than control oocytes in hypotonic solution, (1.5%/min versus 0.75%/min). This increase was not inhibited by 3mM Hg^{++}, 100μM Cu^{++} or 100μM phloretin. MIP is a poor water channel compared to the channel formed by CHIP28, which increases the rate of swelling of oocytes ten- to fifty-fold and is mercury sensitive. MIP RNA-injected oocytes showed no increased permeability to deoxyglucose, inositol, urea, sorbitol or reduced glutathione, compared to controls. MIP RNA-injected oocytes transported more glycerol in 20 minutes than controls (39±4.3 pmol versus 25±5.6 pmol; n=4). The relevance of this observation to lens physiology remains unclear.

Supported by NIH Grant EY06391

Tu-Pos441

VOLUME REGULATION IN CULTURED HUMAN RETINAL PIGMENT EPITHELIUM. ((B.G. Kennedy)) Northwest Cntr. Medical Education. Indiana Univ. Sch. Med., Gary IN 46408

The retinal pigment epithelium (RPE) is an epithelial cell layer which separates the sensory retina from its choroidal blood supply. Laser light scattering and isotopic flux measurements were used to examine volume regulation in cultured human RPE (HRPE). Cell volume decreased and then gradually returned toward control level after exposure to a hypertonic (390 mOs) media. Conversely, volume increased and then relaxed back toward normal levels after hypotonic (190 mOs) challenge. Cultured HRPE catalyze both regulatory volume increase (RVI) and regulatory volume decrease (RVD). Bumetanide-sensitive 86-Rb influx (used as a congener for K) increased 3 fold upon exposure to the hypertonic media. On the other hand, hypotonic challenge, as well as NEM (2 mM) treatment, activated bumetanide-insensitive Rb influx. Additionally, Rb efflux also transiently increased after exposure to the hypotonic media. The K-channel blocker barium (5 mM) partially inhibited both RVD and hypotonically activated Rb efflux. HRPE cells seem to possess volume-sensitive Na-K-Cl cotransport, K-Cl cotransport and K channel activities. (Supported by the Helmsly Fund of Fight for Sight, Nat. Soc. to Prevent Blindness).

Tu-Pos442

EFFECT OF ISOSMOTIC REMOVAL OF EXTRACELLULAR SODIUM ON CELL VOLUME AND MEMBRANE POTENTIAL IN BARNACLE MUSCLE CELLS. ((C. Peña-Rasgado, J. C. Summers, K. McGruder, J. DeSantiago and H. Rasgado-Flores)) Dept. Physiol & Biophys. UHS/Chicago Medical School. N. Chicago, IL 60061.

Isosmotic removal of extracellular Na^+ (Na_o) is a frequently performed manipulation. Using isolated, voltage-clamped barnacle muscle cells, the effect of this manipulation on isosmotic cell volume was studied. Replacement of Na_o by Tris produced membrane depolarization (~20 mV) and cell volume loss (~14%). The membrane depolarization was verapamil-insensitive but depended on extracellular Ca^{2+} (Ca_o) and was probably due to activation of intracellular Ca^{2+}, Ca_i-dependent non-selective cation channels; the cell volume loss was membrane depolarization-independent but depended on Ca_o. This was due to an increase in Ca_i mediated by activation of Ca^{2+} influx via Na/Ca exchange. Na_o-replacement by Li also promoted membrane depolarization (~20 mV) and cell volume loss (20%). Both effects were reduced (~73%), but not abolished by Ca_o-removal. Under this condition, the remaining membrane depolarization was due to a higher membrane permeability of Li^+ over Na^+. The remaining cell volume loss was due to the membrane depolarization which probably induced Ca^{2+} release from intracellular stores.

Supported by NIH (R29-AR-39522) (to H.R-F.).

Tu-Pos443

EFFECT OF ISOSMOTIC REMOVAL OF EXTRACELLULAR CALCIUM AND OF MEMBRANE POTENTIAL ON CELL VOLUME IN BARNACLE MUSCLE CELLS. ((Peña-Rasgado, K. McGruder, J. C. Summers, and H. Rasgado-Flores)) Dept. Physiol & Biophys. UHS/Chicago Medical School. N. Chicago, IL 60061.

Isosmotic removal of extracellular Ca^{2+} (Ca_o) and changes in membrane potential (V_M) are frequently performed to examine their effects on several physiological parameters in cells. Using isolated, voltage-clamped barnacle muscle cells, the effect of these manipulations on isosmotic cell volume were studied. To prevent intracellular Ca^{2+} (Ca_i) release from the sarcoplasmic reticulum (SR), cells (Ca_i-loaded) were incubated in Ca^{2+}-free solutions for 3-4 hrs (Ca_i-depleted) in a series of experiments. Replacing Ca_o by Mg^{2+} induced: 1) verapamil-sensitive, extracellular Na^+ (Na_o)-dependent membrane depolarization; 2) membrane depolarization-dependent cell volume reduction in Ca_i-loaded cells; 3) cell volume increase in Ca_i-depleted cells or in Ca_i-loaded cells whose V_M was held constant. Membrane depolarization induced: 1) volume reduction in Ca_i-loaded cells; or 2) verapamil-sensitive volume increase in Ca_i-depleted cells. This suggests that membrane depolarization induces SR Ca^{2+} release which promotes volume reduction. Volume increases from Na^+ influx through a verapamil-sensitive pathway (e.g., Ca^{2+} channels) is revealed by Ca_o removal (in Ca_i-depleted cells or when V_M is held constant) or by membrane depolarization (in Ca_i-loaded cells).

Tu-Pos444

CO-EXPRESSION OF SERCA2A AND PHOSPHOLAMBAN WITH FUNCTIONAL COUPLING IN SF21 CELLS. ((Joseph M. Autry, Steven E. Cala, Bruce T. Scott, and Larry R. Jones)) Krannert Institute of Cardiology, Indiana University Medical School, Indianapolis IN 46202

We have analyzed the functional interaction between the cardiac sarcoplasmic reticulum Ca-transport ATPase (SERCA2a) and phospholamban (PLB) by co-expressing both proteins in Sf21 insect cells. SERCA2a and PLB were cloned from a canine cardiac lambda gt10 library and expressed using the baculovirus system. Specific monoclonal antibodies (mAbs) documented that the two proteins were efficiently produced. ATP-supported Ca transport by whole cell homogenates was measured at nM ionized Ca, and Ca accumulation in the presence or absence of anti-PLB mAb 2D12 was compared as a test for functional interaction between the proteins. SERCA2a expressed by itself exhibited high Ca uptake which was unaffected by PLB mAb. Co-expression of SERCA2a and PLB greatly inhibited Ca accumulation; however, pre-incubation with mAb reversed this effect with a 6 fold stimulation of Ca uptake. Thus, SERCA2a and PLB are functionally coupled when expressed in Sf21 insect cells. We have also expressed mutant subunits of PLB (L37A and L44A), which are unable to form the pentameric structure of wild-type PLB in insect cells. Studies are currently in progress to determine if the monomeric form of PLB is sufficient to regulate SERCA2a in Sf21 cells, or if the oligomeric structure of PLB is required for functional coupling.

Tu-Pos445

RECOMBINANT PHOSPHOLEMMAN FORMS CHLORIDE CHANNELS IN PLANAR LIPID BILAYERS. ((G.C. Kowdley, J.R. Moorman, S.J. Ackerman, G. Szabo, L.R. Jones)) Indiana University and University of Virginia.

Phospholemman (PLM), a major substrate for protein kinases in heart and other tissues, is a small sarcolemmal protein of 72 amino acids with a single membrane spanning domain. When expressed in oocytes, PLM induces chloride currents. We now find that PLM forms chloride channels in lipid bilayers. The protein was expressed and purified from SF21 insect cells by monoclonal antibody affinity chromatography, and the sequence was verified through 54 contiguous residues by gas-phase sequencing. The channels,which are of high conductance and do not close, are modified by affinity-purified antibodies generated to either the amino or carboxyl ends of PLM. In 11 experiments we saw complete closures (2), transitions to lower conductance (6), or no effect (3). The Figure shows bilayer current during a 20 sec voltage ramp in 200:50 mM KCl. The extrapolated reversal potential indicates anion selectivity. The conductance of 3 nS had not changed for 1 hour when N-terminal antibodies were added 3 to 4 min previously. The fall in conductance to 0.3 nS did not reverse. Since the highly purified protein induces currents that are altered by site-specific antibodies, we conclude that PLM is an ion channel.

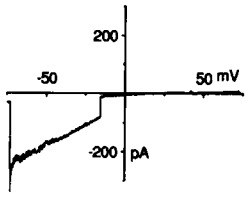

Tu-Pos446

VOLTAGE-DEPENDENT ION SELECTIVITY OF PHOSPHOLEMMAN CHANNELS IN PLANAR LIPID BILAYERS. ((S.J. Ackerman, G.C. Kowdley, L.R. Jones, G. Szabo, J.R. Moorman)) Indiana University and University of Virginia.

To analyse ionic selectivity of currents through phospholemman (PLM) channels reconstituted in lipid bilayers, we applied voltage ramps in 200:50 mM KCl solutions and estimated the cation-anion permeability ratio P_K/P_{Cl} from the reversal potential. Surprisingly, we find transitions between anion-selective and cation-selective unitary currents. In the left panel, a 20 sec voltage ramp elicits a 730 pS current with E_{rev} 12.5 mV (arrow) which makes transitions to and from a 500 pS conductance with E_{rev} - 14.0 mV (double arrows). The right panel is a frequency histogram of selectivity as a function of conductance for 736 events in 14 bilayers. The lefthand axis is P_K/P_{Cl}; events to the right of 1 are anion-selective. The righthand axis is conductance. Though most events are anion-selective with $P_K/P_{Cl} < 0.3$ to 0.4, many are cation-selective. Nearly all the cation-selective currents appeared at negative voltages. We speculate that the selectivity filter of this 72 amino acid ion channel undergoes voltage-dependent conformational changes in which cation or anion binding sites are exposed.

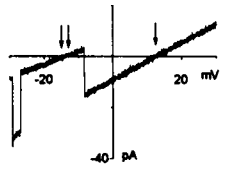

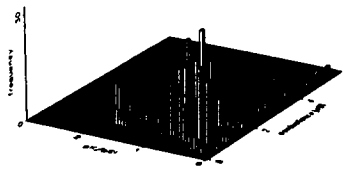

Tu-Pos447

CO-INJECTION OF PROTEIN KINASE A mRNA INCREASES PHOSPHOLEMMAN CHLORIDE CURRENTS IN *XENOPUS* OOCYTES. ((J.P. Mounsey, L.T. Horne, J.E. John, K.P. Lu, A.R. Means, L.R. Jones, J.R. Moorman)) Indiana University and University of Virginia.

Phospholemman (PLM), a major substrate for protein kinases, induces a Cl^- current $I_{Cl(PLM)}$ when expressed in *Xenopus* oocytes. To test the idea that PLM phosphorylation by protein kinase A (PKA) affects $I_{Cl(PLM)}$, we compared currents in oocytes injected with PLM mRNA alone to currents in oocytes coinjected with mRNA for the catalytic subunit of cAMP-dependent protein kinase (PKA). The Figure shows leak-corrected currents during voltage clamp steps from -10 mV to -150 mV. We find that coinjection of PKA mRNA results in a 17-fold increase in $I_{Cl(PLM)}$ (4 frogs, n=39 PLM, 44 PLM plus PKA) at this potential. This increase was apparent only when control $I_{Cl(PLM)}$ was small. The PKA effect was not present in oocytes expressing a phos(-) PLM mutant in which all the potential phosphorylation sites were disabled by Ser to Ala substitution (4 frogs, n=36 mutant, 27 mutant plus PKA). We conclude that the amplitude of $I_{Cl(PLM)}$ is modulated by phosphorylation by protein kinase A at one or more of the four potential phosphorylation sites. Mechanisms might include an increase in PLM expression, or a changes in PLM channel conductance or gating.

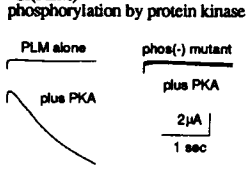

Tu-Pos448

PHOSPHOLEMMAN EXPRESSION AND PHOSPHORYLATION BY PROTEIN KINASE A INCREASE THE VOLUME OF *XENOPUS* OOCYTES. ((K. Wang, J.R. Moorman, J.E. John, L.R. Jones, C.M. Baumgarten)) Medical College of Virginia, Indiana University, and University of Virginia.

Phospholemman (PLM) is a 72-amino acid protein which functions as a Cl^- channel and is an important substrate for phosphorylation. Because of the role of Cl^- in cell volume regulation, we tested the idea that PLM modulates cell volume. Oocyte volume was determined by digital video microscopy assuming spherical geometry. The volume of oocytes varies between frogs, so the volumes of uninjected oocytes from a single frog were averaged and compared to the average of other mRNA-injected oocytes from the same frog. The volume of uninjected oocytes was 0.786 ± 0.042 (SE) mm^3 (18 frogs; n=126 oocytes). Expression of PLM after injection of 20-30 ng of mRNA, an amount that induced large Cl^- currents, increased oocyte volume by 11.0 ± 2.7% ($p < 0.004$; 9 frogs, n= 61 PLM, 67 uninjected). In contrast, injection of an amount of PLM mRNA (2 ng) which induced only very small currents did not alter oocyte volume (-0.4 ± 2.8%; 3 frogs, n=16 PLM, 22 uninjected). Coexpression of protein kinase A (PKA) and PLM increases the Cl^- current. Therefore, we tested the effect of coinjection of PKA catalytic subunit mRNA with PLM mRNA on oocyte volume. Compared to oocytes expressing just PLM, coexpression of PLM and PKA increased cell volume an additional 9.4 ± 3.3% ($p < 0.024$; 5 frogs, n=31 PLM, 23 PLM plus PKA). These data indicate that PLM and its phosphorylation by PKA modulate oocyte volume and lead to the hypothesis that phospholemman contributes to cell volume regulation in heart.

Tu-Pos449

SWELLING OF CILIARY BODY EPITHELIAL CELLS IS ACCOMPANIED BY CHANGES IN CHLORIDE CONDUCTANCE AND INTRACELLULAR [Ca]. ((L.M. Botchkin and G. Matthews)) Dept. of Neurobiology, SUNY, Stony Brook, NY 1794-5230.

The ciliary body secretes the aqueous humor of the eye and regulates intraocular pressure. Volume regulation was studied in nonpigmented epithelial cells from rabbit ciliary body, using whole-cell patch clamp combined with fura-2 measurements of $[Ca]_i$. Hypotonic external solution caused cells to swell and activated Cl current, which was blocked by DIDS (see Fig.). Swelling was also accompanied by an increase in $[Ca]_i$ (right panel in Fig.; hypotonic solution indicated by dark bars; circles show current at +95 mV). However, Cl current is likely not activated by the rise in $[Ca]_i$, because increases in Ca elicited by ionomycin did not activate the current and 10 mM internal EGTA did not prevent development of the current upon swelling. Increases in $[Ca]_i$ comparable to that upon swelling were also seen in response to mechanical stimulation of cells unrelated to swelling. The data suggest that changes in Cl conductance and in $[Ca]_i$ may be involved in regulation of cell volume and fluid secretion in the ciliary body. (Supported by NIH grant EY08673)

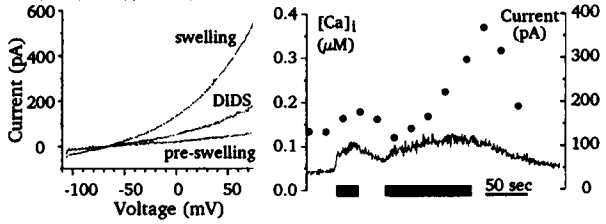

Tu-Pos450

THE ROLE OF V-TYPE PROTON ATPASES IN A HIGH RESISTANCE BLOOD-BRAIN BARRIER.
((P.J.S.Smith and A.M.Shipley)),
NVPF, Marine Biological Laboratory, Woods Hole, Ma 02543
(sponsored by J.R.Demarest)

High resistance blood-brain barriers are present where the brain microenvironment differs markedly from the composition of the blood. Two groups demonstrate such systems in a well developed form - the mammals (≈1800Ωcm) and the insects (≈900-1200Ωcm). Both use elements of mesodermal and neuroectodermal origin. The barrier in the insect ***Periplaneta americana*** has been implicated in brain homeostasis by several studies, - the authors recent application of the voltage sensitive vibrating electrode being one. Here, steady-state currents are recorded arising from the abdominal ganglia ($3\mu A.cm^{-2}$), returning via the peripheral nerves and interganglionic connectives. It is reasoned that in the insect the barrier excludes the unusually high or unstable levels of blood potassium. Further study, with both voltage and ion selective probes, shows that the major ion carrying the outwardly directed current is potassium but that the motive force behind this flux is a vacuolar-type ATPase linked to a H^+/K^+ antiport. This conclusion is based primarily on an insensitivity to vanadate but a relatively rapid shutdown when exposed to n-ethylmaleimide. To date the location of the pump is not known but we hypothesize that it is positioned in basolateral membrane folds of the mesodermally derived sheath cells surrounding the ganglia. These cells are rich in mitochondria and appear to be an active transporting epithelium.

Tu-Pos451

LINEAR PROPERTIES OF ELECTRORECEPTIVE AMPULLARY EPITHELIUM ISOLATED FROM SKATES SHOW UNDERLYING NEGATIVE CONDUCTANCE BEHAVIOR. ((Jin Lu and Harvey M. Fishman))Dept. of Physiology & Biophysics, Univ. of Texas Medical Branch Galveston, TX 77555

We confirmed the sensitivity of ampullae of Lorenzini to low level electric fields by recording changes in afferent nerve discharge in response to μV stimuli across isolated organs (canal, ampulla and nerve) from skates. The amplitude range for a linear current response to a sinusoidal (0.5 Hz) voltage clamp of an organ, was assessed by spectral analysis of the harmonics generated. The current response of the ampullary epithelium was exquisitely linear (total harmonic generation <0.1%) in the range 7.1 to 424 μV (rms) and linear (<1% harmonics) up to 1 mV (rms). Thus, the ampullary epithelium appears to respond linearly to stimuli that produce changes in spike firing rate over the entire working range of the afferent nerve. Admittance determinations were made to characterize the steady state trans-epithelial electrical properties of the ampullary epithelium under voltage clamp conditions with perturbations in the range 1.9 to 94 μV (rms). Complex admittances show a negative real part (interpreted as negative conductance) at low frequencies (<20 Hz). The negative conductance behavior was also confirmed by the direction of current flow through the ampullary epithelium in response to step voltage clamps. We conclude that the steady state negative conductance is an essential property of the ampullary epithelium and that the interplay (neutralization) of negative and positive conductances in receptor cell membranes generated by ion channels may contribute significantly to the electric field sensitivity of ampullary organs. Supported by ONR Grant N00014-90-J-1137.

Tu-Pos452

ION CHANNELS IN THE PLASMA MEMBRANES OF MURINE MAMMARY EPITHELIAL CELLS.
((Christopher D. Watters[x], Mark Nelson[*], and Joseph Patlak[*])) [x]Middlebury College, Dept. of Biology, and University of Vermont, Depts. of [*]Pharmacology and [*]Molecular Physiology and Biophysics, CMRF, 55A South Park Drive, Colchester VT 05446-2500

Milk contains a unique mixture of ions which, along with protein, fat and carbohydrate constituents, are secreted by mammary epithelial cells. To study the early stages of ion secretion, we isolated individual epithelial cells and secretory acini from mice at mid-lactation (10-15 days post-partum) with a standard collagenase procedure. Using cell-attached and excised patch-clamp techniques we have identified the following voltage-insensitive channels in the plasma membrane of freshly isolated cells: 1) a putative chloride channel with a unitary conductance of 10 pS and a reversal potential of about -45 mV; 2) A putative potassium channel with a unitary conductance of 14 pS and a reversal potential near -70 mV; and 3) A putative, non-selective cation channel with a unitary conductance of 12 pS and a reversal potential of about 0 mV. The potassium and cation currents resembled those described for cultured murine mammary epithelial cells (*Furuya, et al., 1989, Pflugers Arch. 414:118-124*). The chloride channel current was particularly noisy: that is, it exhibited multiple levels of open channel conductance. To study a specific plasma membrane domain on more healthy cell populations, we also patch-clamped the exposed basolateral surfaces of epithelial cells in freshly isolated acini. Such acini preparations generally showed less channel activity than single cells and exhibited primarily chloride and, much less frequently, potassium currents. (Supported by funds from Middlebury College, NSF-ROA to CDW, and NSF-DCB-9010563 to MN).

Tu-Pos453

MULTIFUNCTIONAL CALCIUM/CALMODULIN-DEPENDENT PROTEIN KINASE ACTIVATES A NON-SELECTIVE CATION CURRENT IN T84 HUMAN EPITHELIAL CELLS. ((A.P. Braun and H. Schulman)) Dept. Molecular Pharmacology, Stanford University Medical Center, Stanford, CA 94305.

Activation of ion fluxes by secretagogues is critical in fluid secretion/absorption by epithelium. Agents which raise intracellular calcium cause chloride secretion by a mechanism involving CaM kinase. Using whole cell voltage clamp methodology, we have identified a calcium-activated, non-selective (CAN) cation current in T84 cells. The CAN cation current, measured at the chloride reversal potential (-44mV), conducted inward Na^+, K^+, Cs^+, and TEA, but not N-methyl-D-glucamine, and was not blocked by 100μM amiloride. Dialysis of cells with agents to alter the dynamics of protein phosphorylation and dephosphorylation (ie. ATP[S], microcystin, okadaic acid) similarly prolonged the calcium-dependent activation of both the chloride and CAN cation currents. Dialysis of cells with selective peptide inhibitors derived from the α subunit of CaM kinase (281-302 and 291-317) blocked the calcium-dependent activation of both the chloride and CAN cation currents, but not the hypotonicity-induced chloride current. A truncated control peptide (284-302) had no effect on the activation of these currents. In inside/out membrane patches, CAN cation single channel events could be activated in a calcium-dependent manner. Ensemble averages of single channel events following voltage steps reproduced CAN cation tail current behavior observed under whole cell conditions, suggesting that such events may underly the macroscopic current. Collectively, these observations suggest that CaM kinase can activate a CAN cation current in T84 cells. Such a mechanism may contribute to the coordinated secretion of both cations and chloride by calcium elevating agents in epithelium.

Tu-Pos454

VOLUME REGULATION AND MDR1 PROTEIN FUNCTION IN MDR1-TRANSFECTED AND PARENTAL CELL LINES ((James L. Weaver[1], Leslie McKinney[2], Patricia V. Schoenlein[3], Sarah Goldenberg[4], Michael M. Gottesman[4], and Adorjan Aszalos[1])) [1]Molecular Pharmacology, DRT, CDER, FDA, Washington, DC; [2]Department of Physiology, AFRRI, Bethesda, MD; [3]Dept. of Anatomy & Cell Biology, Medical College of Georgia, Augusta, GA; [4]Laboratory of Cell Biology, NCI, NIH, Bethesda, MD.

The MDR1 protein (P-glycoprotein) is a cell membrane ATPase responsible for resistance to several anti-tumor drugs. Gill et al. (Cell 71:23-32, 1992), demonstrated an *MDR1*-transfection associated hypotonic stress-induced Cl^- current. They proposed that drug transport and Cl^- channel functions of MDR1 were separable and mutually exclusive. These hypotheses were tested in four pairs of isogenic cell lines by measuring (1) the effect of hypotonic stress and Cl^- channel blockers on the ability of cells to exclude the MDR1 substrate rhodamine 123 (R123) from their cytoplasm, and (2) the ability of MDR vs parental cells to undergo a regulatory volume decrease (RVD) following hypotonic stress. We found that R123 exclusion from MDR1 transfectants and its regulation by cyclosporin A were unaffected by hypotonic conditions or by Cl^- channel blockers DIDS, SITS or flufenamic acid. The kinetics of RVD were indistinguishable in MDR and parental cells, and MDR1-associated Cl^- channel blockers had no differential effect on RVD. The number of MDR1 antibody binding sites/cell ranged from 8,000 to 55,000 in the different cell lines used, sufficient for RVD. We conclude that MDR1 function is not impaired under hypoosmotic conditions, and that the osmotically-induced Cl^- conductance associated with MDR1 expression observed under patch clamp conditions does not contribute to volume regulation in intact cells.

Tu-Pos455

MODELLING BLOOD-BRAIN BARRIER (BBB) MECHANISMS AGAINST NEUROTOXIC ALKALOIDS. ((Harold Lecar and C. E. Morris*)) Molecular & Cell Biology, UC Berkeley CA 94720 and Loeb Institute*, Ottawa K1Y 4E9.

To reach CNS targets, neurotoxic alkaloids like nicotine and morphine must circumvent any BBB mechanisms acting against them. Although it is has been assumed that a blood-brain interface can present no barrier to alkaloids as membrane-permeant as nicotine, evidence from insects indicates that a BBB to such compounds can exist (eg. Morris 1984 *J. Exp. Zool.* 229:361). To establish the range of effectiveness of BBB mechanisms that can protect the CNS from alkaloids, we are taking an experimental (Murray et al 1994 *J. Neurobiol.* (Jan.)) and a modelling approach to the study of an extreme case, that of nicotine at the blood-brain interface of the tobacco-feeding caterpillar, *Manduca*.

Using compartmental models of varying complexity, we are looking at: the deployment of the P-glycoprotein multidrug pump, the contribution of intracellular detoxifying enzymes, the impact for barrier function of the tortuous diffusion pathway leading to the barrier's tight junctions, the consequences of compartmental pH variation, and the possible involvement of a vacuolar compartment for the drug pumps. Supported by grants from NSERC, Canada.

Tu-Pos456

ION SPECIFICITY AND STOICHIOMETRY OF THE INOSITOL TRANSPORTER IN CARDIAC SARCOLEMMAL VESICLES. ((C.C. Hale, L.J. Berve, C.B. Waters, and L.J. Rubin)) Dalton Cardiovascular Res. Cntr. and Vet. Biomed. Sci., University of Missouri, Columbia, MO 65211.

Cardiac myocytes have a transport mechanism that catalyzes the transmembranal movement of extracellular inositol. Cardiac inositol transport is an electrogenic, Mg^{2+}-dependent, Na^+ co-transport process (*J. Mol. Cell. Cardiol.* 25:721-731, 1993). In the present study, we characterized the ion specificity and stoichiometry of cardiac inositol transport. Cardiac sarcolemmal (SL) vesicles were prepared from bovine ventricular tissue. SL vesicles were equilibrated in K^+ and/or Na^+ buffer (pH 7.4) and where indicated ^{3}H-inositol. All buffers had a final monovalent cation concentration of 160 mM. Transport was initiated by dilution of vesicles in the indicated buffers at 37°C. The reaction was terminated by filtering and washing the vesicles. ^{3}H-inositol transport into cardiac SL vesicles was observed in the presence of an inwardly directed Na^+ gradient but not with either K^+ or Li^+. Inositol transport was not dependent on Cl^- as replacement with the non permeant anion methylsulfate had no affect. The stoichiometry of Na^+ and inositol in the transport reaction was derived by determining the null point of ^{3}H-inositol flux under conditions where the inside and outside concentration (ratio) of inositol and Na^+ were controlled (*J. Mem. Biol.* 67:73-80, 1982). When the ratio of inositol (inside to out) was 4 in the presence of 10 mM Na^+ (inside), the experimentally determined null point was 40 mM Na^+ (outside) suggesting a stoichiometry of 1 Na^+ per each inositol molecule transported. Supported by the AHA (CCH) and AHA-Missouri Affiliate (LJB).

GRAMICIDIN CHANNELS

Tu-Pos457

THE DETERMINATION OF BINDING CONSTANTS OF MICELLAR-PACKAGED GRAMICIDIN A BY ^{13}C AND ^{23}NA NMR.

(Naijie Jing, Kari U. Prasad and Dan W. Urry*) Laboratory of Molecular Biophysics, The University of Alabama at Birmingham, VH300, Birmingham, Alabama 35294-0019.

Based on the malonyl Gramicidin A structure of a single-stranded head to head hydrogen bonded right-handed $\beta^{6.3}$-helix in dodecyl phosphocholine (DPC) micelles (Jing and Urry, in preparation), the determination of cation binding sites for Gramicidin in DPC micelles becomes a significant step in the study of ion transport through this model channel. First, the investigation of cation binding sites in DPC micellar-packaged Gramicidin A (GA) was achieved by ^{13}C-NMR experiments at 30°C using four C-13 labeled GA samples; where the chemical shifts ($\Delta\delta$) of carbonyl carbon (C = O) enriched [1-^{13}C] $Trp^{9,11,13,15}$ Gramicidin A are induced as a function of ion concentration. The results are that (1) the binding site is located between the carbonyl groups of Trp^{11} and Trp^{13}; and (2) the electrostatic interaction between two ions within micellar-packaged GA pushes the bound ions outward from the sequence of $Trp^{9,11,13}$ for one ion to the Trp ^{11,13,15} sequence in the presence of two ions. The distance between the two cation binding sites was approximated to be 16 Å for the right-handed β-helical structure in DPC micelles. Second, analyses based on two different equations, one for single and one for double occupancy, were employed to evaluate the correct occupancy model for GA in DPC micelles. The results clearly indicate double occupancy to be correct. The binding constants for GA in DPC micelles obtained from the analyses are 40/M and 4/M for Na^+; 60/M and 3/M for K^+; 80/M and 2.5/M for Rb^+; 80/M and 4/M for Cs^+; and 1000/M and 30/M for Tl^+. Finally, the binding constants for the Na^+ ion were also estimated by measurement of the longitudinal relaxation time (T_1) using ^{23}Na-NMR of the same sample at the same temperature as used for the ^{13}C NMR study. The binding constants obtained from ^{23}Na NMR are essentially equivalent to those determined from the ^{13}C chemical shifts.

Tu-Pos458

ION PAIR BINDING OF Ca^{++} AND Cl^- IONS IN MICELLAR-PACKAGED GRAMICIDIN A.

(Naijie Jing, Kari U. Prasad and Dan W. Urry*) Laboratory of Molecular Biophysics, The University of Alabama at Birmingham, VH300, Birmingham, Alabama 35294-0019

Two independent NMR experiments were performed to investigate the interaction between $CaCl_2$ and a Gramicidin A (GA) ion transport competent state, using ^{13}C-enriched GA and GA molecules incorporated into dodecyl phosphocholine (DPC) micelles. Based on the comparison of the CD spectra, the structure of the GA molecules in DPC micelles is the same as that of malonyl-GA molecules in DPC micelles, which was identified as a right-handed, head-to-head, hydrogen bonded, single-stranded, $\beta^{6.3}$-helical dimer (Jing and Urry, in preparation). The chemical shifts of C-13 labeled carbonyl carbons vs. $CaCl_2$ concentration demonstrate that Ca^{++} and Cl^- ions interact as an ion pair within the GA structure with the Cl^- ion located near the position of the carbonyl group of the Trp^{11} residue some 5.5 Å from the mouth of the GA helix, and the Ca^{++} ion bound at the position of the carbonyl group of the Trp^{15} residue some 2.5 Å from the entrance to the helical pore. This Ca^{++} interaction is distinctly different from that of Gramicidin A in lysophosphatidylcholine membranes. The binding constants for the singly and doubly occupied states, K^t_b and K^w_b of the GA in DPC determined by the analysis of the ^{13}C chemical shifts, are 180/M and 6/M for Ca^{++} ions, and 120/M and 6/M for Cl^- ions. The measurements of the ^{35}Cl line widths and transverse relaxation times illustrate that interaction occurs between Cl^- ions and GA in DPC when in $CaCl_2$ solution, that no interaction is detected between Cl^- ions and GA in DPC when in NaCl solution, and that the interaction between Cl^- ions and GA in DPC when in $MgCl_2$ solution is much weaker than in $CaCl_2$ solution. In short, a Cl^- ion can enter the GA when it is paired with a divalent Ca^{++} ion; and Ca^{++} and Cl^- ions as a pair exchange rapidly with sites of the GA dimer. This is qualitatively consistent with less effective reduction of single channel current on adding $MgCl_2$ than on adding $CaCl_2$ (Bamberg and Lauger, 1977).

Tu-Pos459

MODULATION OF SELECTED GRAMICIDIN SIDE CHAINS BY COVALENT ACYLATION

((R. E. Koeppe II, J. A. Killian+, T. C. B. Vogt+, B. de Kruijff+, D. V. Greathouse and M. J. Taylor)) Dept. Chem. Biochem., Univ. of Arkansas, Fayetteville, AR, USA 72701; +Dept. of Biochemistry of Membranes, Univ. of Utrecht, The Netherlands.

We have investigated the perturbation of the side chains of Trp-9, Leu-10, and Trp-11 of the gramicidin A (gA) channel by a long fatty acyl chain covalently attached to the ethanolamine end of gramicidin. In a sodium dodecyl sulfate (SDS) environment, one of the β-hydrogens of Leu-10 of gA is severely deshielded by an aromatic ring to a negative chemical shift; this deshielding disappears upon acylation. In a phospholipid environment of DMPC bilayers, the deuterated side chains of Trp-9 and Leu-10 are significantly influenced by acylation, whereas the side chain of Trp-11 is unaffected. This suggests that the acyl chain extends from its attachment site on the ethanolamine to make contact with the side chains of Trp-9 and Leu-10. Together, the ^{1}H and ^{2}H NMR results strongly suggest that the indole ring of Trp-9 is situated near the side chain of Leu-10 in both the SDS and DMPC environments, and that the ring moves away upon acylation. Based on these results, we conclude that the ring of Trp-9 is oriented similarly in SDS and DMPC.

Tu-Pos460

^{23}Na NMR STUDIES OF Na^+ TRANSPORT VIA GRAMICIDIN INCORPORATED INTO LIPID VESICLES AND HUMAN ERYTHROCYTES.

((Arron S.L. Xu#, Philip W. Kuchel# and Bruce A. Cornell*)) #Department of Biochemistry, University of Sydney, NSW 2006, Australia. *Division of Food Science and Technology, CSIRO, PO Box 52, North Ryde 2113, Australia.

We present here the data from studies of transmembrane exchange of Na^+ via gramicidin incorporated in membranes of large unilamellar vesicles (LUV) and human erythrocytes. LUV of egg yolk phosphatidyl choline were prepared by reverse phase evaporation and membrane extrusion. Incorporation of gramicidin into the LUV and erythrocytes was achieved by heat incubation. ^{23}Na NMR spectra of suspensions of LUV and erythrocytes both showed well resolved resonances from the solute populations of the internal/intracellular and external/extracellular compartments when the paramagnetic shift reagent, dysprosium tripolyphosphate (DyPPP), was present in the suspension medium. By using ^{23}Na NMR magnetisation transfer techniques the rate of rapid equilibrium exchange of Na^+ via gramicidin was measured to be ~4000 s^{-1} $dimer^{-1}$, at 25 °C. The activation energies for the equilibrium-exchange influx and efflux of Na^+ were determined in an Arrhenious analysis to be 14.1 ± 1.6 and 17.1 ± 4.1 kJ mol^{-1}, respectively. The kinetics of competitive transport of Na^+ and other alkali metal cations via the gramicidin in LUV were also studied. Phosphatidyl cholines with various lengths of fatty acyl carbon chain were used to prepare LUV of different membrane thickness. The effects of an increase in membrane thickness on the transport activity of gramicidin were investigated. The results are discussed in the context of the frequency of formation of head-to-head active channels of gramicidin in the membrane of various thickness.

Tu-Pos461

AMBIDEXTROUS GRAMICIDIN CHANNELS ((G. Saberwal[a], D. Greathouse[b], R.. E. Koeppe II[b], O. S. Andersen[a])) [a]Dept. Physiol. & Biophys., Cornell Univ. Med. Coll., New York, NY 10021, and [b]Dept. Chem. & Biochem., Univ. Arkansas, Fayetteville, AR 72701. (Spon. by D. Gardner)

The naturally occurring gramicidins form channels that are dimers of right-handed $\beta^{6.3}$ helices. When the chirality of each of the 14 chiral centers in gramicidin A (gA) is inverted, the resulting analogue (gramicidin A$^-$, gA$^-$) forms channels that are left-handed. Here we report the synthesis of a gramicidin analogue that retains the chiral centers of gA and that forms both left- and right-handed channels. This analogue is [Val^5,D-Ala^8]gLW: formyl-L-Val-Gly-L-Ala-D-Leu-L-Val-D-Val-L-Val-D-Ala-L-Leu-D-Trp-L-Leu-D-Trp-L-Leu-D-Trp-L-Leu-ethanolamine. The handedness of [Val^5,D-Ala^8]gLW channels was determined in hybrid-channel formation experiments with gA and with the right-handed analogue des-Val^1-[D-Ala^2]gA, and with the left-handed analogues des-Val^1-[Gly^2]gA$^-$ and des-Val^1-[D-Ala^2]gA$^-$. Heterodimers were observed with all four combinations of [Val^5,D-Ala^8]gLW and the reference compounds. In addition, the circular dichroism spectrum of [Val^5,D-Ala^8]gLW in dimyristoylphosphatidylcholine vesicles is consistent with a mixture of left- and right-handed molecules. Thus, the handedness of gramicidin channels has been changed by making sequence changes that retain the chirality of each residue.

Tu-Pos462

MEMBRANE CURVATURE AND GRAMICIDIN CHANNEL FUNCTION ((J. Girshman, J. A. Lundbæk, L. L. Providence, and O. S. Andersen)) Dept. Physiol. & Biophys., Cornell Univ. Med. Coll., New York, NY 10021. (Spon. H. J. Sackin)

The function of membrane proteins can be modified by altering the spontaneous curvature of the membrane lipids; the mechanisms responsible for this control of membrane protein function are not known. We have examined the effect of lipids that can alter the spontaneous curvature on the duration of gramicidin channels in diphytanoylphosphatidylcholine/*n*-decane bilayers. In the presence of the micelle-forming lysophosphatidylcholine (LPC) at a molar ratio of 1:4 in the membrane-forming solution, the average channel duration is increased three-fold. In the presence of cholesterol (molar ratio 4:1), which can promote H_{II} phase formation, the average channel duration is decreased three-fold. In the presence of the bilayer-forming glycerolmonooleate (GMO) at a molar ratio of 1:1, the average channel duration is not affected. Gramicidin channel formation is associated with a membrane deformation, and the average duration of gramicidin channels is a complex function of membrane thickness compressibility, surface tension, and monolayer bending (splay). The present experiments do not separate among these contributions, but the opposite effects of LPC and cholesterol - and the lack of an effect of GMO -suggest that the gramicidin channel duration is a function of the spontaneous curvature of the lipid monolayers. Such alterations in the spontaneous curvature will alter the membrane deformation energy and thereby the energetics of channel formation and stability. The spontaneous curvature of lipids in a membrane may similarly modify integral membrane protein function by affecting the energetic cost of membrane deformations associated with alterations in the proteins' quaternary structure.

Tu-Pos463

CONTACTS THAT ARE GOOD FOR YOU: SIDE CHAIN CONTACTS IN THE GRAMICIDIN CHANNEL ((G. Saberwal[a], D. Greathouse[b], R. E. Koeppe II[b], O. S. Andersen[a])) [a]Dept. Physiol. & Biophys., Cornell Univ. Med. Coll., New York, NY, [b]Dept. Chem. & Biochem., Univ. Arkansas, Fayetteville, AR. (Spon. by L. G. Palmer)

At the join between the monomers in gramicidin A (gA) channels, residue 1 of one monomer (#1) is adjacent to residue 5 of the other monomer (#2). There is also contact between residue 2 of monomer #1 and residue 4 of monomer #2; and between the residues at position 3 in each monomer. Channel structure and function are influenced by these contacts. Channel stability, for example, is reflected in its average duration (τ): attractive side chain-side chain interactions will increase τ; repulsive interactions will decrease τ. More rigorous evaluation of these interactions is obtained in heterodimer experiments. The relative appearance rates of heterodimers and homodimers and their τ's provide for a quantitative estimate of the channel stabilization by interresidue contacts: in gA homodimers the contacts between Val^1 (in monomer #1) and Ala^5 (in monomer #2) could be favorable; as would the contacts between Ala^1 (in #1) and Val^5 (in #2) in [Ala^1,Val^5,D-Ala^8]gA homodimers; in heterodimers formed between gA and [Ala^1,Val^5,D-Ala^8]gA, however, there would be little contact between Ala^1 (in #1) and Ala^5 (in #2), and an unfavorable contact between Val^1 (in #1) and Val^5 (in #2). The barrier to the formation of heterodimers is 0.3 kJ/mol greater than that for the formation of homodimers, and the difference in free energy between heterodimers and homodimers is +1.7 kJ/mol. In this example, heterodimer formation is energetically costly, which highlights the importance of side chain interactions between opposing monomers for channel formation and stability, and shows that Val-Ala interactions are more favorable than Val-Val or Ala-Ala interactions.

Tu-Pos464

TRYPTOPHANS AND GRAMICIDIN CHANNEL FUNCTION ((L. L. Providence[a], R. Smith[b], T. Milne[b], F. Separovic[c], R. E. Koeppe II[d], and O. S. Andersen[a])) [a]Dept. Physiol. & Biophys., Cornell Univ. Med. Coll., New York, NY; [b]Dept. Biochem., Univ. Queensland, QLD, Australia; [c]CSIRO Food Research Lab., North Ryde, NSW, Australia; [d]Dept. Chem. & Biochem., Univ. Arkansas, Fayetteville, AR

In order to further evaluate the role of Trp residues for gramicidin channel structure and function we have examined the gramicidin analogue [D-Trp^{10,12,14}]gramicidin A (gW), in which there are seven Trp residues in the C-terminal half of the molecule. gW forms a single type of single-stranded channels with a conductance (*g*) of 4.5 pS and an average duration (τ) of 80 ms (1.0 M NaCl, 200 mV, diphytanoylphosphatidylcholine/*n*-decane membranes). The reduction in *g* relative to gramicidin A (gA) channels (15 pS) is surprising, as *g* usually increases as the number of Trp residues at positions 9, 11, 13, and 15 is increased (Becker et al., *Biochemistry* 30:8830, 1991). The reduced single-channel conductance does not appear to result from an increased ion affinity of the gW channels, as *g* in 0.5 M NaCl is 3.7 pS - less than in 1.0 M NaCl. In CsCl the corresponding values were 26 pS (1.0 M) and 16 pS (0.5 M). gW channels are predominantly right-handed, because gW forms hybrid channels with gA, while hybrid channels were not observed in experiments with the enantiomeric analogue des-Val^1-[D-Ala^2]gA$^-$. Given that gW channels are structurally equivalent to gA channels, the reduced single-channel conductance could indicate that the orientation of the Trp residues (relative to the channel axis) at positions 10, 12 and 14 differs from that of the Trp residues at position 9, 11, 13, and 15. This conclusion must be tempered, however, because Trp-Trp interactions might lead to conductance alterations by other mechanisms as well.

Tu-Pos465

DEUTERIUM NMR STUDIES OF LEUCINE AND VALINE SIDE CHAINS IN GRAMICIDIN CHANNELS
((Roger E. Koeppe II, J. Antoinette Killian+, Denise V. Greathouse, and Jennifer Loukota)) Dept. Chem. Biochem., Univ. of Arkansas, Fayetteville, AR, USA 72701; +Dept. of Biochem. of Membranes, Univ. of Utrecht, The Netherlands.

To gain information about the orientations and motions of side chains in a phospholipid environment, we have analyzed ^{2}H NMR spectra of specifically labeled Val and Leu residues in hydrated, oriented samples of gramicidin A:DMPC (1:10). Previously, we showed that if the side chain of Val-1 occupies a fixed orientation in space, then the ^{2}H spectra are consistent only with a χ_1 torsion near -5° or -20° (Killian et al., Biochemistry **1992**, 31, 11283). We now extend the analysis of Val-1 to show that two rapid two-fold side-chain jump models are also consistent with the data: "hopping" between χ_1 of 175° (67% occupancy) and 300° (33%), or between 175° (76% occupancy) and 65° (24%). With either a static or a rapid "hopping" model, there is a significant stabilizing hydrophobic interaction between Val-1 of one monomer and Ala-5 of the other, as confirmed by functional studies. The spectra for Leu-10 can also be fit by either a fixed side chain orientation or by one of several two-fold rapid-jump models. If fixed in space, the Leu-10 side chain could be motionally restrained by the nearby indole ring of Trp-9. In contrast to Val-1 and Leu-10, the side chain of Val-7 occupies two orientations--or perhaps two sets of orientations--that interconvert slowly on the NMR time scale.

Tu-Pos466

TWO-DIMENSIONAL NMR ANALYSIS OF THE STRUCTURE OF [L-ALA^1-D-ALA^2] GRAMICIDIN A IN D_{25} SDS MICELLES.
((Gwendolyn L. Mattice, R. E. Koeppe II)) Department of Chemistry and Biochemistry, University of Arkansas, Fayetteville, AR 72701

Two-dimensional NMR techniques, DQCOSY, NOESY and TOCSY, are being used to investigate the structure of [L-Ala^1-D-Ala^2] gramicidin A in deuterated (d_{25}) SDS micelles. [L-Ala^1-D-Ala^2]gA channels exhibit a higher conductance and longer average lifetime than gramicidin A channels. Circular dichroism results show the secondary structure of this analogue to be similar to gA in both dimyristoylphosphatidylcholine and sodium dodecyl sulfate (SDS) environments. The fingerprint region of the DQCOSY displays fifteen peaks, indicating one structure within the d_{25} SDS micelle. All spectra show the sequence substitutions of Ala^1 and Ala^2 and from the proton assignments, the resonances differing most from those of gA are located at Val^{7,8} and Trp^{9,11}, with one of the Trp^9 ring protons exhibiting the greatest deviation, 0.3 ppm. The additional peaks in the 40 and 100 ms NOESY fingerprint region show $i_{NH} \rightarrow (i+6)_{C\alpha H}$ connectivities for even residues and $i_{NH} \rightarrow (i-6)_{C\alpha H}$ connectivities for odd residues which signifies a single-stranded, right-handed $\beta^{6.3}$ helical conformation. Distance geometry and simulated annealing are being used to refine the three-dimensional structures of the backbone and side chain conformations generated from the 40 ms NOESY data.

Tu-Pos467

DYNAMIC ENERGY PROFILE OF HYDRATED METHYL AMMONIUM IN THE GRAMICIDIN A CHANNEL. ((Yili Hao and David Busath)) BROWN UNIVERSITY, BOX G-B3, Providence, RI 02912

Using the umbrella sampling technique with an atomistic empirical force field, we computed the free energy profile of methyl ammonium for passage through the gramicidin channel. The system consisted of a 316-atom (polar-hydrogen's only) gramicidin A dimer initiated to the Arseniev conformation, an 8-atom methyl ammonium, 22 axial and 195 solvent TIP3 water molecules. The solvent waters were selected from a pre equilibrated droplet and positioned to surround the axial waters and ion. The water-ion column extends at least to the edge of the channel-solvent system for each value of the reaction coordinate and were translated as a unit to initiate each new window. Parameters were from CHARMM v21.3, with methyl ammonium partial charges from Quanta v3.2/Chemnote (MSI, Burlington, MA). The umbrella potential was a harmonic constraint (K=10 kcal/mol-A^2) to a plane perpendicular to the channel axis. Each window required placement of the axial column, 500 steps ABNR minimization, 3 ps heating, 8 ps equilibration, and 10 ps free (except umbrella potential) dynamics. 60 windows were required to cover the 30.75 A reaction path. The free energy in each window was estimated from the probability density in the window after correction for the applied umbrella potential. The overlaps in the windows (2-6 bins) were used to concatenate the window profiles into the total profile. The results from the two identical halves of the channel were compared to obtain an estimate of the cumulative errors. We find an entry energy increase (~11 kcal/mol) at both ends of the channel at ~±10 A and an additional increase (of ~12 kcal/mole) at ~±5 A. At the center there is a decrease in free energy to ~9 kcal/mole (relative to bath). The barriers are too high for the measured channel conductance (Seoh and Busath, 1993), but nevertheless qualitatively illustrate a novel free energy profile shape which should be taken into account in analyzing experimental conductance data.

Tu-Pos468

MOLECULAR DYNAMICS OF GRAMICIDIN A BY SOLID STATE NMR
((S. Huo, K.C. Lee, N.D. Lazo, W. Hu, C.L. North and T. A. Cross))
National High Magnetic Field Laboratory, Institute of Molecular Biophysics and Department of Chemistry, Tallahassee, FL32306

Molecular dynamics of the backbone and sidechains of the gramicidin A channel in DMPC bilayers has been studied by solid state ^{15}N and ^{2}H NMR spin relaxation and tensorial averaging of fast-frozen low-temperature samples. By rapidly freezing the samples and monitoring the temperature dependence of the ^{15}N chemical shift tensor, the local motional amplitude (17-21°) and the motional axis of the peptide plane have been determined for several sites. The Trp side chain dynamics were investigated by similar techniques, revealing amplitudes of 20–30° about C_β–C_γ axis. The ^{15}N and ^{2}H spin relaxation of oriented samples have been analyzed using several models which include the global rotation of the molecule about the channel axis and the independent librational motion of the peptide planes about the C_α–C_α axis, yielding correlation times and motional amplitudes for each peptide plane. To explain the observed nanosecond motion, several possible models for correlated motion are developed. One such model to account for the over-damped correlation times has been computationally simulated by nearest-neighbor jumps among different conformational states in the configurational space. The correlation of the motion is introduced by interactions between neighboring peptide planes mediated by covalent bonds or hydrogen bonds.

Tu-Pos469

HIGH DEFINITION STRUCTURE AND REFINEMENT OF THE GRAMICIDIN CHANNEL BACKBONE AND SIDECHAINS
((Kwun-Chi Lee, Randal R. Ketchem, Shouqin Huo and Timothy A. Cross))
Institute of Molecular Biophysics and Department of Chemistry, Florida State University, Tallahassee, FL 32306

The structure and large amplitude dynamics for each of the valine and leucine sidechains in the gramicidin channel have been determined. Temperature dependent ^{2}H powder pattern spectra as well as spectra of oriented preparations in hydrated lipid bilayers have been analyzed for this effort. χ_1 torsional motions have been characterized for Val_1 and Val_7 as three site jumps between rotameric states in which one state is dominant. Val_8 and Val_8 do not show these large amplitude motions. Analysis of the leucine sidechain dynamics will also be presented.

Using the ^{2}H quadrupolar splittings as orientational constraints, conformational solutions were determined and a least squared fitting calculation was used to determine the unique sidechain conformation. Such calculations were done in conjunction with the constrained and refined backbone structure (Ketchem, et. al., Science, Vol. 261, No. 5127, pp. 1457-1460, 1993). The initial backbone structure was calculated from the solid state NMR data and refined using a simulated annealing technique developed in this lab. The annealing protocol uses backbone torsional motions to initiate changes in the backbone structure. A penalty is calculated after each structural change based on the rmsd between the calculated and observed data and backbone hydrogen bond distances. The annealing protocol minimizes this penalty. Details of the refinement protocol will be presented as well as estimates of the precision and accuracy of the resultant structure.

Tu-Pos470

^{2}H, ^{15}N AND ^{23}Na NMR STUDIES ON THE FUNCTIONAL ASPECTS OF THE GRAMICIDIN CHANNEL
((S. Arumugam, W. Hu, K. C. Lee, F. Tian, M. Cotten and T. A. Cross))
National High Magnetic Field Laboratory, Institute of Molecular Biophysics and Department of Chemistry, Florida Sate University, Tallahasse, FL 32306-3006.

In order to understand the effect of sidechain orientation and dipole moments on the function of gramicidin, ^{2}H labeled tyrosine-(d-4) has been substituted for tryptophan and ^{2}H NMR experiments were carried out on oriented preparations in DMPC lipid bilayers. The orientations of these sidechains will be reported and will be compared with the tryptophan residues obtained earlier and discussed in light of the functional aspects of the gramicidin channel.

Conformational and/or dynamic changes are induced by the presence of Na^+ in the channel. We will report both backbone and sidechain, ^{15}N and ^{2}H NMR studies of these effects. The ^{15}N and ^{2}H NMR results indicate that the tryptophan sidechain conformations are the same as that in the absence of Na^+. However, the ^{15}N chemical shifts for the Leu_{12} sites and Trp_{13} are shifted significantly. ^{2}H NMR spectra of oriented ethanolamine-(d-4) gramicidin also showed significant changes for the quadrupole splittings in the presence of Na^+.

The interaction of Na^+ with the gramicidin channel has also been studied using ^{23}Na NMR spectroscopy. An effort has been initiated using this spectroscopy to study the insertion of gramicidin into the lipid bilayer and to characterize conformational interconversion that occurs once the polypeptide is in a hydrated lipid bilayer.

Tu-Pos471

BROWNIAN DYNAMICS SIMULATIONS OF CS+ TRANSPORT THROUGH GRAMICIDIN A. ((Pete McGill[1], Sam Bek[2], Mark Schumaker[1], and Eric Jakobsson[2]) [1]Department of Pure and Applied Mathematics, Washington State University, Pullman, WA 99164 and [2]Department of Physiology and Biophysics and the National Center for Supercomputing Applications, University of Illinois, Urbana, IL 61801

Brownian dynamics simulations of diffusive multi-ion transport through a single-file pore are compared with measured conductances of Cs+ through Gramicidin A, previously reported in the literature. The mobility and free energy profile characteristic of individual ions in the channel is determined by fitting the analytical theory of diffusive single-ion transport to gramicidin conductance measurements made at very low Cs+ concentrations. These parameters are then combined with an electrostatic interaction between ions in the simulations of multi-ion permeation. At high permeant ion concentrations, the channel becomes doubly occupied most of the time, and the current-concentration curve shows reduced conductance at high concentrations. The current-concentration behavior is similar to that of a "single-vacancy" conductance mechanism, and also to experiment. Results of the simulations are compared with gramicidin conductances measured at high Cs+ concentrations. These comparisons provide a test of the assumptions underlying the calculations, in particular, the assumption that except for ion-ion electrostatic repulsion, the ions in the multiply-occupied channel behave as they do in the singly-occupied channel.

Supported by the National Center for Supercomputing Applications and the National Science Foundation.

Tu-Pos472

ION-WATER-POLYPEPTIDE INTERACTIONS IN INCREASINGLY FLEXIBLE GRAMICIDINLIKE CHANNELS: IMPLICATIONS FOR INFORMATION TRANSFER. ((K.A. Duca and P.C. Jordan)) Biophysics Program, Brandeis University, Waltham, MA 02254.

Previous work (Duca and Jordan, *Biophys J.*, **64**, 295a [1993]) has indicated that interaction between a gramicidinlike channel (a configurationally constrained polyglycine analog) and sodium differs sharply from that between the channel and potassium or cesium. Much reduced water-water distances and increased orientational ordering were noted for sodium. Attributing these phenomena to its greater ability to polarize water, we hypothesize that water ordering via interactions with the ion (and the polypeptide) may be an important mechanism for the transmembrane transfer of information about the state of the channel and/or the environment the ion is exiting. To test this thesis, we performed molecular dynamics simulations emphasizing two model features: explicit inclusion of polarizability and degree of constraint maintaining helical integrity. In moving from a rigid to a fairly flexible channel ($0.1Å < |r-r_0| < 1.0Å$), intermolecular correlations initially became shorter range as reflected by: increases in channel average water-water radial separations for water pairs not immediately adjacent to the ion; decreases in water dipole moments; association of fewer non-exchangeable waters with the ion for any given region of the channel; reduction in long range angular correlations of channel waters. Eventually the trend reversed and the softer channels resembled the rigid ones more than they did those of intermediate flexibility, probably due to carbonyl groups' larger ability to intercalate into the water chain thereby propagating long range order. Cesium and sodium occupying the channel represented limiting cases, behaving very differently, with potassium being generally intermediate to them and sometimes more cesium or sodium-like.

Tu-Pos473

SOLID-STATE NMR STRUCTURAL DETAILS OF THE TRYPTOPHAN CARBONYLS OF THE GRAMICIDIN A CHANNEL. ((F. Separovic, J. Gehrmann[#], B.A. Cornell, R. Smith[#])) CSIRO Food Research Laboratory, POB 52, North Ryde, NSW 2113 & [#]Biochemistry Department, University of Queensland 4072, Australia.

Gramicidin A analogues, labelled with C-13 at the tryptophan 11 and tryptophan 13 carbonyl carbons, were synthesised using t-Boc protected amino acids. The purified analogues were incorporated into ditetradecylphosphatidylcholine bilayers at a 1:15 molar ratio, and macroscopically aligned between glass coverslips. The orientations of the labelled carbonyl groups within the channel were investigated using solid-state NMR. The effect of a monovalent cation (Na^+) on the orientation of these groups was determined. The presence of sodium ions did not perturb the C-13 spectra of the tryptophan carbonyl groups. These results contrast with earlier results in which the Leu-10, Leu-12 and Leu-14 carbonyl groups were found to be significantly affected by the presence of sodium ions and imply that the tryptophan carbonyl groups are not directly involved in ion binding. The channel form of gramicidin A has been demonstrated to be the right handed form of the $\beta^{6.3}$ helix. Consequently, the tryptophan carbonyls would be directed away from the entrance of the channel, and take part in internal hydrogen bonding, so that the presence of cations in the channel would have less effect on them than on the outer leucines.

MODEL CHANNELS

Tu-Pos474

EFFECT OF SINGLE SITE MUTATIONS ON IONIC CHANNELS FORMED BY CryIA(c) *BACILLUS THURINGIENSIS* (*Bt*) TOXIN ((J.L. Schwartz, L. Potvin[*], J. Laflamme[+], A. Mazza, L. Masson, R. Brousseau and R. Laprade[+])) BRI, National Research Council, Montreal, Que, H4P 2R2 and [+]GRTM, University of Montreal, Montreal, Que, Canada, H3C 3J7.

Two mutants of CryIA(c), a *Bt* lepidopteran-specific toxin, were studied in planar lipid bilayer (PLB) experiments. The wild-type toxin formed 500-pS cation-selective channels[1]. The 45-59 region of the N-terminal half of the toxin, which is involved in channel formation, is a conserved hydrophobic region in *Bt* CryI proteins. In our first mutant, P52R, the proline in position 52 was replaced by the positively-charged arginine. This should affect the protein structure significantly. The C-terminal half of CryI toxins, which is involved in specificity and binding, contains a highly conserved, arginine-rich region. In our second mutant, R526G, the positively charged arginine in position 526 was replaced by the neutral aminoacid glycine. Both mutants were tested by lawn assays[2] on Cf-1 cells (*Choristoneura fumiferana*, spruce budworm). R526G toxicity was comparable to that of the wild-type toxin, but P52R was much less toxic. Both mutants partitioned in PLB. In 450:150 mM KCl, the conductances of R526G and P52R channels were around 730 pS and 850 pS respectively. The channels of both mutants were cation-selective. Kinetic patterns and subconductances resembled those of the wild-type toxin.

[1]Schwartz *et al* (1993) Biophys.J. 64:A94; [2]Gringorten *et al* (1990) J.Invert.Pathol. 56:237-242.

Tu-Pos475

MOLECULAR DYNAMICS STUDY OF MEMBRANE IONIC CHANNELS, VIDEO AND PARALLEL COMPUTATION COMPARISONS. ((Y. Chapron, S. Crouzy, J.L. Douvillé, P.E. Bernard and M. Goeschl)) CEA/DSV/DBMS/BMC - CENG GRENOBLE FRANCE.

Throughout the world, many experiments are carried out on ionic channels, using the patch clamp technique, in particular. But understanding ionic transport requires a more structural and dynamical approach. A gramicidin modified by addition of a dioxolan ring, linking in a covalent fashion the two channel constituting monomers, has been chosen for the modelling of channel fluctuations by molecular dynamics, and the theoretical study of the ring gating has been done (Crouzy, S. & Roux, B., in prep.). The requirement to approach as closely as possible the biologic operation of ionic channels implies that phospholipids be taken into account by associating them, to the gramicidin channel, and building more realistic systems with a volume of water hydrating the polar portion of the lipids. Two systems have been designed : first, a minimal system still retaining a physical significance has been built : gramicidin + 12 water molecules into the channel + 2 cylindrical layers of dilaurylphosphatidylethanolamin (56 dlpe) and 716 waters hydrating both polar faces of the cylinder, forming a 4855 atoms structure. A larger one : gramicidin + 11 water + one K ion into the channel + 3 cylindrical layers of "dlpe" (106) and 2270 waters molecules leading to 11615 atoms. A first dynamic over 140 psec with the smaller system, carried out on the Cray II in Grenoble, has required 120 hours of CPU. A video showing the structure of the channel has been produced in the course of this work. The requirement to compute very long trajectories has led us to consider massively parallel computing. Thereafter, parallel Molecular dynamic computations have been carried out on several parallel machines. The CM5 of the IPG in Paris, KSR1 of INRIA, CRAY YMP and C90, and SGI Challenge. The big granularity of the Cray C90 makes it the fastest of the series running XPLOR on the larger system. However, moderated middle grain machines, like the SGI Challenge, have a good promising performance-price ratio.

Tu-Pos476

TOXIN INDUCED PORE FORMATION IN LIPID VESICLE BILAYERS: KINETIC ANALYSIS BASED ON MARKER RELEASE EXPERIMENTS. ((Gerhard Schwarz)) Department of Biophysical Chemistry, University of Basel, Switzerland.

A recently developed theoretical approach to describe marker efflux in terms of the underlying pore kinetics is examined with regard to experimental applications. When the observed signal is linearly related to the extent of release one can directly register in the course of time t a retention function R(t) that is generally related to two kinetic variables determined by the forward pore formation rate and the pore closing rate, respectively. In those popular cases where a self-quenching fluorescent dye is used as a marker no originally linear signal occurs, however. Nevertheless R(t) may then be evaluated from the measured data if the quenching factor of the still encapsulated dye is quantitatively recorded during the release process. Procedures to analyze R(t) in respect of a molecular mechanism are demonstrated in the light of practical examples. Special attention is drawn to the fact that pore formation induced by an added membrane active agent is apparently always slowed down very much after some time.

Tu-Pos477

CHANNEL-LIKE ACTIVITY OF SAPONINS IN CHOLESTEROL-DOPED GIANT LIPOSOMES OBSERVED BY PATCH-CLAMP. ((T. Lefèvre, A. Ghazi and A. Coulombe)) URA CNRS 1121, URA CNRS 1116 Université Paris-Sud, F-91405 Orsay and Hôpital M. Lannelongue (URA CNRS 1159), F-92350 Le Plessis Robinson, FRANCE. (Spon. by G. Vassort)

Saponins are often used as a tool for permeabilization of plasma membranes in order to study intracellular processes. Although it is widely believed that saponins form holes in cholesterol-containing membranes, no direct measurements have yet been performed. Patches excised from giant liposomes were superfused with various concentration of saponins. No effect was observed on asolectin liposomes. However, application of β-escin (conc. ≥ 100 μM) or digitonin (conc. ≥ 10 μM) to patches excised from asolectin liposomes containing 20 or 40% cholesterol, resulted in the induction of channel-like activity (see Figure). Single-channel activity was generally composed of many different current amplitude levels indicating the possibility of various dynamic multimer arrangements giving rise to formation of pores of different sizes. Interestingly, when saponins were applied to liposomes, studied in the "on liposome" configuration, no channel was observed, indicating that these molecules do not cross the seal barrier.

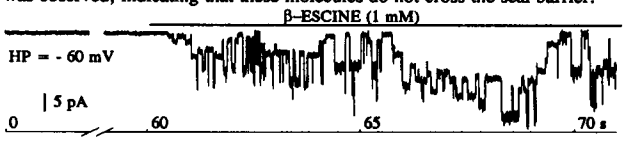

Pipette medium (mM) : 100 NaCl, 10 HEPES, $MgCl_2$ 2, $CaCl_2$ 2, pH : 7 (NaOH).
Bath medium (mM) : 100 KCl, 10 HEPES, pH : 7 (KOH).

Tu-Pos478

DYNAMICS OF MEMBRANE-ASSOCIATED SPIN-LABELED M2α

((Eduardo Perozo, Heinz-Jürgen Steinhoff, Wayne L. Hubbell, Mauricio Montal)) Jules Stein Eye Institute and Department of Chemistry and Biochemistry, UCLA, Los Angeles, CA 90024-7008 and Departments of Biology and Physics, UCSD, La Jolla, CA 92093.

The M2 segment of the α subunit (M2α) has been implicated as a key pore-lining structure of the neuronal acetylcholine receptor. A synthetic M2α peptide forms single channels in bilayers having a conductance of 27 pS (0.5 M NaCl), with very low probability of opening and no apparent voltage dependence. To investigate the structure and dynamics of this peptide in membranes, the single cysteine residue was derivatized with a methanethiosulfonate spin-label and incorporated into bilayers of egg phosphatidylcholine. The spin-labeled side-chain has high mobility in the membrane-bound peptide ($\tau \approx 3$ nsec), and is inaccessible to collision with chromium oxalate in the aqueous phase. These results indicate that the labeled side-chain faces the fluid interior of the bilayer. EPR spectra recorded at 175 °K showed no detectable dipolar interaction between nitroxides. In constrast with this result, analysis of a spin-labeled pentameric association model (Oblatt-Montal et al. (1993) JBC 268:14601) predicts an average inter-spin distance of 20 Å, a separation at which dipolar interactions would be detected. These results are consistent with the membrane bound peptide being in a monomeric state, and suggests a direct correlation between the electrical activity of this peptide and its structure and dynamics. Supported by grants MH-44638, EY-05126 and The Pew Charitable Trust

Tu-Pos479

STRUCTURE OF ALAMETHICIN IN MICELLES AND BILAYERS.

((J.F. Ellena, C.F. Franklin, M.R. Barranger-Mathys, L.P. Kelsh, and D.S. Cafiso)) Dept. of Chemistry and Biophysics Program, Univ. of Virginia, Charlottesville, VA 22904.

Alamethicin is a 20 residue peptide which binds to membranes and forms voltage-gated ion channels. Previously we assigned the H-1 NMR spectrum of alamethicin in sodium dodecylsulfate micelles and obtained 170 NOE distance restraints (Franklin et al. (1993) Biophys. J. 64, A376). These and additional restraints were used to obtain structures by performing simulated annealing followed by restrained energy minimization. Three types of low energy structures were obtained. In each type, residues 1 to 3 and 17 to 20 had variable conformations, residues 4 to 9 formed a right-handed α-helix, and residues 12 to 16 formed an irregular right-handed helix. All three types had bends at α-methylalanine 10 (MeA10). The structures could be interconverted by changing the MeA10 φ or ψ angles. These results suggest that there is conformational variability at MeA10. This may be caused by the lack of backbone hydrogen bonding between residues 10 and 14 (pro) due to the absence of an amide hydrogen on proline. The relationship between the structures and alamethicin function will be discussed.

A series of NMR experiments on isotopically labeled alamethicins incorporated into macroscopically oriented phospholipid bilayers has been initiated in order to determine the structure and orientation of alamethicin in bilayers. N-15ala6 alamethicin has been prepared by utilizing solid phase peptide synthetic techniques. The N-15 chemical shift of the labeled alamethicin in oriented bilayers will provide information on the orientation of the N-terminal helix with respect to the bilayer.

Tu-Pos480

CHANNEL FORMING ACITIVITY OF HUMAN DEFENSINS: DEPENDENCE ON N-TERMINAL RESIDUE.

((D.M. Munoz, Y. Sokolov, T. Ganz, R.I. Lehrer and B.L. Kagan)) UCLA School of Medicine and West L.A. VAMC, Los Angeles, CA 90024

Defensins are a family of small cationic peptides (Mr=3500-4000) found in phagocytic cells of mammals. These peptides possess broad antimicrobial activity in vitro and are thought to contribute to the antimicrobial properties of neutrophils. Previous investigation (Kagan et al., 1990) showed that the defensins known as NP-1 (rabbit) and HNP-1 (human) formed voltage-sensitive channels in lipid bilayers. We report that HNP-2, which differs from HNP-1 by the lack of an N-terminal amino acid, formed voltage sensitive channels when 20-60 μg/ml was added to one side of the bilayer. Appearence of current required a negative voltage (80-100 mV) on the side opposite to that of defensin addition. Multi-level conductance states were seen at both positive and negative voltages. At all negative and low positive voltages (<60 mV) a linear I-V relationship was observed. At higher positive voltages a rapid and sometimes total decrease in conductance was seen. Ion selectivity of the channel was slight to moderately anionic (20-23 mV reversal potential in a 10-fold gradient of NaCl). HNP-3, which differs from HNP-2 only by containing aspartic acid at its N-terminal was inactive in the same conditions. These results suggest that HNP-2 may exert its antimicrobial effect through channel formation, and that the N-terminal amino acid of human defensins plays key role in channel formation.

Tu-Pos481

A COMMERCIAL PREPARATION OF THE COUMARIN ANTIBIOTIC, NOVOBIOCIN, FORMS CATION CHANNELS IN LIPID BILAYERS

((A.M.Feigin, E.V.Aronov, J.H.Teeter, J.G.Brand))
Monell Chemical Senses Center, Univ. of Pennsylvania, Veterans Affairs Medical Center, PA 19104. (Spon. by M.T.Marron)

Commercial preparation of novobiocin added to one or both sides of the lipid bilayer at concentrations of 0.05 - 0.2 mM induces cation selective channels with conductances that are almost identical to those of gramicidin A channel (about 20, 22, 14, 7, and 2 pS for 100 mM NH_4Cl, CsCl, KCl, NaCl and LiCl, respectively). Transference numbers for cations are in the range of 0.97 - 0.98. The equilibrium between open and closed conformations of these channels is voltage independent. The similarity in conductance and ion selectivity between channels formed by novobiocin and gramicidin A may suggest that these structurally dissimilar molecules form channels with comparable internal diameter and internal surface charge distribution. In preliminary experiments we demonstrated that the other coumarin antibiotic - coumermycin A, also forms channels of about 600 pS for 100 mM KCl. Coumarin antibiotics may be a new class of channel-formers that can be used in the studies that relate molecular structure to channel properties.

Tu-Pos482

POTENTIAL DEPENDENT IONIC CHANNELS INDUCED BY AMPHOTERICIN B UPON UNILATERAL INTRODUCTION INTO STEROL-CONTAINING PHOSPHATIDYLCHOLINE BILAYERS.

((R.A.Brutyan)) NIDDK, NIH, Bethesda, MD 20892; Univ. of Maryland, College Park, MD, 20742; Inst.of Biotechnology, Yerevan, 375056, Armenia. (Spon.by V.A. Parsegian)

The investigation of the one-sided ("unilateral") action of amphotericin B (AmB) on model membranes (BLM) containing cholesterol (Chl) or ergosterol (Erl) is essential for elucidating the mechanism of cellular targeting and the severity of host toxicity of this antibiotic. Single ionic channels with ~14 pS conductivity and ~10 sec mean open lifetime were recorded in Erl-DPPC 1:5 (w/w) BLMs with 40 nM AmB added to 2M KCl, pH=6.2 bathing solution. The applied potential was +0.1 V on the side of the drug addition. After switching to -0.1 V potential, these channels had only ~8.5 pS conductance and disappeared over seconds. Replacing Erl with Chl, one again sees highly reproducible channels (80 nM AmB) with a 8-14 pS conductance, whose mean open liftime is ~0.1 s at +0.1 V. At -0.1 V these channels became poorly defined and disappeared. Similar results are seen with DOPC BLMs. The potential dependence of recorded channels can be explained by the Marty/Finkelstein model [J.Gen.Physiol, 65:515,1975] in which applied potentials can reversibly drive K^+-occupied, non-conducting "half pores" across the abstructing monolayer. Application of high potentials allows one to create primarily "unilateral" asymmetric channels even from AmB added to two sides of a BLM, though low applied potentials would permit symmetric channels to form.

Tu-Pos483

ALPHA-HELICAL HYDROPHOBIC POLYPEPTIDES FORM PROTON-SELECTIVE CHANNELS IN LIPID BILAYERS.

((A.E. Oliver and D.W. Deamer)) U.C. Davis, Davis, CA 95616

Proton translocation is important in membrane-mediated processes such as ATP-dependent proton pumps, ATP synthesis, bacteriorhodopsin and cytochrome oxidase function. The fundamental mechanism, however, is poorly understood. To test the theoretical possibility that bundles of hydrophobic α-helices provide a low energy pathway for ion translocation through the lipid bilayer, polyamino acids were incorporated into extruded liposomes and planar lipid membranes. Proton and potassium ion translocation were measured through these membranes. Liposomes with incorporated long-chain poly-L-alanine or poly-L-leucine were found to have proton permeability coefficients 5-7 times greater than control liposomes, an effect similar to that caused by alamethicin in the same peptide to lipid range. In contrast, short-chain polyamino acids had relatively little effect. Potassium permeability was not markedly increased by any of the polyamino acids tested. Fourier transform infrared spectroscopy indicated that a major fraction of the long-chain hydrophobic peptides existed in an α-helical conformation. Single channel recording in both 0.1 M HCl and 0.1 M KCl was also used to determine whether proton-conducting channels formed in planar lipid membranes (phosphatidylcholine : phosphatidylethanolamine, 1:1). Poly-L-leucine and poly-L-alanine in HCl caused a 10-30 fold increase in frequency of conductive events compared to that seen in KCl or by the other polyamino acids in either solution. This finding correlates well with the liposome observations in which these two polyamino acids caused the largest increase in membrane proton permeability but had little effect on potassium permeability. Poly-L-leucine was considerably more conductive than poly-L-alanine due to larger event amplitudes and a higher event frequency. The channel-like activity appeared to switch between conductive and non-conductive states, with most open-times in the range of 50-200 ms. The proton-selective nature of these defects suggests that protons may be moving through them along hydrogen-bonded strands of water molecules. We conclude that hydrophobic polyamino acids produce proton-conducting defects in lipid bilayers that may be used to model functional proton channels in biological membranes.
Supported by NASA NAGW-1119.

Tu-Pos484

WHY MAGAININ PEPTIDES CAN DISCRIMINATE BETWEEN BACTERIAL AND ERYTHROCYTE MEMBRANES?

((K. Matsuzaki, K. Sugishita, N. Fujii and K. Miyajima)) Fac. Pharm. Sci., Kyoto University, Sakyo-ku, Kyoto 606-01, JAPAN

Magainins (MGs), a class of antimicrobial peptide isolated from *Xenopus* skin, permeabilize bacterial membranes. However, they are practically nonhemolytic. Both membrane systems greatly differ in lipid composition. Thus, we examined the effects of lipid composition on the lytic activity of MG 2 and compared them with those of melittin (ML), a lytic peptide. The lytic power of MG 2 to liposomes of phosphatidylglycerol, abundant in bacterial membranes, was ten times stronger than that of ML. In contrast, the MG2-induced permeabilization of bilayers of phosphatidylcholine, mainly localized in the outer half of the erythrocyte membrane was two orders of magnitude weaker than that by ML, in keeping with MG's much weaker hemolytic activity. The formation of phosphatidic acid on erythrocyte surface by a phospholipase D treatment enhanced the peptide binding to and the lysis of erythrocytes. The incorporation of cholesterol, rich in the erythrocyte membrane, reduced the lysis by MG 2. The application of a transmembrane potential enhanced MG's hemolytic activity. We can conclude that the absence of any acidic lipids on the outer monolayer and the abundant presence of cholesterol, combined with the lack of a transmembrane potential, protect erythrocytes from MG's attack.

Tu-Pos485

ELECTRO-ELASTIC COUPLING IN MODELING IONIC TRANSPORT DYNAMICS IN TRANSMEMBRANE ION CHANNELS.

((M.B. Partenskii and P.C. Jordan)) Dept. of Chemistry, Brandeis University, Waltham, MA 02254.

General analysis and a specific illustration using an exactly soluble "elastic capacitor" model have shown (Partenskii and Jordan, *J.Chem.Phys.* **99**:2992 [1993]) that coupling between quasielastic (of interactive and/or entropic origin) and electrical degrees of freedom can cause such peculiarities at electrified interfaces as a negative branch of differential capacity, multistability and related electrical instabilities and phase transitions. The same mechanism may well have significant impact on the evolution of ionic current through an ion channel. Coupling of a charging process, induced by a transmembrane voltage, with structural changes in the channel (local deformation, bond libration, water dipole alignment, etc.) is described by switching the elastic capacitor in parallel with the pore's internal resistance, $R_{int}(x)$; x is the "gap width" of the capacitor (introduced to model voltage induced structural deformation in the pore-protein system). External resistance R_{ext} accounts for ionic diffusion from the solvent to the channel mouth. The other model parameters are an effective friction, affecting the time evolution of the elastic system, and the applied voltage, V. Analysis of the resulting nonlinear differential equations demonstrates self-oscillation of charge, current and elastic deformation for a range of model parameters. The possible interrelation between this effect and j(t) behavior of single ion channels is discussed.

MOLECULAR MECHANISMS OF MECHANOTRANSDUCTION: FROM BACTERIA TO BUCKMINSTER

W-AM-SymI-1

MECHANOSENSITIVE ION CHANNELS IN THE *E. COLI* CELL ENVELOPE: FROM PATCH-CLAMP STUDIES TO MOLECULAR IDENTIFICATION.

((B. Martinac[1], A.H. Delcour[2], M. Buechner[3], S.I. Sukharev[4], P. Blount[4], J. Adler[5] and C. Kung[4,6])) Dept Pharmacol[1], Univ of Western Australia, Perth, WA, Australia; Dept Biol[2], Univ of Houston, Houston, TX, USA; Dept Biol[3], Johns Hopkins University, Baltimore, MD, USA; Lab Mol Biol[4], Dept Biochem[5] and Dept Genetics[6], Univ of Wisconsin, Madison, WI, USA.

We used the patch-clamp technique to study the mechanosensitive ion channels (MSCs) of *Escherichia coli* in various experimentally-induced giant forms, and also in reconstituted bacterial membrane fractions. The membrane envelope of giant spheroplasts of *E. coli* exhibits activities of two distinct types of MSCs, the small MSC (MscS) and the large MSC (MscL) with conductances of approximately 1 and 3 nS (in 200 mM KCl) respectively. The effects of lysozyme and various amphipathic compounds on the activity of the MscS in membrane patches of giant spheroplasts indicated that (i) the peptidoglycan (cell wall) acted to resist the membrane stretching, and (ii) the lipid bilayer alone could transduce the mechanical force along the membrane plane which opened the channel. Both the MscS and the MscL can be functionally reconstituted into azolectin liposomes, either by fusing native membrane vesicles or by reassembly of the octylglucoside-solubilized membrane extract. This result strongly supported the previous findings that both types of channels are gated by tension transduced via the lipid bilayer. The nonselective MscL activated by high negative pressures and the weakly anion-selective MscS activated by lower negative pressures applied to a patch-clamp pipette appeared more sensitive to suction in liposomes than in spheroplasts. This finding suggested further that the cell wall restrains the membrane stretch. With detergent solubilization of the cell envelope followed by gel filtration of the solubilized membrane extract and patch-clamp sampling of individual fractions reconstituted into liposomes, we demonstrated that the MscL and the MscS are distinct proteins under nondenaturing conditions with approximate m.w. of 60-80 kD and 200-400 kD repectively. In addition, with SDS-PAGE we were able to trace the MscL to a small protein of approximately 17 kD. This protein was electroblotted and microsequenced. The sequence of 37 N-terminal amino-acid residues was found to correspond to a protein of previously unknown function encoded by a gene we have named *mscL* on a genomic fragment at minute 72 of the *E. coli* chromosome. Since insertional disruption of *mscL* removed the channel activity and re-expression of *mscL* carried on an expression plasmid restored its activity, we conclude that the *mscL* gene encodes a protein responsible for the activity of the MscL in *E. coli*.

W-AM-SymI-2

TOUCH INSENSITIVE MUTANTS IN *C. ELEGANS*.

((M. Driscoll)) Dept. of Molecular Biology and Biochemistry, Rutgers University, Center for Advanced Biotechnology and Medicine, 679 Hoes Lane, Piscataway, NJ 08855.

Mechanosensation in the nematode *Caenorhabditis elegans* is mediated by six mechanosensory neurons called touch receptor cells. M. Chalfie and colleagues have identified over 400 mutations that disrupt the function of the touch receptors (*Science* 243:1027 (1989)). These mutations define 15 *mec* genes (so named because elimination of their activity renders animals *mec*hanosensory defective) specifically required for the development and function of the touch receptor neurons. Some of these genes are expected to encode products directly involved in mechanotransduction.

mec-4 encodes a subunit of a newly discovered type of ion channel that is a candidate mechanosensory channel. *mec-4* is also of considerable interest because specific amino acid changes in the MEC-4 protein can induce the degenerative death of the touch receptor neurons. Our structure/function analysis of the MEC-4 protein has highlighted the functional importance of charged and polar amino acid residues which align on one face of the predicted α helix thought to form the second membrane-spanning domain, MSDII. We speculate that MSDII lines the channel pore and that essential amino acids project into the channel lumen to influence ion transport. Other genetic and molecular studies are consistent with a model in which the mechanosensory channel is a multimer that includes more than one MEC-4 subunit and a subunit homologous to MEC-4. We are beginning to test this detailed model of channel structure using biochemical and electrophysiological approaches. Consistent with the claim that mechanosensory channels are ubiquitous, *mec-4* is a member of a rapidly growing family of identified genes from *C. elegans* and higher organisms that appear to be expressed in diverse cell types.

W-AM-SymI-3

PRESSURE-CLAMP MEASUREMENTS OF THE DYNAMIC PROPERTIES OF MECHANO-GATED CHANNELS.

((O.P. Hamill and D.W. McBride, Jr.)) Department of Physiology and Biophysics, UTMB, Galveston, TX 77555.

Mechano-electrical transduction (MET) is typically associated with a generator potential that arises through an increase in membrane conductance to cations (Na^+, K^+ and Ca^{++}). Patch-clamp characterization of a stretch-activated cation channel in skeletal muscle fibers (Guharay & Sachs, J. Physiol, 352:685,1984) demonstrated that mechanical stimulation affected channel gating rather than channel conductance. Subsequently, the development of a pressure-clamp technique (McBride & Hamill, Pflugers. Archiv. 421:606, 1992) has revealed dynamic properties of mechano-gated (MG) channels. Pressure jump analysis of the MG channel in muscle and *Xenopus* oocytes has enabled the characterization of the pressure and voltage dependence of the latency, turn on and turn off kinetics of mechano-gated channels. Adaptation of MG channel activity to sustained stimulation was found in both cell types. In general, adaptation enables mechanotransducers to maintain their dynamic sensitivity over a broad stimulus domain. In nonsensory cells it may also serve to limit Ca^{++} influx. Adaptation of MG channel activity is voltage dependent but occurs in the absence of Ca^{++} (Hamill & McBride, PNAS 89:7462,1992). Mechanical stimulation of the patch can abolish adaptation. This result indicates that membrane-cytoskeleton coupling is important for adaptation.

W-AM-SymI-4

MECHANOELECTRICAL TRANSDUCTION IN THE VERTEBRATE HAIR CELL.

((R.A. Eatock)) Dept. of Otolaryngology, Baylor College of Medicine, Houston, TX 77030.

Hair cells are the mechanoreceptive cells of the lateral line and inner ear. Stimulation deflects the cells' hair bundles: arrays of modified microvilli (stereovilli) that protrude from the apical surfaces. Deflection of the hair bundle modulates channels near the tips of the stereovilli (Jaramillo & Hudspeth, Neuron 7:409, 1991). In the prevailing model of transduction, the channels are gated by elastic elements ("gating springs") that stretch in response to deflections of the hair bundle in one direction and relax during deflections in the opposite direction (Corey & Hudspeth, J. Neurosci. 3:962, 1983). Candidate gating springs, called tip links, have been identified; these are filamentous connections between stereovilli in adjacent rows (Pickles et al., Hearing Res. 15:103, 1984). The transduction process adapts in a calcium-dependent fashion, shifting the operating range in the direction of the stimulus (Eatock et al., J. Neurosci. 7:2821, 1987). One model of adaptation proposes that the gating springs are linked by myosin to the actin cores of the stereovilli and that movement of the myosin along the core restores the gating springs to (near) their resting lengths (Howard & Hudspeth, Proc. Natl. Acad. Sci. 84:3064, 1987; Assad & Corey, J. Neurosci. 12:3291, 1992). An alternative model (Crawford et al., J. Physiol. 419:405, 1989) proposes that calcium ions that enter open transduction channels promote channel closure.